

**Examination of the biomechanical properties of the  
All-on-Four™ treatment concept**

**Árpád László Szabó, D.M.D.**

Ph.D. Thesis

Szeged

2024

University of Szeged  
Albert Szent-Györgyi Medical School  
Doctoral School of Department of Prosthodontics  
Faculty of Dentistry

**Examination of the biomechanical properties of the  
All-on-Four<sup>TM</sup> treatment concept**

Ph.D. Thesis

**Árpád László Szabó, D.M.D.**

Supervisor:

Zoltán Lajos Baráth., Ph.D., Habil. Prof.

Szeged

2024

# CONTENTS

<b>I. PUBLICATIONS</b> .....	3
<b>II. LIST OF ABBREVIATIONS</b> .....	5
<b>III. INTRODUCTION</b> .....	7
<i>A. Global burden of oral disorders and edentulism</i> .....	7
<i>B. Factors affecting implant placement and survival</i> .....	9
<i>C. The All-on-Four<sup>TM</sup> (Ao4) treatment concept</i> .....	13
<i>D. Finite element analysis (FEA)</i> .....	14
<b>IV. AIMS OF THE STUDY</b> .....	17
<b>V. MATERIALS AND METHODS</b> .....	19
<i>1. Clinical study</i> .....	19
<i>2. Finite element analysis (FEA)</i> .....	23
<b>VI. RESULT</b> .....	31
<i>1. Clinical study</i> .....	31
<i>2. Finite element analysis (FEA)</i> .....	36
<b>VII. DISCUSSION</b> .....	43
<i>1. Clinical study</i> .....	43
<i>2. Finite element analysis (FEA)</i> .....	46
<b>VIII. NEW FINDINGS</b> .....	52
<b>IX. SUMMARY</b> .....	53
<b>XI. REFERENCES</b> .....	55
<b>XII. ACKNOWLEDGEMENTS</b> .....	69
<b>XIII. APPENDIX</b> .....	70
<b>XIII. CO-AUTHORS' DECLARATION</b> .....	82

# I. PUBLICATIONS

## 1. Publications related to the subject of the thesis

I. **Szabó ÁL**, Nagy ÁL, Lászlófy C, Gajdács M, Bencsik P, Kárpáti K, Baráth ZL: Distally Tilted Implants According to the All-on-Four® Treatment Concept for the Rehabilitation of Complete Edentulism: A 3.5-Year Retrospective Radiographic Study of Clinical Outcomes and Marginal Bone Level Changes. *Dent J* 2022; 10(5): e82.

**IF<sub>2022</sub>: 2.6, SJR ranking: Q2, Citations: 6 (Independent citations: 5)**

II. **Szabó ÁL**, Matusovits D, Sylteen H, Lakatos ÉI, Baráth ZL: Biomechanical Effects of Different Load Cases with an Implant-Supported Full Bridge on Four Implants in an Edentulous Mandible: A Three-Dimensional Finite Element Analysis (3D-FEA). *Dent J* 2023; 11(11): e261.

**IF<sub>2022</sub>: 2.6, SJR ranking: Q2, Citations: - (Independent citations: -)**

**ΣIF: 5.2**

## 2. Publications not related to the subject of the thesis

I. Körtvélyessy G, **Szabó ÁL**, Pelsőczy-Kovács I, Tarjányi T, Tóth Z, Kárpáti K, Matusovits D, Hangyási BD, Baráth Z: Different Conical Angle Connection of Implant and Abutment Behavior: A Static and Dynamic Load Test and Finite Element Analysis Study. *Materials* 2023; 16(5): e1988.

**IF<sub>2022</sub>: 3.4, SJR ranking: Q2, Citations: 1 (Independent citations: 1)**

**ΣIF: 3.4**

**ΣIF for all publications: 8.6**

### **3. Presentations related to the subject of the thesis**

**I. Szabó ÁL**, Kálmán K, Baráth ZL, Lászlófy C: Az ALL-ON-4 technológia sikerességét befolyásoló tényezők retrospektív vizsgálata és az ALL-ON-4 technika multidiszciplináris sikerei, hibái. In: Seres, László (szerk.) Magyar Arc-, Állcsont- és Szájsebészeti Társaság XXII. Kongresszusa és Szegedi Fogorvos Találkozó. 2018. szeptember 27-29., Szeged, Magyarország.

**II. Szabó ÁL**, Baráth ZL: Biomechanikai feszülések kiértékelése ANSYS végelemes modellen „All-on Four” koncepció esetén. In: SZTE FOK Fogorvosi referáló ülés. 2023. április 21., Szeged, Magyarország.

**III. Szabó ÁL**, Gajdács M, Kárpáti K, Lakatos É, Baráth ZL: Az “All-on Four” implantációs koncepció végelelemes modellezése és biomechanikai feszültségeinek kiértékelése az ANSYS szoftver segítségével. In: Magyar Fogorvosok Egyesülete Fogpótlástani Társaság Magyar Fogorvosok Fogpótlástani Társasága XXV. Konferenciája és Magyar Gnatológiai Társaság I. Konferenciája. Pécs, 2023. szeptember 21-23., Pécs, Magyarország.

## II. LIST OF ABBREVIATIONS

**3D:** three-dimensional

**Ao4:** All-on-Four

**AP:** alveolar process

**ANOVA:** one-way analysis of variance

**BOP:** bleeding on probing

**CAD:** Computer Aided Design

**CBCT:** cone-beam computer tomography

**Co:** cobalt

**Cr:** chromium

**CS:** conical standard

**CT:** computer tomography

**DA:** disto-approximal

**DM:** diabetes mellitus

**E:** Young's modulus/elastic modulus

**FEA:** finite element analysis

**GBD:** Global Burden of Disease

**ISQ:** Implant Stability Quotient

**LC:** load case (loading scheme)

**MA:** mesio-approximal

**MBL:** marginal bone loss

**N:** Newton

**OPT:** orthopantomography

**Pa:** Pascal

**$\rho$ :** density

**p<sub>eqv</sub>**: equivalent stress (von Mises stress)

**p<sub>max</sub>**: maximum principal stress (first principal stress)

**p<sub>min</sub>**: minimum principal stress (third principal stress)

**QoL**: quality of life

**RCT**: randomized controlled trial

**S**: simulation

**SDG**: Sustainable Development Goals

**SEM**: standard error of the mean

**SPSS**: Statistical Package for the Social Sciences

**T**: time point

**Ti**: titanium

**UN**: United Nations

**v**: Poisson's ratio

**WHA**: World Health Assembly

**WHO**: World Health Organization

**YLD**: Years Lived with Disability

**Zr**: zirconia

**ΔBL**: marginal bone level changes

### III. INTRODUCTION

#### A. Global burden of oral disorders and edentulism

Oral health – according to the definition of the World Health Organization (WHO) – is a state where the individual has a healthy dentition without suffering from chronic orofacial pain, and they are also free of birth defects (i.e. cleft lip and palate), oral tissue lesions or oral and pharyngeal tumors; additionally, they should not be affected by any other disorders that may influence the integrity of the oral, dental and craniofacial tissues, or the functionality of the craniofacial complex [1,2]. Oral health is largely dependent on the social, political and economic determinants of health, in addition to the availability of specialized human resources; thus, oral disorders often disproportionately affect the most disadvantaged and vulnerable patients with low socio-economic status [3]. As oral disorders considerably affect everyday functionality and well-being – having physiological (e.g., nutrition, speech), psychological (e.g., confidence, comfort, self-worth) and esthetic aspects – they are important contributors to years lived with disability (YLDs) and decreased quality of life (QoL) [4]. The 74<sup>th</sup> World Health Assembly (WHA; 2021) aimed to draft the “*Global strategy on oral health*” [5]; according to some estimates, there are over 3.5 billion individuals affected by disorders of the oral cavity, with projections that the prevalence of these illnesses will most likely increase, due to global population ageing and growth [6]. Oral disorders of public health importance include untreated dental caries of the permanent teeth, severe periodontal disease, lip and oral cavity cancers, traumatic injuries of the orofacial region, severe tooth loss (partial toothlessness, i.e. having  $\leq 9$  permanent teeth) and edentulism (complete tooth loss) [7]. In addition to inadequate oral hygiene, many modifiable risk factors and lifestyle habits (such as a diet rich in carbohydrates, simple sugars and low in fiber, tobacco consumption, and alcohol use) contribute to the development of oral diseases [8]. As the effectiveness of previous global strategies on oral health were modest at best, the WHA has recommended that current strategies on improving oral health be implemented within existing WHO strategic programmes, such as attaining universal health coverage, global prevention of non-communicable diseases, smoking cessation and health promoting schools [6]. Furthermore, the United Nation’s Sustainable Development Goals (UN SDGs) and oral health goals have considerable overlaps, both in regards to direct (SDG 3: „*Good Health and Well-being*”) and indirect (SDG 1: “*No poverty*”; SDG 2: “*Zero hunger*”; SDG 10: “*Reduced inequalities*”)



effects in attaining SDGs, respectively [9]. Edentulism is a definite condition, which most commonly occurs as a consequence of untreated caries of the permanent teeth and its complications, severe periodontal disease or traumatic injuries, leading to the extraction of affected teeth [10]. Based on the Global Burden of Disease (GBD) database, the estimated incidence and prevalence of edentulism in 2019 were 25 million (19.8 – 30.7) and 352 million (280 – 449) cases, respectively. According to WHO reports, the prevalence of edentulism is ~7% globally, which has increased by 80% in the last 30 years; however, this rate is over 10% in patients >50 years of age [11]. Moreover, edentulism is a considerable contributor to disease burden, causing 9.62 million (6.15 – 14.2) YLDs in 2019, disproportionately affecting low and middle income countries (**Figure 1.**) [11]. In addition to the subsequent oral dysfunction, edentulism is a significant determinant of general health, leading to the increased risk of developing other comorbidities (e.g., cardiovascular diseases [12], gastrointestinal disorders [13], obesity [14], type II diabetes [15], dementia [16], chronic kidney disease [17], various cancers [18], rheumatoid arthritis [19], chronic obstructive pulmonary disease [20], aspiration pneumonia [21], obstructive sleep apnea [22]), and the associated risk of mortality is also higher in these conditions [23].

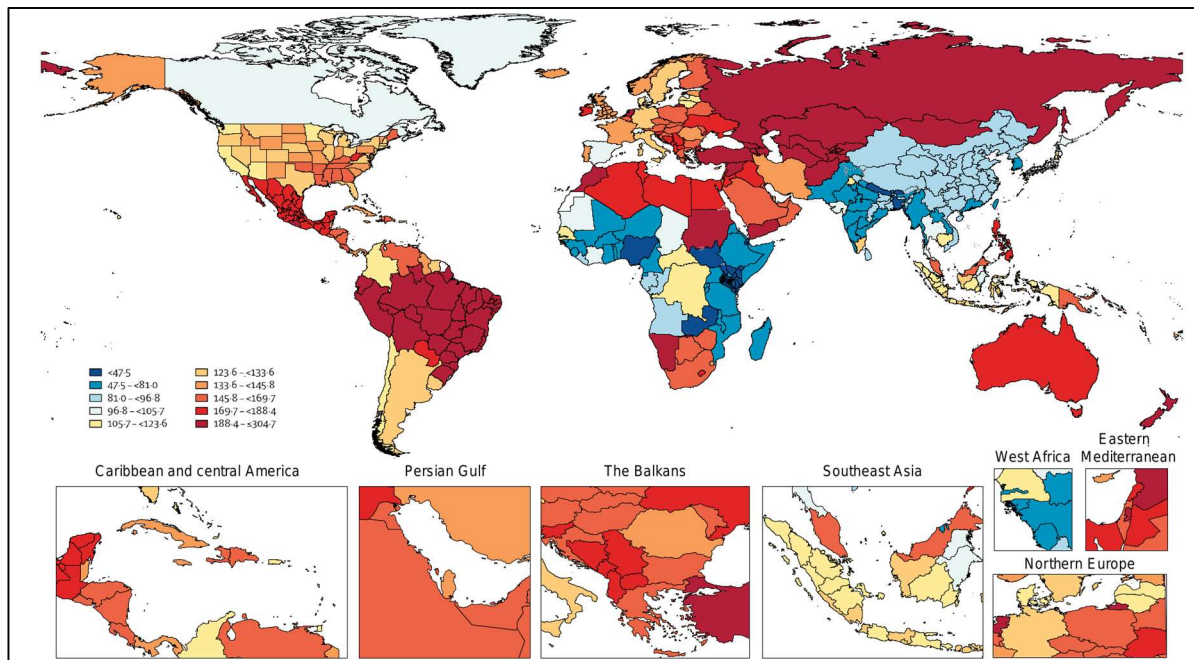


**Figure 1.** Age-standardised number of disability-adjusted life years (DALY) per 100 000 individuals, by location, both sexes combined, based on the GBD database (2019) [11]

## **B. Factors affecting implant placement and survival**

The use of dental implants is often considered a form of tertiary prevention, where the aim is to provide effective treatment and rehabilitation to a condition, which has already led to bodily harm [24]. Endosseous, osseointegrated implant-supported, fixed full-arch restorations are widely recognized as a safe and effective treatment alternative for the oral rehabilitation of edentulous patients [25]. Typically, dental implants – made from an alloplastic material (most commonly titanium [Ti]) – have a screw-like component that helps with insertion into the bone, and serves as a framework for transferring functional and parafunctional forces generated during mastication into the peri-implant tissues [26]. The characteristics of load transmission and stress distribution in the bone and around the implants are important determinants of implant health and survival [27]. The morphology, surface, length, diameter and quantity of the implants, the material properties of the implants and of the prosthesis, the loading type, the quantity and quality of the available alveolar bone all impact load transmission at the bone-implant interface [28]; nevertheless, the material properties, length, diameter, form and number of implants are the few biomechanical factors that are easily modifiable [29]. Previously, conventional (delayed, two-stage) loading protocols were carried out, where patients received their restorations after a healing period of 2–3 months; however, recently, immediate loading (one-stage) protocols have been extensively investigated for their clinical applicability and comparability, where patients receive a preliminary acrylic prosthesis within 48 hours of implant placement, followed by the final prostheses in the coming few months [30,31].

Teeth are anchored into the jaws through the bundle bone, into which, the periodontal ligaments invest. The alveolar process (AP) is a teeth-dependent tissue, which goes through involutionary changes and atrophy following tooth loss or tooth extraction, and the lack of physiological forces of mastication affecting the jawbones [32]. After tooth loss (or extraction), minor dimensional changes are observed in the apical and middle portions of the socket site, on the other hand, the volume of hard tissue lost in the coronal portion of the ridge is usually substantial [33]. These morphological changes in the post-extraction sockets may be described using radiographic methods, study cast measurements or cephalometric measurements [34]. The gross morphological changes (i.e. atrophy of the AP) may be further exacerbated by a history of periodontal disease, periapical pathologies, endodontic lesions, and bone or dental trauma [35]. The rate of atrophy of the AP greatly varies on a person-to-

person basis, influenced by the patient's genetic characteristics, sex, age, immunological status, lifestyle choices (e.g., smoking), hormone levels, the condition of the socket before/after tooth extraction, the number and proximity of extracted teeth, and the time elapsed since the extraction of the teeth [36]. Furthermore, the tissue biotype, and cellular and molecular factors affecting post-extraction wound healing may also have pronounced effects [37].

In addition to the contour changes caused by bone remodeling, clinicians should also be aware of the quality of the available edentulous jaw bone before any interventions, as the status (i.e. volume, favorable architecture) of the AP may hinder the patients from receiving an ideal prosthetic reconstruction (with fixed or removable dentures) following implant-placement from a functional and esthetic point of view [38]. The two most common classification systems to characterize the quality of edentulous jaw bone before implant placement are the Lekholm and Zarb (1985), and the Misch and Judy (1987) categories [39,40]. The former classification describes the ratio of cortical and medullar bone in the AP (with *Type I* having the largest quantity of cortical bone, while *Type IV* is characterized by a majority soft, low-density medullar bone layer, covered by a thin cortical layer only) (**Figure 2.**); overall, high levels of implant mechanical stability and favorable outcomes has been associated with *Type II-III* bone [X]. On the other hand, the latter method describes alveolar bone density, where *D1* bone has the densest structure, and *D4* bone being the least dense (**Figure 2.**) [39,40]. Both categories may be used to predict the success of future implant performance [41]. Following tooth extraction, the greatest amount of bone loss (or remodeling) in the horizontal dimension is usually observed on the facial aspect of the ridge, while the greatest bone loss in the vertical dimension is observed on the buccal aspect [30-33, 42]. Residual ridge resorption (or remodeling) leads to not only decreased bone width and height of the AP – i.e. to an increasingly narrow dental arch – but also to qualitative changes in the remaining bone [30-33, 43]; these post-extraction involutory changes are more severe in the case of the mandible, expressed in bone volume reduction, alterations in the bone architecture and a shift from *D1* bone to *D2* bone. On the other hand, in the maxilla, the thinning of cancellous bone may be observed, the orientation of the trabeculae changes, which may considerably affect the macro-micromorphology and the interactions between the bone and the implant threads [44].

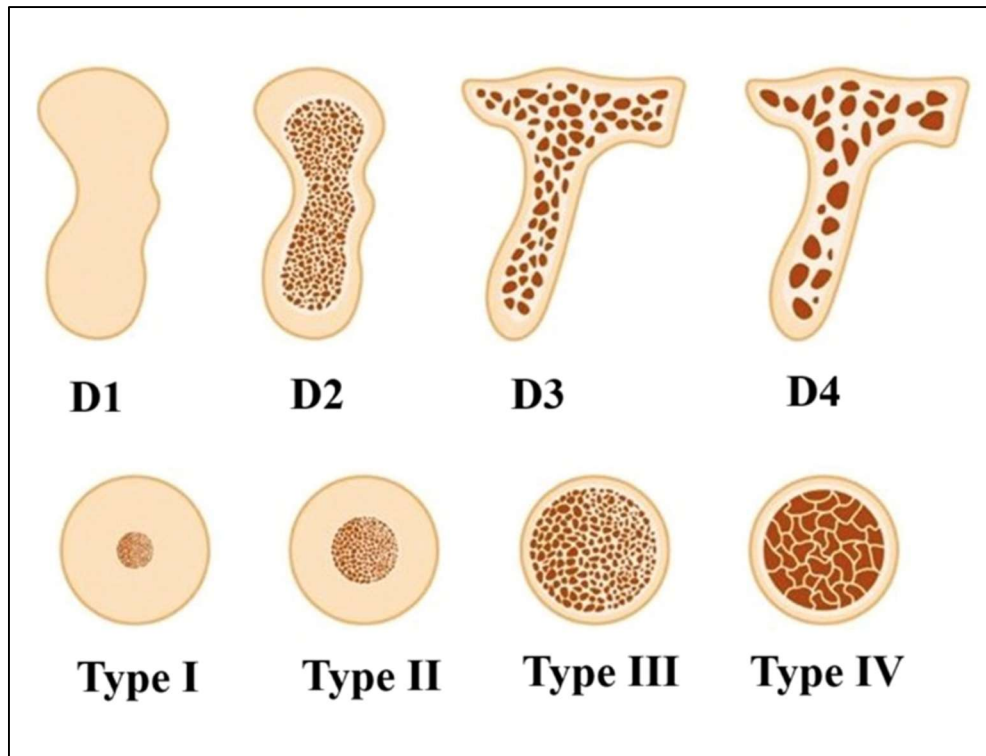


**Figure 2.** Classification systems to characterize the quality of edentulous jaw bone, based on the Misch-Judy (*D1-D4*; top row) and Lekholm and Zarb (*Type I-IV*; bottom row) methods (adapted from [39,40])

An additional aim of providing patients with prosthetic restorations is to establish a load transfer to the surrounding bones in a manner, which closely resembles physiological conditions, slowing down the degeneration of the AP, and restoring long-term functionality [45]. Immediately after the introduction of dental implants, implant survival is dependent upon the interaction of the implant’s alloplastic material (e.g., Ti) with the nearest biological surface (i.e. the bone) [46]. The stability of dental implants may be characterized as *primary* (or mechanical) stability, which affects the immediate outcome of the implant surgery (influenced by bone quality, preparation of the implant bed, and implant geometry); on the other hand, *secondary* (or biological) stability leads to the formation of the implant-bone interface, influenced by underlying patient attributes and implant microtopography [47,48]. The intermediate period between primary and secondary stability is characterized by a “*stability dip*” [49] (**Figure 3.**). Another aspect of primary implant stability is to avoid micromotions at the bone-implant interface at the initial phase of osseointegration; reaching high primary stability is essential for immediate loading protocols to be successful and durable [50]. According to the recent literature, if micromotions are above 50-150  $\mu\text{m}$ , there is the risk of developing a fibrous, non-mineralized, fluid-formed capsule around the implants in

lieu of osseointegrated surfaces [51,52] (**Figure 3**). Similarly to implant stability, implant failure may also be classified into two groups: *early* (primary) implant failure is mostly due to failure of osseointegration, while *late* (secondary) implant failure may occur due to mechanical (screw loosening, implant fracture, prosthetic fracture) or biological (peri-implantitis) reasons [53,54]. Furthermore, both primary and secondary implant failure may be mediated by individual patient factors, such as non-modifiable characteristics like age, sex, chronic underlying conditions and medicines taken for them, inadequate oral hygiene, periodontal disease, bruxism and lifestyle habits [55].

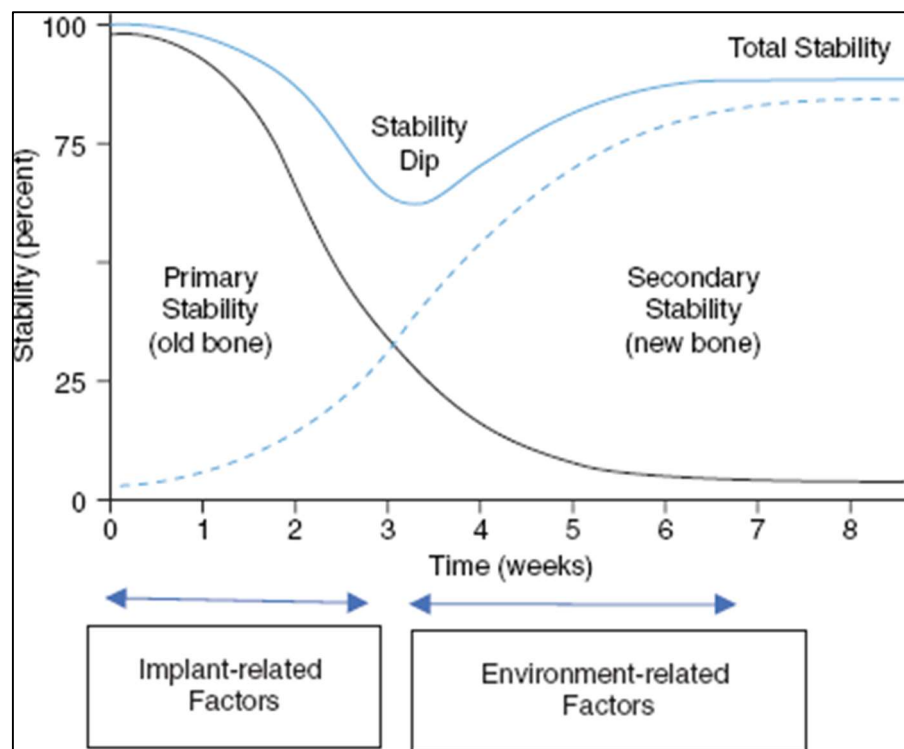


**Figure 3.** Timeline and relevance of early (primary) and late (secondary) stability associated with implant placement [50,51]

### **C. The All-on-Four™ (Ao4) treatment concept**

As stated previously, implant placement may be followed by a delayed (two-stage) or an immediate (one-stage) loading protocol for the oral rehabilitation of edentulous patients; recent studies have shown that overall implant survival rate of immediate loading protocols is comparable to that of the delayed loading schemes [56,57]. Furthermore, as patients prefer reduced treatment durations and esthetic results, restorations based on immediate loading protocols results in greater patient satisfaction rates. However, due to the anatomical constraints of the edentulous jaw (especially in the case of the mandible), or if the quality and the amount of residual alveolar bone is limited, implant-supported prosthetic treatment is impossible without complex surgical interventions preceding implant placement [58,59]. Alveolar crest augmentation, bone grafting, nerve transposition and soft tissue management in the posterior mandible all carry the risk of complications (e.g., loss of soft tissue volume and contours, graft failure, infections), increased morbidity, and poor patient performance, in addition, the reconstructive surgery corresponds to higher costs and longer recovery time intervals [60,61]. Thus, most patients prefer a less invasive and a more economical approach to their dental rehabilitation with a shorter recovery [62]. One of the proposed alternative solutions to these surgical procedures include the use of short and extra-short implants, a long distal cantilever, or increasing the implant diameter, in which cases, a careful selection of the surgical protocol may correspond to favorable clinical outcomes [63,64]. Furthermore, the use of tilted implants in the jaw is another recognized alternative to avoid bone grafting procedures, as no significant clinical difference in success rates compared to axially placed implants, and their acceptability by patients is also higher [65]. Clinical advantages of angled implants are associated with the extension of the distal cantilever, in addition to resulting in better implant survival rates [66]. The bending effect on the single tilting implants may increase the marginal bone stress, but this may be augmented with splinting them into a multiple implant-supported prosthesis [67].

The “All-on-Four” (Ao4) treatment concept—devised by Maló et al. (Nobel Biocare, Göteborg, Sweden) in 2003 – has also been described as a viable method that allows clinicians to overcome the anatomical limitations of the mandibular bone without necessitating advanced and risky surgical techniques [68,69]. This strategy for oral rehabilitation involves the placement of four implants in the interforaminal area of the mandible and the premaxillary region – two axial implants, which are positioned in the anterior alveolar region, while the other two implants are tilted (15–45°) in the posterior region—to support immediately loaded, one-piece full-arch fixed restorations [70]. With

implant angulation in the posterior region, violation of the mandibular nerve is bypassed, the use of longer implants (i.e., resulting in a longer bone-to-implant contact area) is permitted, and the length of the denture cantilevers may also be reduced [71]. Marginal bone loss (MBL) between tilted and axially placed implants demonstrated no difference and presented with no detrimental effects on osseointegration levels [72]. Ao4 procedures often include the use of computer-assisted procedures and implant guides, enhancing the safety and reliability of the procedures [73]. Advantageous results on implant survival rate and the short-term success of the Ao4 concept for the rehabilitation of both maxillary and mandibular arches has been reported by numerous short and medium-term studies [74]. Retrospective studies have reported that MBL levels after 3-5 years were ~0.5-1.5 mm, both in the maxilla and the mandible [75,76]. A ten-year longitudinal study by Maló *et al.* has demonstrated a 98.2% survival rate of mandibular implants [77], while a literature summary by Durkan *et al.* reported success rates ranging between 92.2-100%; however, long-term studies with high evidence rigor are currently lacking [78].

#### **D. Finite element analysis (FEA)**

Considerable gaps still exist in the knowledge regarding the biomechanical stresses observed in the peri-implant bone, implants, and prostheses during the treatment of edentulous jaws. During mastication and parafunctional activities of the oral cavity, dental implants and the surrounding AP are affected by mechanical forces (stresses, loads) [79]. The long-term success and predictability of implant-supported restorations largely depends on the distribution of these forces and the rate of load transfer at the bone-implant interface, as they may affect both primary (critical in immediate loading) and secondary stability (affecting bone remodeling processes) [80,81]. Load transmission at the bone-implant interface is influenced by a variety of factors, including the length, diameter, form, and surface of the implants; material properties of the implant and/or prosthesis; geometry, quality, and quantity of the residual alveolar bone; nonetheless, the properties of the implants are among the few modifiable biomechanical factors [82-84]. Due to the fact that the Ao4 concept operates with fewer implants overall, the characteristics of individual implants have a more pronounced importance [85]. With the use of a lower number of (tilted) implants, one of the disadvantages of the Ao4 concept is that higher stress and strain around the implant and in the bone may exceed the load bearing capacity of the bone (i.e., overload), resulting in microdamage accumulation and marginal bone resorption [86]. This may threaten primary stability and

osseointegration, leading to excessive micromotion and—in severe cases—implant loss or failure [87].

External forces in dental materials and bodies lead to the awakening of internal forces (or stresses) [88]; these stresses may be complex in nature, but may be decomposed into more basic stress types, such as tensile, compressive, and shear stresses [89,90]. Strain – which describes the dimensional changes occurring in a physical bodies or materials – is also an important property, as stress and strain tolerance are often used as characteristic indicators for dental biomaterials [91]. Clinicians should be aware of the various stresses arising in the jawbone from masticatory forces and implants during treatment planning, to ensure a best possible distribution of stresses following prosthetic treatment [92]. In recent studies, the most commonly used indicators to assess the biomechanical properties of the peri-implant bone are the maximum principal stress ( $\mathbf{P}_{\max}$ , first principal stress; representing the strongest *tensile* stress values), minimum principal stress ( $\mathbf{P}_{\min}$ , third principal stress; representing the strongest *compressive* stress values) and equivalent stress ( $\mathbf{P}_{\text{eqv}}$ , von Mises stress; representing the effectiveness of the implant-to-bone load transfer) values [93]. Determination of the biomechanical properties and stress/strain levels in the peri-implant bone or in the implant body were largely achieved by laboratory measurements with mechanical testing machines. In these studies, measurements are performed on cadavers and bone ribbons used as model systems; however, many of these methods are cumbersome to use, and often lack in reproducibility [94].

At the same time, the use of finite element analyses (FEA) to generate three-dimensional (3D) qualitative and quantitative biomechanical data in the field of medicine and dentistry have received substantial attention, and has become a widely accepted, non-invasive research method to estimate specific biomechanical parameters and behaviors in complex biological systems, such as the edentulous mandible, the peri-implant bone or on the restorations [95,96]. During FEA, complex structures and shapes showing irregular geometry (e.g., maxilla and mandible, implants) are discretized into many small elements (a “finite” number of elements, e.g., a tetrahedron), which are connected at the corners through so-called “nodes”; the number of elements and the type of meshing used for a FEA model is a key indicator of model accuracy [97]. The mechanical behavior of every element may be described as a function of node displacement (e.g., due to bite force). One of the main advantages of FEA – keeping in mind the limitations of the method, and the assumptions/restraints made to simulate complex structures – includes its capability to be used for high-throughput analysis [98]; furthermore, FEA is a flexible method, allowing for



running simulations under various conditions, as the geometry of the modelled object, the element number and type, material properties, physical conditions, loading mode and computational accuracy of FEA may be freely selected and changed [99]. Each setting will influence results and their interpretation, therefore the behavior of our model may be determined for numerous materials and under various loading conditions.

## IV. AIMS OF THE STUDY

The Ao4 prosthetic concept has received substantial attention from dentists for the oral rehabilitation of edentulous patients, due to the advantageous, short-term clinical outcomes associated with this treatment protocol; furthermore, implant placement with Ao4 is followed by immediate loading, which is in line with the preferences of the patients. On the other hand, there are substantial gaps in the literature, associated with numerous practical aspects of the Ao4 concept; for example, there are limited number of mid- to long-term retrospective or prospective studies, determining the success rate, survival and peri-implant bone-level changes implant placement according to the Ao4 concept. Furthermore, there is currently no established consensus of the type of loading to be favored, partly due to the limited knowledge of the biomechanical stresses observed in the peri-implant bone, implants, and prostheses following treatment of the jawbone. Therefore, our present study set out the following aims: *i*) to assess the clinical success rate and the marginal bone loss (MBL) levels following the implantation of distally tilted implants according to the Ao4 prosthetic concept, in a retrospective, single-center experience, measured by radiological findings; *ii*) to investigate the biomechanical behavior of an edentulous mandible with an implant-supported full bridge on four implants (aiming to model the Ao4 prosthetic concept) under simulated masticatory forces, in the context of different loading schemes and material properties, in a patient-specific finite element model, using 3D-FEA.

### **The specific goals of the study were the following:**

1. Determination of **implant survival rates (%)** of distally tilted **Ao4 implants at baseline** (T<sub>0</sub>; at the 3-month appointment), and after **18 months** (T<sub>1</sub>; 1.5 years post-restoration), **30 months** (T<sub>2</sub>; 2.5 years post-restoration), and **42 months** (T<sub>3</sub>; 3.5 years post-restoration) of follow-up, in a retrospective fashion
2. Determination of **MBL levels** around **maxillary and mandibular Ao4 implants at baseline** (T<sub>0</sub>; at the 3-month appointment), and after **18 months** (T<sub>1</sub>; 1.5 years post-restoration), **30 months** (T<sub>2</sub>; 2.5 years post-restoration), and **42 months** (T<sub>3</sub>; 3.5 years post-restoration) of follow-up, in a retrospective fashion

3. Determination of **MBL levels** around **tilted (posterior) and axial (anterior) Ao4 implants at baseline** ( $T_0$ ; at the 3-month appointment), and after **18 months** ( $T_1$ ; 1.5 years post-restoration), **30 months** ( $T_2$ ; 2.5 years post-restoration), and **42 months** ( $T_3$ ; 3.5 years post-restoration) of follow-up, in a retrospective fashion
4. Determination of **MBL levels** around the **mesio-approximal (MA) and disto-approximal (DA) aspects of Ao4 implants at baseline** ( $T_0$ ; at the 3-month appointment), and after **18 months** ( $T_1$ ; 1.5 years post-restoration), **30 months** ( $T_2$ ; 2.5 years post-restoration), and **42 months** ( $T_3$ ; 3.5 years post-restoration) of follow-up, in a retrospective fashion
5. Determination of **maximum principal stress [ $P_{max}$ ], minimum principal stress [ $P_{min}$ ] and equivalent stress [ $P_{eqv}$ ]** values in the **cortical and trabecular bone**, corresponding to four sets of **masticatory load cases (LC1-LC4)**, in a patient-specific finite element model of an edentulous mandible
6. Determination of **maximum principal stress [ $P_{max}$ ], minimum principal stress [ $P_{min}$ ] and equivalent stress [ $P_{eqv}$ ]** values in the **cortical and trabecular bone**, corresponding to different **implant-denture material configurations (S1 and S2)**, in a patient-specific finite element model of an edentulous mandible

## V. MATERIALS AND METHODS

### 1. Clinical study

#### 1. A. Study design

A single-center, institution-based retrospective study was carried out at the Faculty of Dentistry, University of Szeged, between 2017.01.01. and 2022.01.01., corresponding to patients – deemed eligible based on the inclusion and exclusion criteria – undergoing an implant surgical procedure with an immediately-loaded, four-implant-supported fixed prosthetic concept, following the Ao4 protocol. The study employed a convenience sampling approach at the study center [100], and has aimed to evaluate radiographic data (peri-implant bone-level changes) longitudinally from included patients.

#### 1. B. Patient recruitment, inclusion and exclusion criteria

Before the initiation of the study, the following inclusion criteria were set for eligibility: *(i)* patients aged 18 years or older, *(ii)* patients in an overall good health condition, able to undergo surgical intervention; *(iii)* patients in need for a complete rehabilitation of the edentulous maxilla or mandible, and the possibility of placing a minimum of 4 implants (at least 10 mm long); *(iv)* sufficient bone height in the sites intended for the placement of implants (min. 6 mm, evaluated by preoperative CT scans analysis). Furthermore, the following exclusion criteria were set: *(i)* presence of an acute infection at the planned implant sites; *(ii)* known coagulopathies or other hematologic diseases; *(iii)* recent occurrence of a severe cardiovascular or cerebrovascular event; *(iv)* diseases affecting the immune system; *(v)* uncontrolled diabetes mellitus (DM); *(vi)* pregnancy or lactation; *(vii)* metabolic illnesses affecting the bones, bisphosphonate therapy; *(viii)* heavy smoking (>10 packs/day); *(ix)* systemic chemotherapy or irradiation of the head and neck region within the last 12 months; *(x)* presence of parafunctional habits, such as severe bruxism or clenching (assessed and identified by clinicians, based on clinical signs and symptoms); *(xi)* inadequate oral hygiene level (full-mouth plaque and bleeding scores over 20%), or poor perceived motivation on the part of the patient to maintain good oral hygiene throughout the study.

## **1. C. Preoperative treatment**

Prior to surgical treatment, the relevant medical and dental history, lifestyle habits (e.g., smoking), and potential drug allergies of the patients were reviewed; the preoperative assessment of the patients was carried out by a prosthodontist and a periodontist. Following the presentation of the treatment plan to the patients and obtaining consent, surgical treatment was scheduled. Cone-beam computed tomography (CBCT) scans (i-CAT cone beam CT-scanner, Imaging Sciences International; Hatfield, PA, United States) were carried out for preoperative assessment. Individuals followed an antibiotic regimen *per os* (amoxicillin 500 mg t.i.d. or clindamycin 300 mg q.i.d.) three days prior to the surgical procedures, in cases where teeth had to be extracted simultaneously. Preceding surgery, local anesthesia was administered (4% articaine containing 1:100,000 epinephrine).

## **1. D. Implant placement protocol**

All relevant operative interventions were performed by the same surgeon with more than twenty years of experience associated with immediate loading procedures. Quantitative and qualitative assessment of the jaw bone was performed by means of preoperative radiographs, visual inspection, and tactile evaluation during drilling; appraisal of bone quality was carried out using the CBCT scans [101]. Each individual received (i) 2 distally tilted implants in the posterior region and, after that, (ii) 2 anterior implants in the maxilla or the mandible. In the maxilla, tilted implants were positioned just anterior to the maxillary sinus, while in the mandible they were positioned anterior to the mental foramen. The placement of implants was according to the Ao4 treatment concept, using the Ao4 surgical guide (Nobel Biocare; Kloten, Switzerland); comprehensive details regarding the procedure have been described elsewhere [102]. Regarding bone regeneration, universal clinical protocols for immediate implant placement were used [103]. Localized bone grafting was performed to cover exposed threads and/or other osseous defects associated with extraction sockets, as needed with demineralized allografts. For the fabrication of the master cast to create the patients' provisional restoration, open-tray multi-unit impression copings were placed on the multi-unit abutments to make an impression using precision impression material (Flexitime, Heraeus Kulzer, Hanau, Germany).

Following the operative procedure, patients were instructed to abstain from brushing in the first 7 days post-op, and to rinse using warm water. For 24 h post-op, instructions and recommendations were given for a soft diet (cold or at room temperature), to be followed by a semi-solid diet for the following three months. Patients were supplied with antibiotics (amoxicillin 500 mg t.i.d. or clindamycin 300 mg t.i.d. for seven days) and analgesics (non-steroid anti-inflammatory drugs) to control post-operative pain and inflammation as per standard guidelines and protocols in oral surgery. To confirm implant positions, and the positions of the prosthetic components, a CBCT scan was taken immediately postoperatively [101].

### **1. E. Restorative protocol**

Prior to the surgical intervention, a heat-cured acrylic resin (Ivocap High Impact acrylic, Ivoclar Vivadent; Amherst, NY, USA) was prefabricated, which was amended to the master model directly after the surgery. Fabrication was carried out using cold curing material (Probase, Ivoclar Vivadent; Amherst, NY, USA). Following 3–4 h after the completion of the operation, the provisional all-acrylic prosthesis was seated. Routine follow-ups were scheduled for the patients after surgery at 7, 14, and 28 days and 3 months after surgery, and on a yearly basis thereafter. Following the 3-month appointment, fabrication of the definitive prosthesis was initiated, consisting of a milled Ti frame with a wrap-around heat-cured acrylic resin (Nobel Procera Implant Bridge Ti framework veneered with composite). The antagonist denture was a fixed denture/implant supported restoration in all cases. A long-cone paralleling method was applied to obtain matched and calibrated orthopantomogram (OPT; panoramic X-ray) images at the 3-month appointment and at the subsequent appointments continuously. The 3-month radiographs after the time of placement of the definitive prosthesis were utilized as a baseline ( $T_0$ ) to assess the bone levels longitudinally. At the respective follow-ups, the implants were assessed for signs of peri-implantitis, plaque, and bleeding on probing (BOP), based on routine clinical guidelines [104].

## 1. F. Radiographic Assessment: Calculation of Marginal Bone Loss

Peri-implant bone-level changes were measured by matched and calibrated OPT images taken at the 3-month appointment (i.e., baseline,  $T_0$ ) and follow-ups after 18 months ( $T_1$ ; 1.5 years post-restoration), 30 months ( $T_2$ ; 2.5 years post-restoration), and 42 months ( $T_3$ ; 3.5 years post-restoration); marginal bone level (the most coronal bone-to-implant contact) was assessed on the MA and DA aspects. An independent researcher—not affiliated with the primary center and investigators—evaluated the OPT images. Radiographs were digitized in a 640 (H)  $\times$  480 (V) pixel matrix image with an 8-bit depth. The density and contrast were then adjusted for optimal visualization of the marginal bone, and the digital images were saved as a .TIF extension image. The 2D images were then exported and analyzed using the CLINIVIEW image analysis software (MI Dental; Knowsley, Prescott, UK). Calibration for image analysis was performed on an individual implant-level ( $n = 288$ ) to achieve the most accurate results possible, where the known size and specifications of the individual documented implants were used as the basis for calibration, to allow for the calculation of marginal bone level changes in the area. Assessment of bone levels were carried out and captured separately on the MA and DA sides of the implant. The change in marginal bone levels (expressed in mm) from the baseline ( $T_0$ ) to the values recorded at the follow-ups  $T_1$ ,  $T_2$ , and  $T_3$  were calculated.

## 1. G. Outcome Variables Assessed

During the study, the following primary outcome measures were assessed: **(i) implant survival rate (%)**, at baseline ( $T_0$ ; at the 3-month appointment), and after 18 months ( $T_1$ ; 1.5 years post-restoration), 30 months ( $T_2$ ; 2.5 years post-restoration), and 42 months ( $T_3$ ; 3.5 years post-restoration), defined as Ao4 implants being stable and functional (implant stability was assessed using pressure from two opposing instruments following the unscrewing of the prosthesis), lack of peri-implant radiolucency on radiographs, lack of suppuration or pain associated with the implant site, no signs of peri-implantitis, and lack of neuropathies or persistent paresthesia; **(ii) MBL levels** around Ao4 implants from the baseline ( $T_0$ ) to the values recorded at the follow-ups  $T_1$  (1.5 years),  $T_2$  (2.5 years), and  $T_3$  (3.5 years) post-implantation. MBL levels were compared around the following implant subgroups: *a.*)

maxillary vs. mandibular implants; *b.*) tilted (posterior) and axial (anterior) implants; *c.*) MA and DA implants.

## 2. Finite element analysis (FEA)

### 2. A. Study design, model origin

To perform FEA in the context of our study, a patient-specific finite element model was constructed using pre- and post-implantation CT images of a 63-year-old male patient with adequate bone supply, who was eligible for treatment with an implant-supported full bridge on four implants. Implant placement occurred 6 months post-extraction. The patient's final prosthesis consisted of a milled cobalt–chromium (Co–Cr) alloy frame with a cold-curing pour-type acrylic denture base (Vertex Dental B.V., Soesterberg, The Netherlands) and Ivoclar Vivadent (Schaan, Liechtenstein) denture teeth. A CBCT image corresponding to the patient's baseline state and the panoramic radiograph 4-year post-implant placement are presented in **Figures 4.** and **5.**, respectively.

To ensure the most accurate bone modelling possible, finite element models of the trabecular and the compact bone were created by the segmentation of the CT images of the pre-implantation edentulous mandible. This prevented the adverse effect of X-ray image artifacts in the environment of metallic materials on the subsequent material properties. The geometry and precise location of the implants in the jawbone were obtained by processing the post-implantation CT images. The two datasets—obtained by separate segmentations—were fused to create the final model including the trabecular bone, compact bone, and implants.

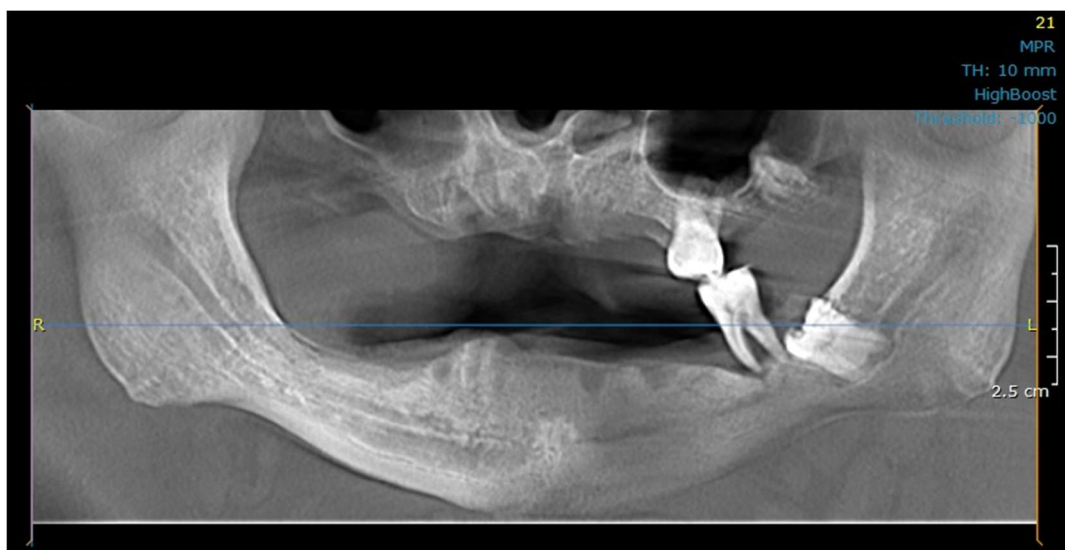


**Figure 4.** Cone-beam CT (CBCT) image corresponding to the patient's baseline state.





**Figure 5.** Panoramic radiograph of the patient 4 years post-implant placement.

## **2. B. Modeling**

CT images (in .dicom format) were imported into the 3D Slicer Computer Aided Design (CAD) software [105]. To find the best display of the mandible, brightness and contrast were adjusted manually on the CT images, which were then loaded into 3D Slicer to create a 3D model, by combining the slices together [106]. Segmentation of the mandibular bone was completed manually using the “*Threshold*” command of the 3D Slicer Segmentation module. After the generation of the initial 3D model, the “*Scissor*” and “*Island*” tools were used to eliminate noise (i.e., excessive bone, small islands) from the model. The “*Smoothing*” command with the median smoothing option—which removed small extrusions and filled small gaps, while keeping smooth contours mostly unchanged—was used to eliminate roughness on the surface of the 3D model [106]. The segmentation of the mandible was finalized by the elimination of the residual metal support by the “*Scissor*” tool. To generate the cortical (compact) bone section, the “*Hollow*” command was used to create a new segment—which was a replica of the mandibular surface—at a thickness of 2.5 mm, with the assumption that the cortical bone layer thickness was regular. The trabecular (cancellous) bone section was simulated by subtracting the cortical bone segment from the mandible.

The 3D geometry of the cylindrical implants was constructed using the same patient’s CT images, who received four implants in both the maxilla and the mandible, according to the SmartGuide<sup>®</sup> protocol (iRES<sup>®</sup>, Mendrisio, Switzerland) [107]. The two anterior implants

(MultiNeO™ with a Conical Standard (CS) implant-abutment connection platform, Alpha-Bio Tec Ltd., Petah Tikva, Israel) were threaded, with angled multi-unit abutments (Alpha-Bio Tec Ltd., Petah Tikva, Israel; 17°/2.5 mm and 30°/2.5 mm, respectively) and dimensions of 4.2 × 11.5 mm and 3.75 × 13 mm (diameter and length), respectively, were placed straight and parallel to each other. Two distally tilted implants (MultiNeO™ CS, Alpha-Bio Tec Ltd., Petah Tikva, Israel; the implants were threaded with a diameter and length of 4.2 × 11.5 mm) with angled multi-unit abutments (Alpha-Bio Tec Ltd., Petah Tikva, Israel; 17°/2.5 mm) were placed in the posterior region of the mandible [108]. The distance between the anterior two implants in the mandible was 15.5 mm, while the distance between the anterior and posterior implants was 11.0 mm and 9.16 mm, respectively. Steps to generate the 3D view of the implants were similar to those described for the mandible, their positioning inside the mandible was identical to the source material. The resulting CAD models were recorded in “.step” and “.iges” formats, which could be imported into the ANSYS SpaceClaim software (ANSYS 19.1, Canonsburg, PA, USA) to create the solid body mesh of the implants and mandible components [109].

## 2. C. Meshing, boundary conditions

SOLID187 (a 10-node, higher order 3D element with quadratic displacement behavior, ideal for modeling irregular meshes) and CONTA174 (an 8-node 3D element used to model contact and sliding between surfaces) elements were used to generate the mesh of the mandible and the implants using ANSYS SpaceClaim [110,111]. Element size was adjusted to be finer at the implants and the contact surfaces with the mandible bone, on the other hand, the mesh was coarser at the rest of the mandible body. The number of elements and nodes of the models were 569,588 and 1,430,889, respectively. A simplified denture was included in the simulations with a metallic base and applied with a realistic geometry. The denture was assumed to be a horseshoe-shaped curved cylinder, with a diameter of 2 mm, running about 2 mm over the mandible surface, which was created by the “*Spline*” (used to create a curved line), “*Pull*” (used to generate volume elements from surface elements, or surface elements from line elements), and “*Fill*” (used to convert the object into a solid body) commands of ANSYS SpaceClaim (**Figure 6**). After checking for vertical alignment with the implants, the denture was integrated into the implant mesh, creating a single facet

interpenetrating the mandible, which was then subtracted from the model of the cortical and trabecular bone.

Following the automatic and manual geometric repair of meshing errors, the facet mesh was converted into solid body mesh (**Figure 7**). As the present study focused on the functional behavior of the implants inside of the mandibular bone, the boundary conditions were fixed, the movements of the temporo-mandibular joint were neglected, and a fixed support was applied close to the vicinity of the joint [112]. In order to keep the number of elements at a reasonable level, the model considers the wire supporting the prosthesis, instead of the entire prosthesis, as the medium transmitting the masticatory loads to the implant. As the stiffness of the entire prosthesis is mainly provided by the Ti wire mentioned above, in our analyses, the distribution of the masticatory forces on the denture and the wire are assumed to be similar. For similar reasons, to reduce the complexity of the model, the geometry of the implants obtained from the post-implantation CT image of the same patient was used.

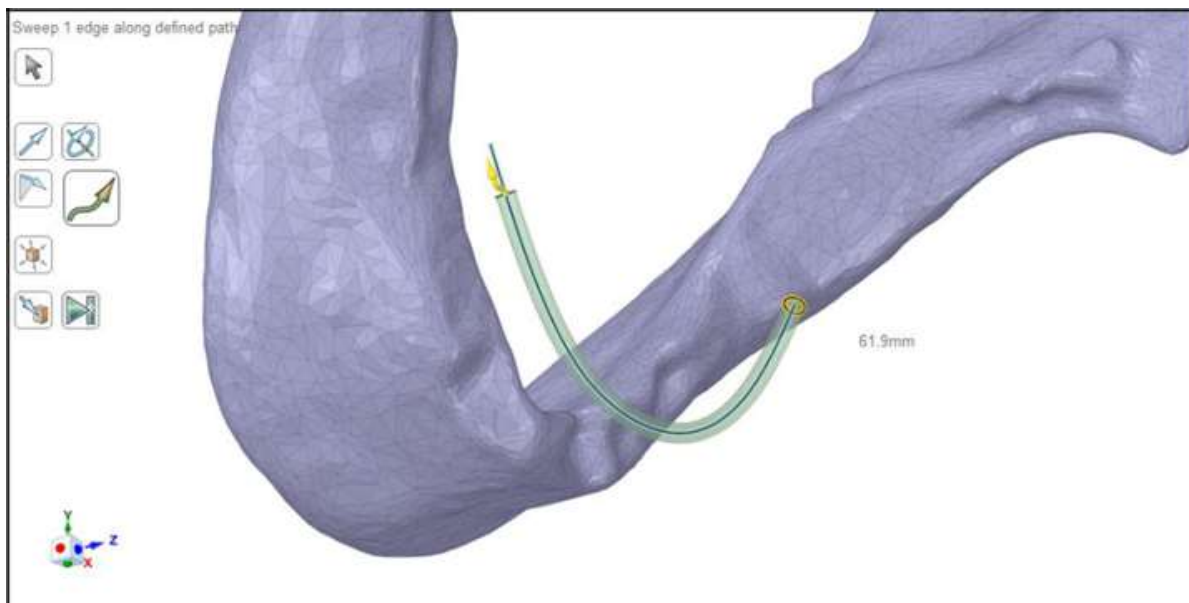


**Figure 6.** Creation of the simplified denture during the modeling process

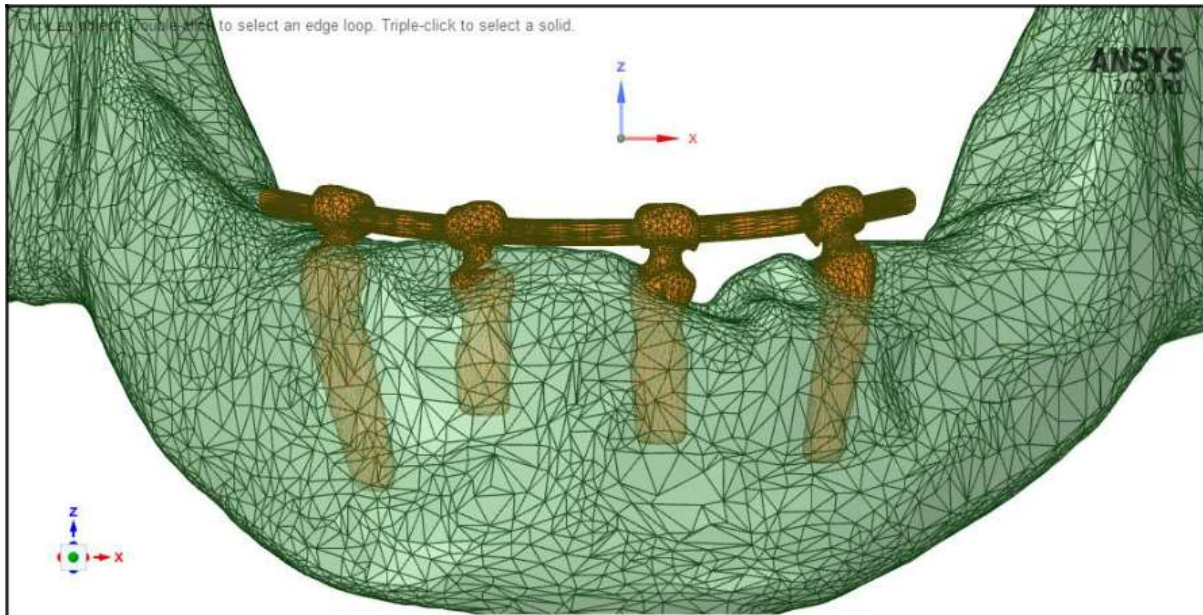


**Figure 7.** Finite element mesh of the implant-denture and the mandible models

## 2. D. Material Properties

The peri-implant bone in the model was made up of cortical and trabecular bones, with a transition region that extends past the implant's outermost edge. The interface between the bone and the implant was set as bonded; osseointegration was assumed to be 100% [113]. Based on previous literature findings, the material properties, which define the physical properties of the modelled structures, were entered into the software, according to the values presented in **Table 1**. The physical features of the peri-implant bone were modelled to reflect the features of *type II* bone, according to the Lekholm and Zarb classification [39]. All parts in the model were accepted as homogeneous, isotropic, and linear elastic [114]. With the aim of simulating framework material changes, two sets of simulations were performed: *i*) in the first set of simulations (denoted as **S1**), the denture body and the implant bodies were assigned the same material (Ti, i.e., TiAl6V4), *ii*) in the second set of simulations (denoted as **S2**), different material properties were assigned to the implant bodies (TiAl6V4) and the denture bodies (a Co-Cr alloy in 70–30% ratio, i.e., CO-CR-01-P.30CR).

**Table 1.** Material properties used in the FEA

<b>Materials</b>	<b>Density <math>\rho</math> [g/cm<sup>3</sup>]</b>	<b>Young's Modulus E [GPa]</b>	<b>Poisson's Ratio <math>\nu</math></b>
<b>Titanium</b> [115,116] <b>(TiAl6V4)</b>	4.51	102	0.36
<b>Cobalt–Chromium</b> [115,116] <b>(CO–CR-01-P.30CR)</b>	10	210	0.29
<b>Cortical bone</b> [117,118]	1.6	15	0.3
<b>Trabecular bone</b> [117,118]	0.2	0.096	0.3

## 2. E. Loading, occlusal cases

The finite-element simulation to model the state of the peri-implant bone and the stress distribution was carried out using the ANSYS Workbench software (ANSYS 2020 R1, Canonsburg, PA, USA). As a part of our study, the effects of different occlusion settings – i.e., the appropriate location of the masticatory force – was assessed. For the sake of comparability, the vertical components of the masticatory forces were included in the calculations; these were set at 300 N to be exerted on the denture in four different simulated load cases [119], as seen in **Figure 8** and described below:

- **Load case 1 (LC1):** the distributed masticatory force that covers the entire surface of the denture
- **Load case 2 (LC2):** similar to the LC1 case, but the force excludes the cantilevers of the denture stretching behind the terminal implants
- **Load case 3 (LC3):** the masticatory force was exerted on the denture at the premolar region, at the area extending between the front and side implants
- **Load case 4 (LC4):** similar to the LC3 case, a nonsymmetrical distributed force, but applied on only one side of the denture

In the case of linear analysis, it is assumed that the relationship between the force acting on the examined body and the deformation caused by the mentioned force is linear [120]. In subsequent analyses, positive (+) values represent tension, while negative (-) values represent compression stress. Stress outputs for the mandible from the ANSYS Workbench were taken as *maximum principal stress* (or first principal stress/tensile stress,  $[P_{\max}]$ , representing the strongest tensile stress at the point of interest), *minimum principal stress* (or third principal stress/compressive stress,  $[P_{\min}]$ , representing the strongest compressive stress), and equivalent stress (or von Mises stress,  $[P_{\text{eqv}}]$ , representing the stress around the implant, i.e., where the load is transferred to the bones) [121].

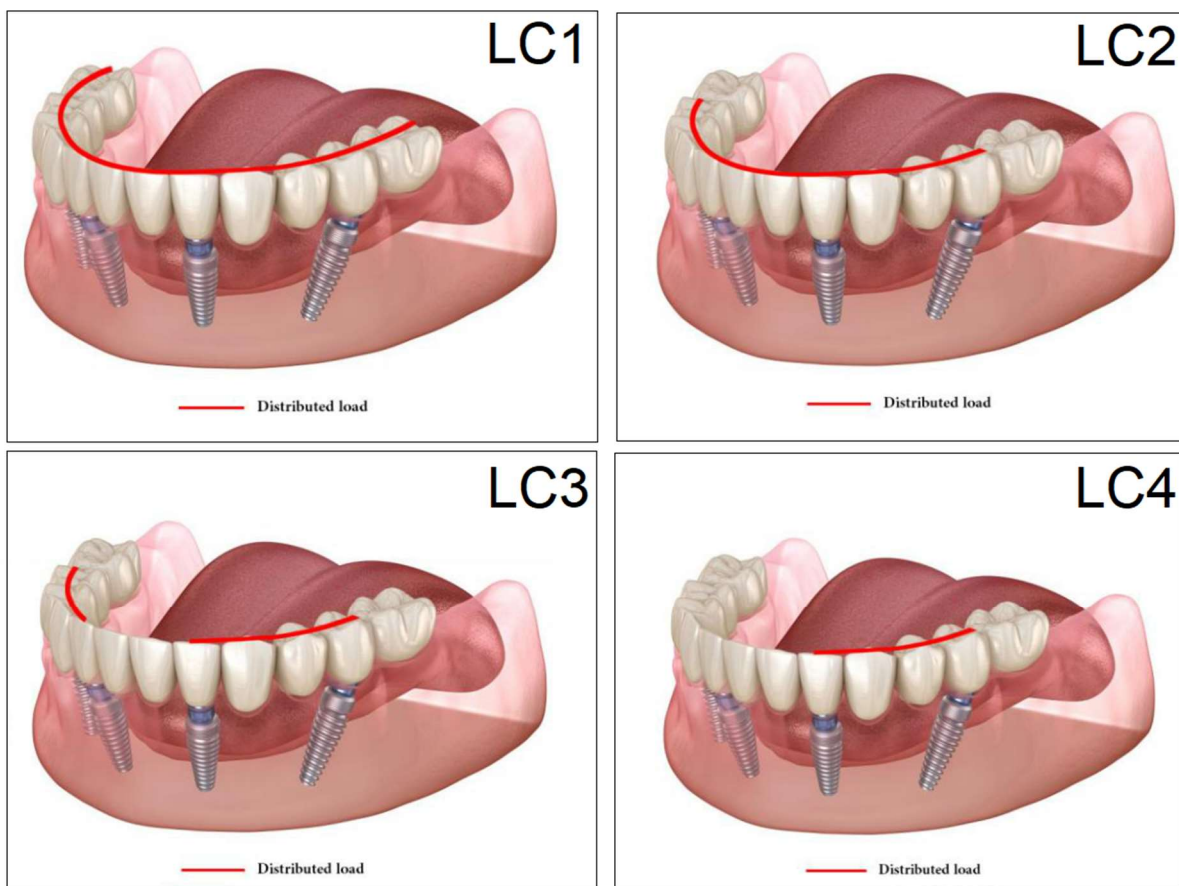


**Figure 8.** Load cases (LC1–4) used in the study.

The **red line** represents the distributed load applied in the FEA.

### **3. Ethical considerations**

The studies 1 (clinical study) and 2 (FEA) were conducted in accordance with the Declaration of Helsinki and national and institutional ethical standards. Ethical approval for the study protocols were obtained from the Human Institutional and Regional Biomedical Research Ethics Committee, University of Szeged (registration number: 158/2021-SZTE [5035]). All participants (including were informed of the nature and aims of the study and the data collected; all participants of the study signed an informed consent form.

### **4. Statistical analysis**

#### **4. 1. Clinical study**

Descriptive statistics (including means  $\pm$  SEM (standard error of the mean), ranges and percentages) was performed using Microsoft Excel 365 (Microsoft Corp., Redmond, WA, USA). Statistical analyses were carried out by the SPSS v. 22.0 (IBM Corp., Endicott, NY, USA); the normality of variables was tested using the Shapiro–Wilk test; inferential statistics were performed using independent-sample t-test, one-way analysis of variance (ANOVA) with Tukey's *post hoc* test and Pearson's correlation ( $r$ ) coefficient.  $p$  values  $< 0.05$  were considered statistically significant.

#### **4. 2. Finite element analysis (FEA)**

The results of FEA do not have variance, therefore there was no need to perform statistical analysis.

## VI. RESULTS

### 1. Clinical study

During the study period,  $n = 36$  patients ( $n = 24$  [66.7%] males and  $n = 12$  [33.3%] females) with complete records of periapical radiographs underwent implant placement using the Ao4 concept at the Faculty of Dentistry, University of Szeged, and have been rehabilitated. The mean age of patients at the time of fixture installation was  $58.75 \pm 13.71$  years (range: 19–90 years). In sum,  $n = 144$  and  $n = 144$  implants (Nobel Biocare) were placed in the maxilla and mandibles of patients, respectively, therefore the analysis of  $n = 288$  individual implant data was carried out. During the 42-month study period, no implants have failed, resulting in 100% overall survival rate (100% for T<sub>0</sub>, T<sub>1</sub>, T<sub>2</sub> and T<sub>3</sub>, respectively). No patients ( $n = 0$ ) were lost to follow-up at either time points (i.e. at 3 months, at 18 months, at 30 months, and at 42 months post-restoration, respectively), all patients complied with the set timetables.

The radiographic mean MBL at baseline (T<sub>0</sub>) were  $0.181 \pm 0.011$  mm (mean  $\pm$  SEM; maxilla ( $n = 144$ ):  $0.178 \pm 0.017$  mm vs. mandible ( $n = 144$ ):  $0.184 \pm 0.015$  mm;  $p > 0.05$ ); in the subsequent analyses, marginal bone level changes ( $\Delta$ BL) at T<sub>1</sub>, T<sub>2</sub>, and T<sub>3</sub> follow-up times were compared to these initial values. Levels of marginal bone loss according to different correlates are presented in **Table 2.** (maxilla vs. mandible), **Table 3.** (axial vs. posterior implants) and **Table 4.** (MA vs. DA), respectively; in addition, the extent of bone loss on an individual implant-level is represented in **Table 5.** and **Table 6.** The mean MBL rate after the 1.5-year follow-up was  $0.558 \pm 0.029$  mm and  $0.484 \pm 0.024$  mm, while by the 3.5-year mark, MBL rate was  $0.770 \pm 0.029$  mm and  $0.713 \pm 0.026$  mm regarding the implants placed in the maxilla and mandibular bone, respectively; bone-level changes were significant over time ( $p = 0.035$  and  $p = 0.033$ , respectively), while the alterations observed around the maxilla and mandibular implants did not differ significantly ( $p > 0.05$ ) (**Table 2.**).

Measured bone loss was significantly higher in posterior implants throughout the follow-up period (**Table 3.**); in addition, bone-level changes were significant over time ( $p = 0.041$  and  $p = 0.039$ ). No significant differences were observed in the measured bone-level changes on the MA and DA aspects of the implants throughout the study period ( $p > 0.05$  in all cases; **Table 4.**), while bone loss increased consistently during the follow-up periods in both the MA ( $p = 0.029$ ) and DA ( $p = 0.035$ ) aspects.



**Table 2.** Marginal bone-level changes around implants located in the maxilla and mandible during the 42-month study period

<b>Marginal bone level changes (<math>\Delta</math>BL) (mm <math>\pm</math> SEM)</b>			
<b>Follow-up</b>	<b>Maxilla (<math>n = 144</math>)</b>	<b>Mandible (<math>n = 144</math>)</b>	<b><math>p</math>-value (between groups)**</b>
<b>T<sub>1</sub></b>	-0.558 $\pm$ 0.029 <sup>a</sup>	-0.484 $\pm$ 0.024 <sup>a</sup>	$p > 0.05$
<b>T<sub>2</sub></b>	-0.747 $\pm$ 0.030 <sup>b</sup>	-0.678 $\pm$ 0.036 <sup>b</sup>	$p > 0.05$
<b>T<sub>3</sub></b>	-0.770 $\pm$ 0.029 <sup>b</sup>	-0.713 $\pm$ 0.026 <sup>b</sup>	$p > 0.05$
<b><math>p</math>-value (between follow-ups)*</b>	<b><math>p = 0.035</math></b>	<b><math>p = 0.033</math></b>	

\*based on ANOVA analysis, significant differences ( $p < 0.05$ ) among groups (as demonstrated by post-hoc tests) are indicated by different superscript letters (*a* and *b*);

\*\*based on independent-sample t-test;  $p$ -values below 0.05 are shown in **boldface**

**Table 3.** Marginal bone-level changes around axial and tilted implants during the 42-month study period

<b>Marginal bone level changes (<math>\Delta</math>BL) (mm <math>\pm</math> SEM)</b>			
<b>Follow-up</b>	<b>Axial (anterior) (<math>n = 144</math>)</b>	<b>Tilted (posterior) (<math>n = 144</math>)</b>	<b><math>p</math>-value (between groups)**</b>
<b>T<sub>1</sub></b>	-0.405 $\pm$ 0.021 <sup>a</sup>	-0.637 $\pm$ 0.027 <sup>a</sup>	<b><math>p = 0.008</math></b>
<b>T<sub>2</sub></b>	-0.592 $\pm$ 0.024 <sup>b</sup>	-0.676 $\pm$ 0.028 <sup>a</sup>	<b><math>p = 0.048</math></b>
<b>T<sub>3</sub></b>	-0.606 $\pm$ 0.022 <sup>b</sup>	-0.833 $\pm$ 0.029 <sup>b</sup>	<b><math>p = 0.002</math></b>
<b><math>p</math>-value (between follow-ups)*</b>	<b><math>p = 0.041</math></b>	<b><math>p = 0.039</math></b>	

\*based on ANOVA analysis, significant differences ( $p < 0.05$ ) among groups (as demonstrated by post-hoc tests) are indicated by different superscript letters (*a* and *b*);

\*\*based on independent-sample t-test;  $p$ -values below 0.05 are shown in **boldface**

During subgroup analysis, a tendency was shown for higher bone loss rates for both MA (T1:  $-0.586 \pm 0.043$ , T2:  $-0.716 \pm 0.046$ , and T3:  $-0.767 \pm 0.042$ ) and DA (T1:  $-0.545 \pm 0.051$ , T2:  $-0.757 \pm 0.063$ , and T3:  $-0.825 \pm 0.060$ ), however these differences were not statistically significant ( $p > 0.05$ ) (**Table 4.**).

**Table 4.** Marginal bone-level changes on the mesio- (MA) and disto-approximal (DA) aspects of the implants during the 42-month study period

<b>Marginal bone level changes (<math>\Delta</math>BL) (mm <math>\pm</math> SEM)</b>			
<b>Follow-up</b>	<b>Mesio-approximal (MA) aspect (<math>n = 144</math>)</b>	<b>Disto-approximal (DA) aspect (<math>n = 144</math>)</b>	<b><math>p</math>-value (between groups)**</b>
<b>T1</b>	$-0.519 \pm 0.024^a$	$-0.522 \pm 0.029^a$	$p > 0.05$
<b>T2</b>	$-0.697 \pm 0.025^b$	$-0.728 \pm 0.032^b$	$p > 0.05$
<b>T3</b>	$-0.729 \pm 0.024^b$	$-0.793 \pm 0.029^b$	$p > 0.05$
<b><math>p</math>-value (between follow-ups)*</b>	<b><math>p = 0.029</math></b>	<b><math>p = 0.035</math></b>	

\*based on ANOVA analysis, significant differences ( $p < 0.05$ ) among groups (as demonstrated by post-hoc tests) are indicated by different superscript letters (*a* and *b*);

\*\*based on independent-sample t-test;  $p$ -values below 0.05 are shown in **boldface**

The degree of bone resorption was also assessed on an individual implant-level separately in the maxilla and mandible, presented in the **Tables 5.** and **6.** In the case of the maxilla, higher bone loss was observed for the teeth 14DA (with  $-1.001 \pm 0.101$  mm at T<sub>3</sub>, range:  $-0.3$ - $1.7$  mm) and 24DA (with  $-1.066 \pm 0.081$  mm at T<sub>3</sub>, range:  $-0.6$ - $1.8$  mm), which were significantly higher than the values compared to most other teeth ( $p < 0.05$ ) (**Table 5.**). Highest rate of bone loss in the mandible were shown for the teeth 34DA (with  $-0.872 \pm 0.044$  mm at T<sub>3</sub>, range:  $-0.6$ - $1.3$  mm) and 44MA (with  $-0.789 \pm 0.066$  mm at T<sub>3</sub>, range:  $-0.4$ - $1.5$  mm); bone resorption at 34DA was significantly higher rates observed for other teeth ( $p < 0.05$ ), with the exception of 32MA and 44MA (**Table 6.**). Significantly increasing levels of bone loss were seen in all respective cases, both for maxillar and mandibular implants ( $p < 0.05$ ).

Furthermore, it was tested whether the age of the patients was a relevant correlate regarding bone resorption levels; overall, we did not find any significant linear correlation ( $r < 0.2$ ,  $p > 0.05$ ) between the degree of bone resorption and age. However, in case of 12MA in the maxilla, a positive (but non-significant) tendency could be observed.

**Table 5.** Marginal bone-level changes around individual implants in the maxilla during the 42-month study period

Marginal bone level changes ( $\Delta$ BL) (mm $\pm$ SEM)								
Follow-up	12DA ( <i>n</i> = 18)	12MA ( <i>n</i> = 18)	14DA ( <i>n</i> = 18)	14MA ( <i>n</i> = 18)	22DA ( <i>n</i> = 18)	22MA ( <i>n</i> = 18)	24DA ( <i>n</i> = 18)	24MA ( <i>n</i> = 18)
<b>T<sub>1</sub></b>	-0.378 $\pm$ 0.051 <sup>a</sup>	-0.489 $\pm$ 0.063 <sup>a</sup>	-0.728 $\pm$ 0.093 <sup>a</sup>	-0.567 $\pm$ 0.074 <sup>a</sup>	-0.361 $\pm$ 0.061 <sup>a</sup>	-0.439 $\pm$ 0.055 <sup>a</sup>	-0.844 $\pm$ 0.095 <sup>a</sup>	-0.538 $\pm$ 0.053 <sup>a</sup>
<b>Range (mm)</b>	-0.0-0.7	-0.0-1.1	-0.2-1.4	-0.0-1.2	-0.0-0.8	-0.0-1.0	-0.4-1.8	-0.0-1.2
<b>T<sub>2</sub></b>	-0.583 $\pm$ 0.042 <sup>b</sup>	-0.661 $\pm$ 0.051 <sup>b</sup>	-0.950 $\pm$ 0.105 <sup>b</sup>	-0.733 $\pm$ 0.072 <sup>b</sup>	-0.489 $\pm$ 0.062 <sup>b</sup>	-0.605 $\pm$ 0.067 <sup>b</sup>	-1.033 $\pm$ 0.087 <sup>b</sup>	-0.722 $\pm$ 0.056 <sup>b</sup>
<b>Range (mm)</b>	-0.3-1.0	-0.1-1.1	-0.3-1.7	-0.2-1.2	-0.1-0.8	-0.4-1.4	-0.6-1.8	-0.1-1.3
<b>T<sub>3</sub></b>	-0.711 $\pm$ 0.061 <sup>c</sup>	-0.717 $\pm$ 0.054 <sup>b</sup>	-1.001 $\pm$ 0.101 <sup>b</sup>	-0.772 $\pm$ 0.074 <sup>b</sup>	-0.553 $\pm$ 0.053 <sup>b</sup>	-0.667 $\pm$ 0.065 <sup>b</sup>	-1.066 $\pm$ 0.081 <sup>b</sup>	-0.789 $\pm$ 0.066 <sup>b</sup>
<b>Range (mm)</b>	-0.3-1.1	-0.2-1.1	-0.3-1.7	-0.3-1.5	-0.1-0.8	-0.4-1.4	-0.6-1.8	-0.1-1.3
<b>Statistical significance<sup>1</sup></b>	*	*	*	*	*	*	*	*

<sup>1</sup>based on ANOVA analyses, level of significance: \* denotes  $p < 0.05$ ; significant differences ( $p < 0.05$ ) among groups (as demonstrated by post-hoc tests) are indicated by different superscript letters (*a*, *b* and *c*)

**Table 6.** Marginal bone level changes around individual implants in the mandible during the 42-month study period

<b>Marginal bone level changes (<math>\Delta</math>BL) (mm <math>\pm</math> SEM)</b>								
<b>Follow-up</b>	<b>32DA (n = 18)</b>	<b>32MA (n = 18)</b>	<b>34DA (n = 18)</b>	<b>34MA (n = 18)</b>	<b>42DA (n = 18)</b>	<b>42MA (n = 18)</b>	<b>44DA (n = 18)</b>	<b>44MA (n = 18)</b>
<b>T<sub>1</sub></b>	-0.256 $\pm$ 0.051 <sup>a</sup>	-0.550 $\pm$ 0.078 <sup>a</sup>	-0.622 $\pm$ 0.052 <sup>a</sup>	-0.494 $\pm$ 0.058 <sup>a</sup>	-0.344 $\pm$ 0.054 <sup>a</sup>	-0.422 $\pm$ 0.066 <sup>a</sup>	-0.344 $\pm$ 0.054 <sup>a</sup>	-0.538 $\pm$ 0.053 <sup>a</sup>
<b>Range (mm)</b>	-0-0.6	-0.1-1.1	-0.2-1.0	-0.1-0.9	-0-0.8	-0.1-1.0	-0.2-1.0	-0.1-1.4
<b>T<sub>2</sub></b>	-0.388 $\pm$ 0.053 <sup>b</sup>	-0.689 $\pm$ 0.082 <sup>b</sup>	-0.827 $\pm$ 0.053 <sup>b</sup>	-0.678 $\pm$ 0.063 <sup>b</sup>	-0.494 $\pm$ 0.046 <sup>b</sup>	-0.627 $\pm$ 0.062 <sup>b</sup>	-0.494 $\pm$ 0.046 <sup>b</sup>	-0.722 $\pm$ 0.056 <sup>b</sup>
<b>Range (mm)</b>	-0.1-0.7	-0.1-1.4	-0.4-1.3	-0.2-1.0	-0.1-0.8	-0.2-1.2	-0.3-1.1	-0.3-1.4
<b>T<sub>3</sub></b>	-0.444 $\pm$ 0.051 <sup>c</sup>	-0.722 $\pm$ 0.081 <sup>b</sup>	-0.872 $\pm$ 0.044 <sup>b</sup>	-0.717 $\pm$ 0.059 <sup>b</sup>	-0.555 $\pm$ 0.051 <sup>b</sup>	-0.694 $\pm$ 0.051 <sup>b</sup>	-0.555 $\pm$ 0.051 <sup>b</sup>	-0.789 $\pm$ 0.066 <sup>b</sup>
<b>Range (mm)</b>	-0.1-0.8	-0.1-1.4	-0.6-1.3	-0.3-1.1	-0.2-0.9	-0.4-1.1	-0.3-1.3	-0.4-1.5
<b>Statistical significance<sup>1</sup></b>	*	*	*	*	*	*	*	*

<sup>1</sup>based on ANOVA analyses, level of significance: \* denotes  $p < 0.05$ ; significant differences ( $p < 0.05$ ) among groups (as demonstrated by post-hoc tests) are indicated by different superscript letters (*a*, *b* and *c*)

## 2. Finite element analysis (FEA)

During our analyses, stress results associated with the four sets of masticatory load cases (i.e. LC1–LC4), corresponding to different implant-denture material configurations (i.e. S1 and S2) were expressed in MPa, as the maximum principal stress ( $P_{\max}$ ; peak tension stress), minimum principal stress ( $P_{\min}$ ; peak compressive stress), and equivalent stress ( $P_{\text{eqv}}$ ) values in the cortical and the trabecular bone. Results of the stress values in mandibular bone structure are shown in **Table 7**. Furthermore, stress heatmaps with range scales (shown in different colors) for maximum and minimum principal stresses are demonstrated for each load case for the cortical and trabecular bodies, respectively; as representative figures, the stress heatmaps for the S1 LC1 and S2 LC1 cases for the cortical bone segment and mandibular bone segment of the mandible are shown in **Figures 9-10**. and **Figures 11-12.**, respectively. On the other hand, the stress heatmaps for the S1 LC2 and S2 LC2 cases for the cortical bone segment and mandibular bone segment are shown in **Appendix 1-2**. and **Appendix 3-4.**, for the S1 LC3 and S2 LC3 cases for the cortical bone segment and mandibular bone segment, they are shown in **Appendix 5-6**. and **Appendix 7-8.**, while for the S1 LC4 and S2 LC4 cases for the cortical bone segment and mandibular bone segment, they are presented in **Appendix 9-10**. and **Appendix 11-12.**, respectively. For more visibility, implants were not included in these stress maps.

Overall, based on the stress maps for principal stress distribution, the highest stress values were always seen at the implant–bone interface. Compressive stress values were 1.5–2.5-times higher and 1.1–1.4-times higher than tensile stress values in the cortical bone and trabecular bone, respectively (**Table 7**). The highest maximum principal stress values were observed for the load case LC2, both regarding the cortical bone (S1  $P_{\max}$ : 89.57 MPa, S2  $P_{\max}$ : 102.98 MPa) and the trabecular bone (S1  $P_{\max}$ : 3.03 MPa, S2  $P_{\max}$ : 2.62 MPa). The highest tensile stress for LC2 was seen near the top of the third implant for the cortical bone, and near the top of the second implant for the trabecular bone. The highest minimum principal stress values for the cortical bone were seen in the S2 LC2 ( $P_{\min}$ : –265.35 MPa) and S1 LC3 cases ( $P_{\min}$ : –172.30 MPa), while in the case of the trabecular bone, these were seen in the case of LC4 (S1  $P_{\min}$ : –3.49 MPa, S2  $P_{\min}$ : –3.52 MPa), respectively, which were seen near the top of the second implant. Nevertheless, all other load cases (including LC3 and LC4) showed higher  $P_{\max}$  and  $P_{\min}$  values for both simulations and bone segments, compared to LC1, where the force covers the entire surface of the denture, including the extension surface

(cortical bone: S1  $P_{\max}$ : 76.39 MPa, S2  $P_{\max}$ : 88.51 MPa; S1  $P_{\min}$ : -115.30 MPa, S2  $P_{\min}$ : -222.76 MPa; trabecular bone: S1  $P_{\max}$ : 2.49 MPa, S2  $P_{\max}$ : 2.24 MPa; S1  $P_{\min}$ : -2.81 MPa, S2  $P_{\min}$ : -2.89 MPa). Peak equivalent stress values were highest in the case of LC1 (166.40 MPa) and LC2 (279.69 MPa) for S1 and S2, respectively; the lowest equivalent stress was observed at LC4 (142.27 MPa) for S1, and LC1 (244.92 MPa) for S2 (**Table 7**).

**Table 7.** Peak tension ( $P_{\max}$ ), compression ( $P_{\min}$ ) stress, and equivalent stress ( $P_{\text{eqv}}$ ) values in the different parts of the mandibular bone structure [MPa].

		LC1		LC2		LC3		LC4	
		S1	S2	S1	S2	S1	S2	S1	S2
<b>Cortical bone</b>	$P_{\max}$ [MPa]	<i>76.39</i>	<i>88.51</i>	<b>89.57</b>	<b>102.98</b>	85.63	95.48	81.02	93.15
	$P_{\min}$ [MPa]	<i>-115.30</i>	<i>-222.76</i>	-136.4	<b>-265.35</b>	<b>-172.30</b>	-252.61	-125.20	-235.32
<b>Trabecular bone</b>	$P_{\max}$ [MPa]	<i>2.49</i>	<i>2.24</i>	<b>3.03</b>	<b>2.62</b>	2.95	2.52	2.92	2.59
	$P_{\min}$ [MPa]	<i>-2.81</i>	<i>-2.89</i>	-3.34	-3.38	-3.25	-3.25	<b>-3.49</b>	<b>-3.52</b>
$P_{\text{eqv}}$ [MPa]		<b>166.40</b>	<i>244.92</i>	166.36	<b>279.69</b>	164.36	265.58	<i>142.27</i>	260.77

The values in *italics* represent the lowest, while values in **boldface** represent the highest tension stress ( $P_{\max}$ ), compression stress ( $P_{\min}$ ), and equivalent stress ( $P_{\text{eqv}}$ ) values in each case; **LC1–LC4**: load case 1–4; **S1**: material assigned for denture body and implant bodies is TiAl6V4; **S2**: material assigned for implant bodies was TiAl6V4, while this was a Co-Cr alloy for the denture body; **MPa**: megapascal.

Peak maximum principal stress values in the cortical bone were 15.87%, 14.97%, 11.50%, and 14.97% higher in the case of S2, for the LC1, LC2, LC3, and LC4 load cases, respectively. In light of this, peak minimum principal stress values in the cortical bone were 93.20%, 94.54%, 46.61%, and 87.96% higher in the case of S2, for the LC1, LC2, LC3, and LC4 load cases, respectively. Peak maximum principal stress values in the trabecular bone were 11.16%, 15.65%, 15.87%, and 15.87% higher in the case of S1, for the LC1, LC2, LC3, and LC4 load cases, respectively. On the other hand, differences in the peak minimum principal stress values in the trabecular bone were considerably smaller, i.e., 2.85%, 1.20%, 0.0%, and 0.86% higher in the case of S2, for the LC1, LC2, LC3, and LC4 load cases, respectively. Equivalent (von Mises) stress values were higher 47.19%, 68.12%, 61.58%, and 83.29% higher in the case of S2, for the LC1, LC2, LC3, and LC4 load cases, respectively (Table 7).

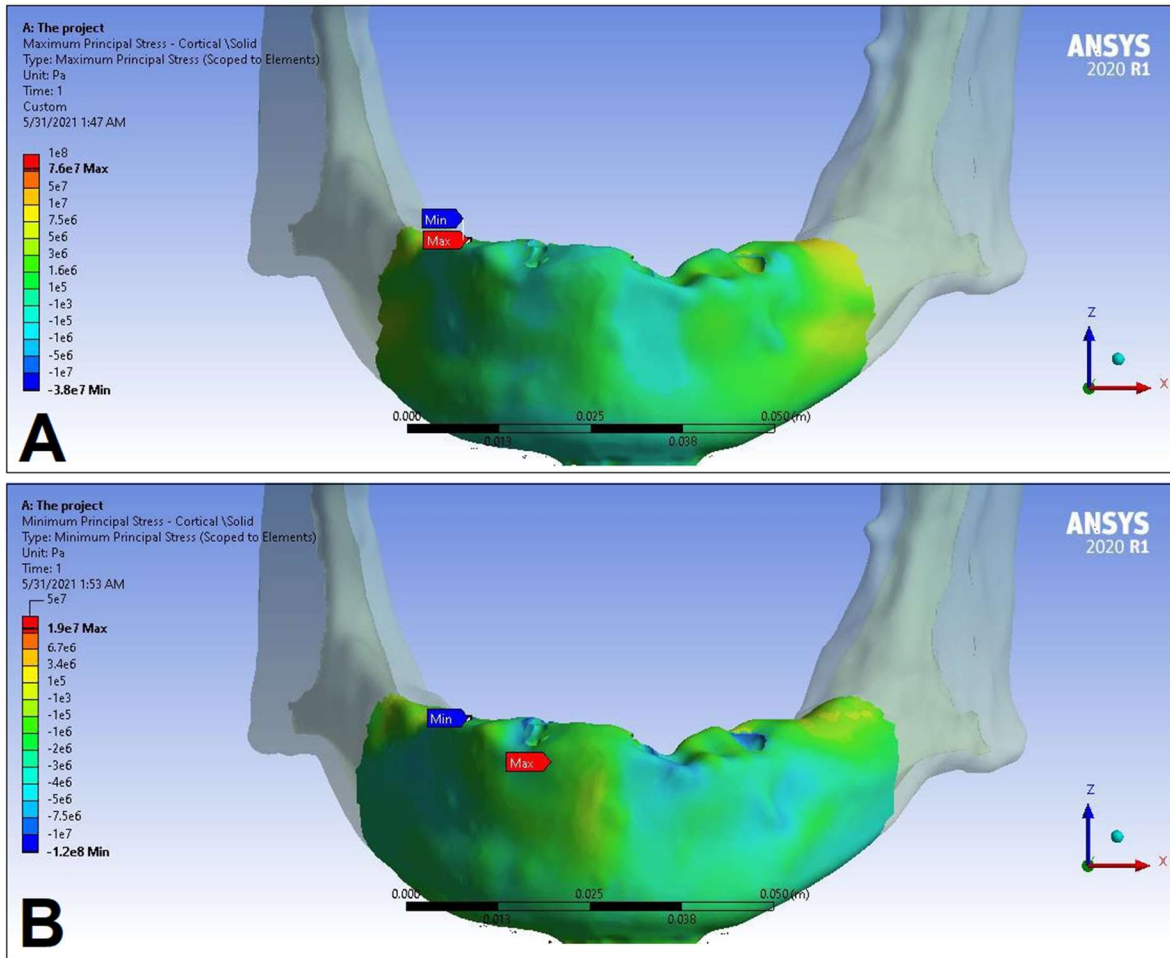


**Figure 9.** Maximum ( $P_{\max}$ , **A**) and minimum ( $P_{\min}$ , **B**) principal stress distributions in the *cortical* bone segment of the mandible for the S1 LC1 simulation case. The heatmap shows the distribution of stresses according to the color scale, while the maximum and minimum values for stresses are also denoted (e.g., 8E3 corresponds to  $8 \times 10^3$ ).



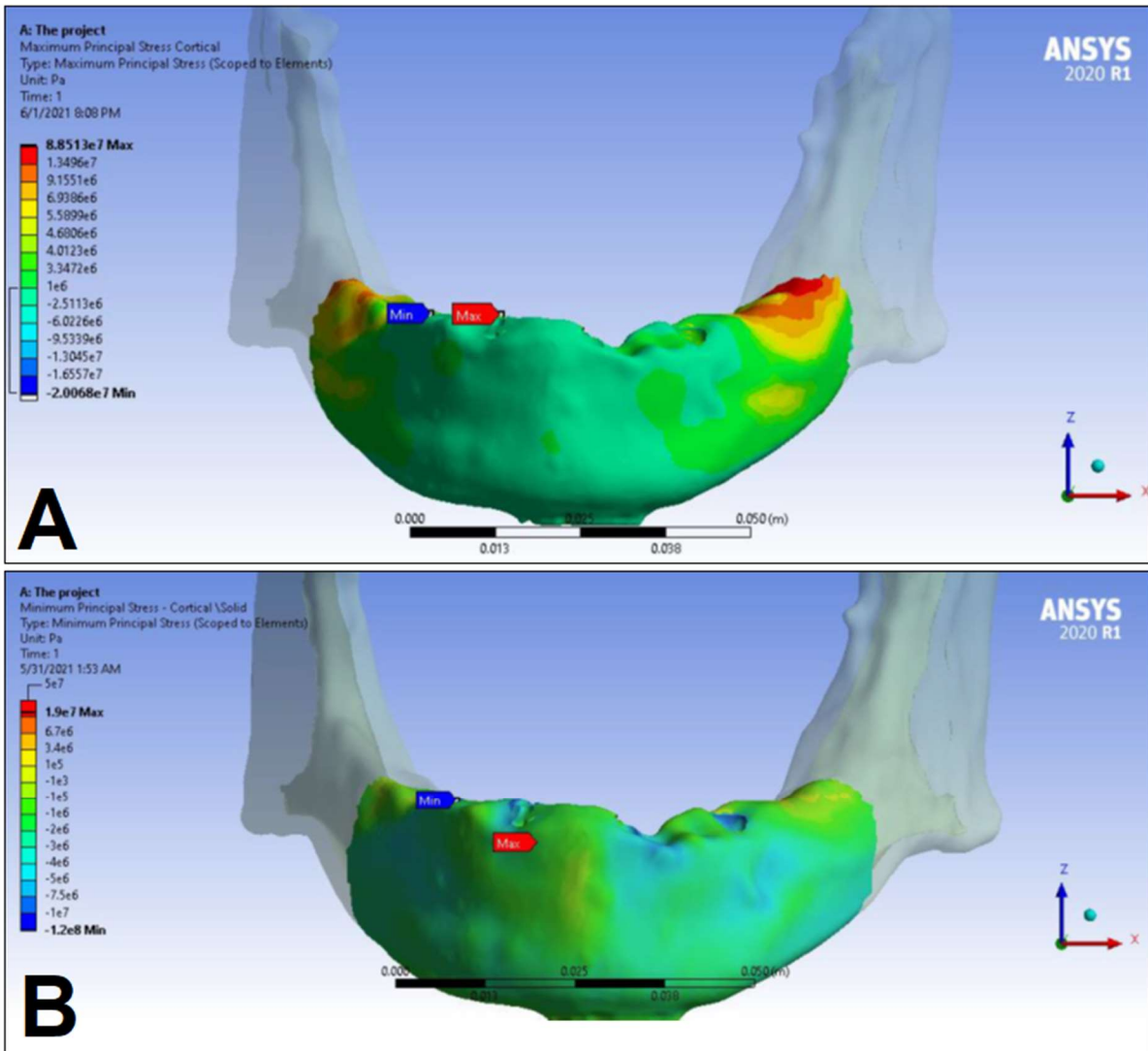


**Figure 10.** Maximum ( $P_{\max}$ , **A**) and minimum ( $P_{\min}$ , **B**) principal stress distributions in the *cortical* bone segment of the mandible for the S2 LC1 simulation case. The heatmap shows the distribution of stresses according to the color scale, while the maximum and minimum values for stresses are also denoted (e.g., 8E3 corresponds to  $8 \times 10^3$ ).

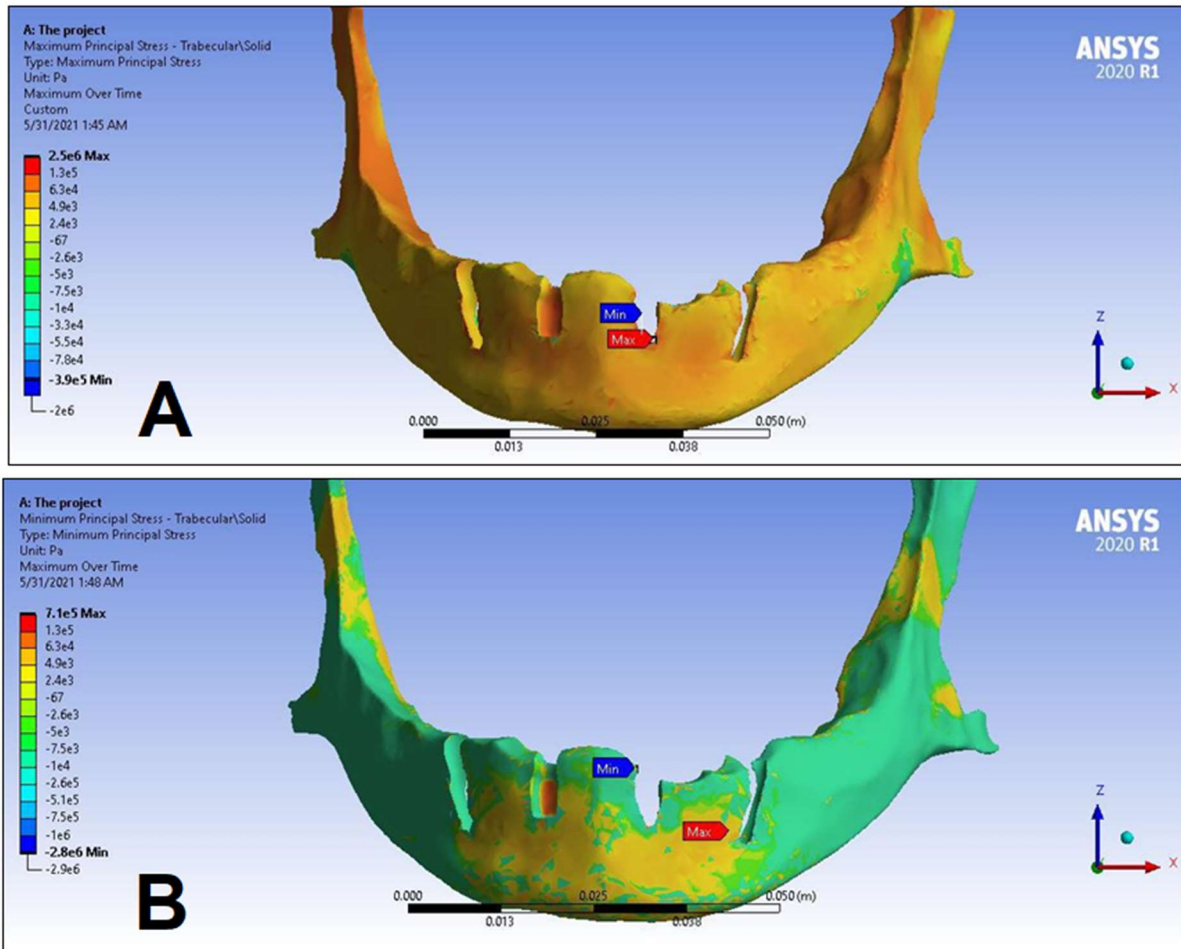


**Figure 11.** Maximum ( $P_{\max}$ , **A**) and minimum ( $P_{\min}$ , **B**) principal stress distributions in the *trabecular* bone segment of the mandible for the S1 LC1 simulation case. The heatmap shows the distribution of stresses according to the color scale, while the maximum and minimum values for stresses are also denoted (e.g., 8E3 corresponds to  $8 \times 10^3$ ).

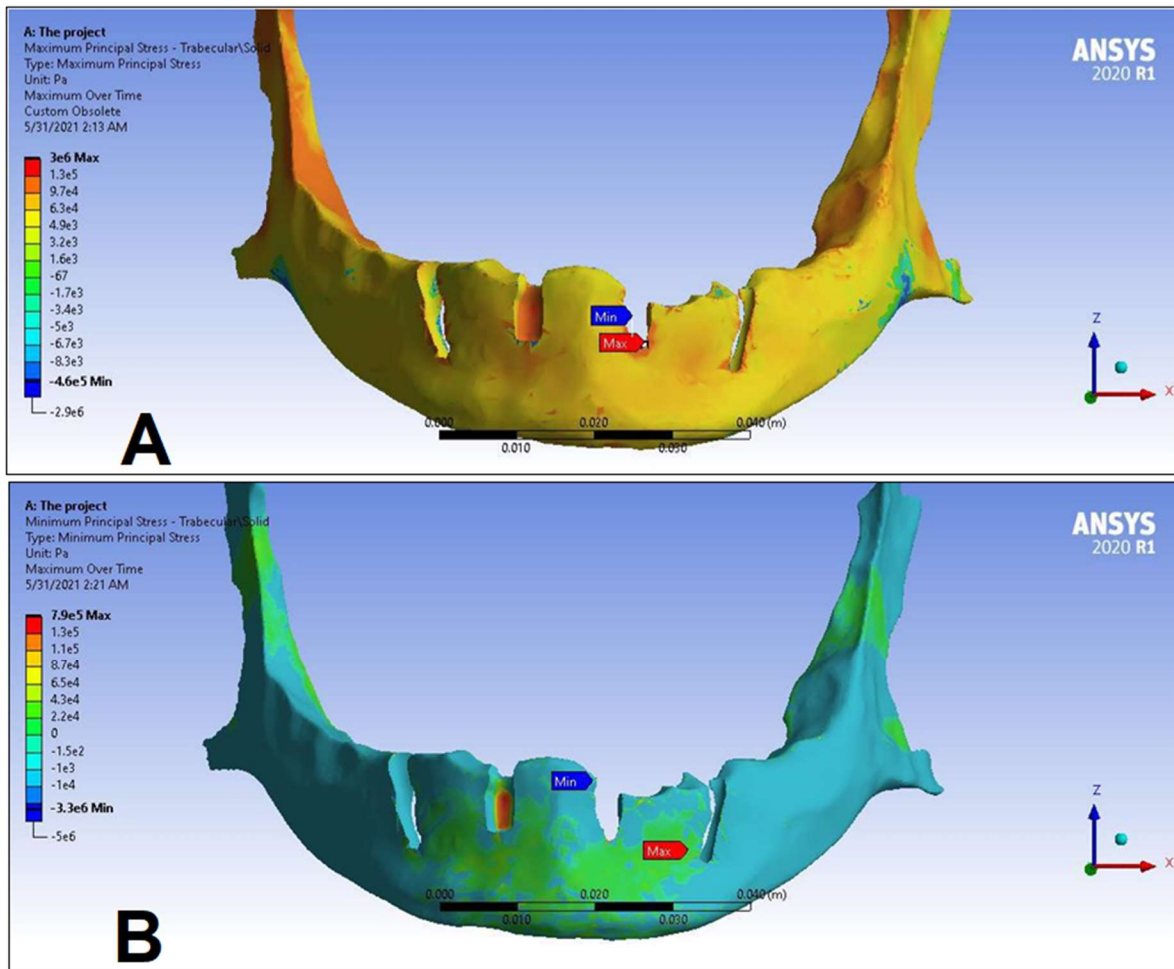


**Figure 12.** Maximum ( $P_{\max}$ , **A**) and minimum ( $P_{\min}$ , **B**) principal stress distributions in the *trabecular* bone segment of the mandible for the S2 LC1 simulation case. The heatmap shows the distribution of stresses according to the color scale, while the maximum and minimum values for stresses are also denoted (e.g., 8E3 corresponds to  $8 \times 10^3$ ).

## VII. DISCUSSION

### 1. Clinical study

The aim of the retrospective clinical study was to provide additional evidence on the clinical outcomes associated with distally tilted implants according to the Ao4 therapeutic concept, and to assess the rates of marginal bone loss as a function of the elapsed time and patient characteristics using radiographic findings. Various procedures preceding implant placement (e.g., impression, drilling, and introduction of tools) may lead to inflammation and consequently, a baseline level of bone resorption will inevitably occur [122]. Additionally, recent studies provide evidence that repeated abutment manipulation, in the case of implants with platform-switching, may lead to detrimental changes in soft and hard tissues (i.e., tissue remodeling as measured by mucosal margins, implant shoulder, apical extension of the long junctional epithelium and most coronal bone-level in contact with the implant) [123]. Thus, on one hand, the use of implants with fixed abutments (i.e. the “*one abutment–one time*” concept) may greatly stabilize peri-implant soft and hard tissues, while immediate implant placement may significantly reduce the initial unavoidable bone loss [124]. Only around two-thirds of patients are completely complication-free following the restoration of the implant-supported fixed prostheses; these complications may include biological adverse events (e.g., peri-implantitis or loss of alveolar bone) and technical complications (screw loosening, retention loss, or fractures in the superstructures), that may lead to implant failure [125-127]. The clinical utility of the Ao4 treatment concept has been demonstrated in numerous clinical studies, showing that this technique is distinguished by a predictable, positive prognosis and high patient satisfaction rates [78,128]. The superiority of this concept is associated with the implementation of an atrophic maxilla or mandible, less complicated surgery and upkeep, and masticatory forces in the satisfactory range [78].

The initial hypotheses for our study were: (i) no differences in peri-implant bone levels among axial and tilted implants during follow-ups, and (ii) no differences in peri-implant bone levels measured at the MA and DA aspects of implants during follow-ups. The 3.5-year-long follow-up period involved thirty-six patients, with an overall implant survival rate of 100%, highlighting the clinical success of the Ao4 concept. High implant survival rates have been consistently reported for this technique; the previously mentioned longitudinal

study of Maló *et al.* and the narrative review of Durkan *et al.* all reported high implant survival rates, with no differences between tilted and axial implants in clinical success rates [77,78]. Based on our MBL at baseline ( $T_0$ ;  $\sim 0.18$  mm) and at the three follow-up points ( $T_1$ ,  $T_2$ , and  $T_3$ ), bone loss showed the kinetics characteristic for a saturation curve, i.e., showing relatively high  $\Delta$ BL values at the first-follow-up, with bone-levels changes “flattening out” the curve. By the third follow-up, mean bone loss in our patients was around 0.7–0.8 mm in both the maxilla and mandible, with specific positions in the maxilla and the mandible disproportionately affected; while a tendency for higher peri-implant bone loss was seen on the DA aspects, no significant differences were shown MA vs. DA aspects during follow-ups. Bone resorption measured on the MA aspects may be mediated by masticatory forces generated on extension surfaces and the negative torque generated by the bucco-lingual forces, which exerts tensile stresses on these surfaces – which were previously verified via FEA studies – which can enhance bone resorption [129].

The literature shows wide variation for MBL rates among studies, which is also considerably influenced by the follow-up period associated with the study. Similar kinetics in bone-loss were observed by Hürzeler *et al.* [130], showing MBL of 1.5 mm in the first year post-implantation, followed by  $0.2 \pm 0.5$  mm in the subsequent years (in a 5-year follow up study), and Widmark *et al.* [131], with MBL of 1.0 mm in the first year post-implantation, followed by 0.2 mm in the subsequent years (with follow-ups ranging between 3–5 years). In a study involving thirty-nine patients, Makary *et al.* assessed the clinical success of an early loading protocol by controlling for thread depth according to the bone density of the implant site. They showed a decrease in Implant Stability Quotient (ISQ) values in the early periods of healing – associated with the transition from primary to secondary stability – following the surgical intervention, with the average marginal bone loss recorded at  $0.12 \pm 0.12$  mm at 12 months post-loading with a 100% survival rate. In their study, no differences were shown between the MA and DA aspects of implants [132]. Similarly to this study, no differences were observed between MBL at the MA and DA aspects by Barone *et al.* (0.4 mm vs. 0.5 mm) [133]. In a retrospective, CBCT-based study, Roe *et al.* reported a  $0.82 \pm 0.64$  mm vertical, and  $1.23 \pm 0.75$  mm horizontal bone height reduction at 1-year follow-up after immediate implant placement [134]. Interestingly, the study of Maló *et al.* reported implant failure in similar positions where our study presented with the highest levels on an individual implant-level [135].

On the other hand, bone loss levels were significantly higher around tilted implants compared to axial implants at every time-point. Tilted or short implants provide viable alternatives to bone grafting; on the other hand, they may lead to increased stress on the surrounding bone due to bending [136,137]. A finite-element analysis performed by Rubo *et al.* showed that the presence of distally tilted implants in an Ao4 concept would result in higher maxillary bone stress compared to vertical implants, highlighting that the proportion of increased stress is proportional to the increased length of the cantilever [138]. In contrast, the paper by Durkan *et al.* reports bone loss levels within the range of 0.34–1.14 mm for axial, and 0.43–1.13 mm for angled implants, with no significant differences between them [78]. The study by Pera *et al.* compared the clinical outcomes of immediate and delayed-loading procedures in edentulous maxillae with full-arch fixed prostheses, where all prostheses provided satisfactory function and no significant differences were shown in the cumulative survival rate of implants (one-stage: 93.3% vs. two-stage: 94.9%), while MBL was significantly lower in the immediate-loading group [75]. In a prospective 6-year study from the same authors, the clinical reliability of the immediate-loading protocol was further demonstrated, noting no significant differences in bone loss when comparing tilted vs. axial implants [76]. Implant length may also considerably affect implant survival and MBL, as demonstrated by the meta-analysis conducted by Fernandes *et al.*: based on the randomized controlled trials (RCTs) included in the analysis, survival rate of extra short ( $\leq 6$  mm) and longer (6 mm) implants were similar (93.12% vs. 95.98%). In addition, average marginal bone loss at 1-year-, 3-year-, 5-year- and 8-year follow-ups were  $-0.71$  mm,  $-0.42$  mm,  $-0.69$  mm, and  $-1.58$  mm for extra short implants, while  $-0.92$  mm,  $-0.43$  mm,  $-0.46$  mm, and  $-2.46$  mm for longer implants, respectively. In summary, published clinical studies have shown that bone loss was lower in extra short implants [139]. Overall, our study has concluded that the use of Ao4 prosthetic concept for total arch rehabilitation yields higher MBL in association with tilted implants and, in some cases, on the MA surfaces at vertically positioned implants after  $>40$  months of function. The present study highlights some areas of concern during prosthetic rehabilitation with the Ao4 concept. The limitations of our study – including the retrospective, single-center study design, the relatively low number of subjects and the time of follow-up – should be taken into consideration when interpreting the results.

## 2. Finite element analysis (FEA)

Our 3D-FEA-based study aimed to evaluate the biomechanical effects of different occlusion/load cases and implant-denture material properties in an edentulous mandible (constructed using authentic CT scans of a patient) with an implant-supported full bridge on four implants, to model the biomechanical properties of the Ao4 concept. The initial hypotheses our study were the following: (i) the LC where the masticatory force covers the entire surface of the denture (including the cantilever) is the most advantageous, when considering stress distributions, (ii) material properties assigned to the denture body and the implant considerably affect stress levels and stress distribution characteristics. Due to the bone's elastic material properties, tensile and compressive stress values were deemed appropriate to evaluate biomechanical properties in this study [140]. Based on previous literature findings, the cortical bone is most mechanically resistant to compressive forces, less resistant to tensile force, and the least resistant to shear forces, respectively [141]. Based on our analyses, the LC1 modeled was noted as the safest option, confirming our initial hypotheses. This load case was characterized by the most uniform stress distribution, and the lowest peak  $P_{max}$  and  $P_{min}$  values in the mandible body, throughout all simulations. On the other hand, LC2 – the load case where the force excluded the cantilevers of the denture extending behind the terminal implants – showed the highest peak  $P_{max}$  values in both cortical and trabecular bone for S1 and S2, respectively; therefore, it was the least desirable option in our analyses. For  $P_{min}$ , the situation was a bit more complex: in case of the cortical bone, LC2 for S2 and LC3 for S1 showed the highest values (–265.35 MPa and 172.30 MPa, respectively), while in the case of the trabecular bone, LC4 had the highest peak values (both for S1 and S2). Overall, all other load cases in most simulation parameters showed higher stress values than LC1. As seen on the stress distribution maps (as shown in the Results and in the Appendix), noted stress values were peak values denoted at a specific position; however, in reality, these maximum stresses occur as a load transmitted at the bone–implant interface, not at a single point [142]. Although comparisons may be hindered by the different model characteristics set by researchers, our results have yielded similar  $P_{max}$  and  $P_{min}$  values, in the same order, to other previously published reports assessing stresses on mandibular bone tissue [112,113,121,140,143-146]. The mandibular bone adapts to its loading, and responds to stresses by bone formation or resorption, i.e., neither unloaded nor overloaded areas are desirable due to long-term consequences [147]. Thus, the longevity of an implant may be ensured by keeping the stresses of the bone in the physiological range, with the most even

stress distribution possible [148]. Overloading and subsequent bone resorption would occur if the tensile and compressive values exceed the physiological limits posed by the ultimate strength of the bone; stress values resulting from our FEA were below these physiological limits in all simulations and load cases [149]. In addition, the rigid full-arch restoration and the spread of the implants in the mandible will further reduce stress on an individual implant-level.

The Ao4 treatment concept has been widely popularized in the recent years for the oral rehabilitation of an atrophic mandible, due to high level of functionality and patient satisfaction rates [150]. The clear advantages of this technique include the small number of implants needed, less complex surgery, the use of longer, tilted distal implants (resulting in a shorter cantilever), and large inter-implant distances, leading to improved anchorage to the bone and higher primary stability [151]. Based on various clinical reports, the use of shorter implants has been discouraged, due to their lower success rate; on the other hand (when implant diameter is kept constant), there are considerable benefits to increasing implant length in enhancing bone-implant contact area and primary stability, but only up to a cut-off point of around 12–15 mm [152]. Studies have demonstrated that increased stress in the implant and in the peri-implant area is proportional to longer cantilever lengths. According to the study by Bevilacqua *et al.*, it was shown that decreasing the cantilever length – irrespective of distal implant inclination angles (0°, 15°, 30° and 45°) – led to a reduction in all modelled stress values [153]. Thus, due to the tilted distal implants, shorter cantilever length will subsequently lead to lower stress and strain values. The 3D-FEA study of Liu *et al.* also highlighted this, when assessing the stress distributions of immediate- and delayed-loaded Ao4 implants in an edentulous maxilla; their study included various implant inclination angles (0°, 15°, 30°, and 45°) for posterior implants, where a multivectoral load of 150 N was applied to the distal cantilever of the superstructure. In the immediate-loading cases, the highest  $P_{\max}$  and  $P_{\min}$  values in the cortical bone were seen for the 0° inclined implants, while these stresses decreased by 24.91% and 53.00%, respectively, for the 45° implants. The average  $P_{\max}$  and  $P_{\min}$  values (corresponding to the load on the entire model) decreased with the increasing inclination angles in all measurements [112]. Malhotra *et al.* studied the effect of distal implant angulation with different cantilever lengths in a mandibular Ao4 model, where unilateral and bilateral axial and oblique forces were applied and  $P_{\text{eqv}}$  stress and strain distribution was measured. Their results showed that there were significant differences in the  $P_{\text{eqv}}$  values between 30° and 45° implants, while no such differences were shown for



increasing the cantilever length from 4 mm to 12 mm [154]. Their results are in concordance with the report of van Zyl *et al.*, demonstrating that the ideal level of cantilever loading exists up to 15 mm, while over this threshold value, buccal and lingual cortical plates may be under considerably greater stresses, risking implant failure [155]. Overall, their studies have also underlined that longer cantilever lengths should be avoided.

One of the main findings of the current study is the considerable effect that the load positions had on the distribution of the tested stresses. It should also be noted that in our FEA model, peak stress values were measured near the implant–bone interface, which may be explained by the stress distribution characteristic of the cylindrical implants modeled in the present study [156]. The geometry of the implant body and surface thread may have considerable effects on load transfer characteristics: while smooth, cylindrical implants may transfer dangerous shearing effects at the bone-implant interface (resulting in higher rates of implant failure), while through the introduction of (micro)threads to the implant architecture – as a surface function – these shear forces may transform into more tolerant force forms transferred to the bone surface [157]. Wu *et al.* performed an *in vitro* experiment coupled with 3D-FEA to assess the effects of implant design on the stress distribution in mandibular Ao4 implants; in their study, three distinct loading positions were defined (i.e., at the central incisor area, and at molar regions with or without cantilever load) and they showed that the peak stress values were 36–62% and 45–57% higher, respectively, in the non-cantilever load case [158]. Horita *et al.* performed a FEA-based micromotion and stress analysis in an edentulous mandible; in their analysis, peak  $P_{\min}$  values were higher in the immediate-loading case, both with and without cantilever loading, while for non-cantilever loading, a ~45–50% reduction in stress values were shown. Their 3D model showed peak  $P_{\min}$  and  $P_{\max}$  in the bone around the neck of the right distal implant in the tested cases, which may be due to the relatively high Young's modulus of the cortical bone, which lies in the closest vicinity of the occlusal loading area and the implant neck. Furthermore, in their report, the framework material did not have a pronounced effect on the results [159]. One of the considerable advantages of using standardized FEA models to compare the stress distribution of various LCs is that the intended (study) factors may be changed at will, while keeping all other study factors constant, ensuring all changes in the simulation outcome are due to the effect of the studied variable [112,114,160]. In contrast to our initial hypotheses, the framework applied (S1 and S2), had a relatively small effect regarding  $P_{\max}$  values in the cortical bone (difference: 11.50–14.97%) and trabecular bone (difference: 11.16–15.87%); on the other

hand,  $P_{\min}$  values in the cortical bone (difference: 46.61–94.54%) and  $P_{\text{eqv}}$  values (difference: 47.19–83.29%) were considerably higher in the case of S2 (i.e., the simulated Ti and Co–Cr framework). The study by Bhering *et al.* compared biomechanical stresses in the maxilla for Ao4 and “All-on-Six” implants using different framework materials (Ti, Co–Cr, and Zr); the study showed that  $P_{\max}$ ,  $P_{\min}$ , and  $P_{\text{eqv}}$  values for the cortical and cancellous bone and implant displacement were significantly lower for the All-on-Six model, associated with the higher number of implants. On the other hand, the different framework materials had no considerable effect on implant displacement or on any of the stresses modelled [161]. A finite-element micromotion analysis performed by Sigüira *et al.* – using parallel-implant and Ao4 implant configuration models in an edentulous mandible – highlighted the influence of trabecular bone thickness (defined as high and low-density) on preventing micromotion, while cortical bone thickness seemingly played a smaller role. In their Ao4 model, the maximum micromotion for non-cantilever loading was one-third of that with cantilever loading [162]. Although the limitations of the study should be taken into account, the overall findings were the following: (i) among our mandibular models, the LC where masticatory forces covered the entire mesio–distal surface of the denture, including the cantilever, was identified as the most advantageous (with the most uniform stress distribution and the lowest peak stress values), while the LC where the modelled masticatory forces excluded the cantilevers was observed as the least desirable option in our analyses, (ii) material properties of the denture in our models had a considerable influence on the  $P_{\min}$  values in the cortical bone and on  $P_{\text{eqv}}$ , while the same was not noted in for  $P_{\max}$  values. To assess the real-life clinical consequences of the presented LCs and stress distributions on implant survival and MBL, more robust evidence—such as long-term clinical studies—would be needed.

To perform our analyses, some biologically complex objects (e.g., the anatomical complexity of the mandible, macrostructure, and microstructure of the implants, boundary conditions) and variable factors were considered constant out of necessity, e.g., all materials were considered homogeneous, isotropic, and linear elastic, a *Type II* bone was used for simulation, and osseointegration was assumed at 100% [112,114,160]. The present study employed a patient-specific 3D finite element model, where the patient had adequate bone supply and was eligible for treatment with an implant-supported full bridge on four implants. However, additional studies involving patients with limited bone supply and/or underlying conditions, which would potentially affect short and long-term implant survival, would be welcome. While it is important to highlight that modeling the size of the implants was accurate and the model was based on CT scans of a patient with adequate bone supply,

anisotropy better reflects material properties in dentistry, and osseointegration is a gradual process; thus, changes in these parameters may lead to different results in the FEA. The reliability of the 3D FEA stress analysis largely depends on the number and ratio of elements and nodes (including the use of higher order elements) in the model [107,111,160]; in our case, the number of elements and nodes is in line with other studies already published to ensure maximum sensitivity of the model. Nevertheless, increasing their number would further enhance the reliability of the simulations. Mastication is a sophisticated and complex process, which makes its accurate estimation difficult for FEA studies: in this study, masticatory forces – which are multivectoral (vertical, horizontal, and oblique) under real circumstances – were modeled using a linear, continuous force exerted vertically on the simplified denture [163]. Therefore, in future studies, the introduction of multiple-bite forces, LCs, load directions, magnitudes, material properties, and implant types are needed to complement and confirm our findings.

Overall, our research – both the retrospective clinical study and our FEA analyses – has shown the clinical utility and predictability of the Ao4 therapeutic concept, with highlighting some potential areas of interest for researchers and clinicians from the standpoint of prosthetic rehabilitation. To ensure the long-term maintenance and longevity of Ao4 concept – especially from the standpoint of the edentulous mandible, where the available bone supply, due to the post-extraction involutionary changes, is often limited – efforts to determine the stresses of the surrounding bone in the physiological range, with the most even stress distribution possible, have paramount importance. Furthermore, the longevity of an implant may be ensured by keeping the stresses of the bone in the physiological range, with the most even stress distribution possible [164]. In our clinical study, we have shown the highest marginal bone loss levels around the DA aspects of tilted implants, and the MA aspects of axial implants, which corresponded to 0.7-0.8 mm of marginal bone loss – both in the maxilla and the mandible, after 3.5-years of follow-up; this rate of bone loss is comparable to the values found in the literature, corresponding to similar follow-up times. The results in the clinical study were further underlined in our FEA simulations: maximum stress values (tensile, compressive and equivalent, respectively) were observed at the implant-bone interface, most commonly localized near the top area of the second implant. Furthermore, according to our 3D-FEA models, highest peak tension stress ( $\sim 100$  MPa in the cortical bone,  $\sim 3$  MPa in the trabecular bone) and highest peak compressive stress ( $\sim -265$  MPa in the cortical bone,  $\sim -3.5$  MPa in the trabecular bone) values were all within the range that could be withstood by the jawbones (according to the physiological limits posed by the

ultimate strength of the bone), without the fear of pathological complications. During treatment planning, care should be taken to reduce stress levels at the implant-bone interface in these highlighted areas of interest (e.g., by the appropriate choice of masticatory load distributions) to reduce marginal bone loss levels post-implant placement, and to ensure implant stability.

## VIII. NEW FINDINGS

**a. During Ao4 treatment, rates of marginal bone loss around tilted (posterior) implants were consistently higher:** significantly higher rates of marginal bone loss were observed around tilted (posterior) implants – compared to axial (anterior) implants – throughout all the follow-up measurements in the 3.5-year study period.

**b. During Ao4 treatment, the rates of marginal bone loss around mesio-approximal (MA) and disto-approximal (DA) aspects of implants were similar:** no significant differences were observed in marginal bone loss levels between the MA and DA aspects of implants, throughout all the follow-up measurements in the 3.5-year study period. Overall, highest marginal bone loss levels in our study were shown around the DA aspects of tilted implants, and the MA aspects of axial implants.

**c. During 3D-FEA, the load case where linear masticatory forces covered the entire mesio–distal surface of the denture – including the cantilever – was the most advantageous:** among our mandibular models, lowest maximum and minimum principal stress values, both in the cortical and trabecular bone, and the most uniform stress distribution was observed for load case 1 (LC1), where the masticatory force covers the entire surface of the denture, including the extension surface. In contrast, LC2 – where the linearly modelled masticatory forces excluded the cantilevers – was the least advantageous, with the highest observed maximum and minimum principal stress values.

**d. During 3D-FEA, material properties of the implant and denture bodies has considerable effects on the stress values observed in the cortical bone:** during the simulations (S2) where different material properties were assigned to implant bodies (TiAl6V4) and the denture bodies (Co-Cr), maximum principal stress values, minimum principal stress values and equivalent (von Mises) stress values were 11.50-15.87%, 46.61-94.54% and 47.19-83.29% higher, respectively (compared to S1, where implant and denture bodies were both TiAl6V4). In contrast, similar differences were not observed for the trabecular bone.

## IX. SUMMARY

The “All-on-Four” (Ao4) prosthetic concept – developed by Maló *et al.* in 2003 – employs implant placement followed by immediate loading, which has received substantial attention from dentists for the oral rehabilitation of edentulous patients, due to the advantageous, short-term clinical outcomes associated with this treatment protocol. Ao4 allows clinicians to overcome the anatomical limitations of the edentulous mandible, without necessitating advanced and risky surgical techniques. The long-term success and predictability of implant-supported restorations largely depends on the distribution and the rate of load transfer at the bone-implant interface, as it may affect both primary (critical in immediate loading) and secondary stability (affecting bone remodeling processes); however, considerable gaps in knowledge still exist regarding the biomechanical stresses observed in the peri-implant bone, implants, and prostheses during the treatment of edentulous jaws. The aims of our study were the following: *i*) to assess the clinical success and marginal bone loss (MBL) levels following the implantation of distally tilted implants according to the Ao4 prosthetic concept; *ii*) to investigate the biomechanical behavior of an edentulous mandible with an implant-supported full bridge on four implants under simulated masticatory forces in a patient-specific finite element analysis (FEA) model. A single-center, institution-based retrospective study was carried out at the between 2017.01.01. and 2022.01.01., corresponding to  $n=36$  patients (i.e.  $n=288$  implants) eligible to receive an immediately-loaded, four-implant-supported fixed prosthetic restoration, following the Ao4 protocol. In addition to implant survival rate, MBL was measured around the mesio-approximal (MA) and disto-approximal (DA) aspects of the implants, by matched and calibrated orthopantomography images taken at baseline and follow-ups until 3.5-years post-restoration. A 3D finite element model was constructed using pre- and post-implantation CT images of a 63-year-old male patient with adequate bone supply, who was eligible for treatment with an implant-supported full bridge on four implants. Vertical components of the masticatory forces were included in the simulations set at 300 N, with four different simulated load cases; furthermore, two sets of simulations (Ti and Ti, and Ti and Co-Cr) were performed with different denture body and the implant body materials set. During FEA maximum principal stress, minimum principal stress and equivalent stress values were determined. In our clinical study, we have observed a 100% implant survival rate during the 3.5-year study period, and have shown the highest marginal bone loss levels around the DA aspects of tilted implants, and the MA aspects of axial implants. In the FEA model, highest stress values were always seen at the implant—bone interface. Among the mandibular

FEA models, the load case, where masticatory forces covered the entire mesio–distal surface of the denture, including the cantilever, was identified as the most advantageous, with the most uniform stress distribution and the lowest peak stress values. In contrast, the load case where the modelled masticatory forces excluded the cantilevers was observed as the least desirable option in our analyses. The framework material had pronounced effects on the minimum principal stress and equivalent stress values in cortical bone (46.61–94.54% and 47.19–83.29% higher for the simulated Ti and Co–Cr framework, respectively), while it had limited effects on maximum principal stress values. During treatment planning, care should be taken to reduce stress levels at the implant–bone interface in these highlighted areas of interest (e.g., by the appropriate choice of masticatory load distributions) to reduce marginal bone loss levels post-implant placement, and to ensure implant stability. Overall, our research – both the retrospective clinical study and our FEA analyses – has shown clinical utility and predictability of the Ao4 therapeutic concept, with highlighting some potential areas of interest for researchers and clinicians from the standpoint of prosthetic rehabilitation.

## XI. REFERENCES

1. World Health Organization (WHO). Oral health. Available online: [https://www.who.int/health-topics/oral-health#tab=tab\\_1](https://www.who.int/health-topics/oral-health#tab=tab_1) (Accessed on: 2024.05.01.)
2. Jain N, Dutt U, Radenkov I, Jain S. WHO's global oral health status report 2022: Actions, discussion and implementation. *Oral Dis* 2023;30:73-79.
3. National Institutes of Health (NIH). Oral health in America: Advances and Challenges. Bethesda (MD): National Institute of Dental and Craniofacial Research(US); 2021 Dec. Section 1, Effect of Oral Health on the Community, Overall Well-Being, and the Economy. Available online: <https://www.ncbi.nlm.nih.gov/books/NBK578297/> (Accessed on: 2024.05.01.)
4. Grace RG, Jagtap M. Impact of Swallowing Impairment on Quality of Life of Individuals with Dysphagia. *Indian J Otolaryngol Head Neck Surg* 2022;74:5473-5477.
5. Lobbezoo F, Aarab G, Kapos FP, Dayo ADF, Huang Z, Koutris M, Peres MA, Thymi M, Haggman-Henrikson B. The Global Need for Easy and Valid Assessment Tools for Orofacial Pain. *J Dent Res* 2022;101:1549–1553.
6. World Health Organization (WHO). Global oral health status report: Towards universal health coverage for oral health by 2030. Available online: <https://www.who.int/team/noncommunicable-diseases/global-status-report-on-oral-health-2022> (Accessed on: 2024.05.01.)
7. Petersen PE, Bourgeois D, Ogawa H, Estupinan-Day S, Ndiaye C. The global burden of oral diseases and risks to oral health. *Bull World Health Org* 2005;83:661-669.
8. Petersen PE. Sociobehavioural risk factors in dental caries-an international perspective. *Comm Dent Oral Epidemiol* 2005;33:274-279.
9. Huang YK, Chang YC. Oral health: The first step to sustainable development goal 3. *J Formosan Med Assoc* 2022;121:1348-1350.
10. Al-Rafee MA. The epidemiology of edentulism and the associated factors: A literature Review. *J Family Med Prim Care* 2020;9:1841-1843.
11. GBD 2017 Oral Disorders Collaborators. Global, Regional, and National Levels and Trends in Burden of Oral Conditions from 1990 to 2017: A Systematic Analysis for the Global Burden of Disease 2017 Study. *J Dent Res* 2020;99:362-373.
12. Qin X, Chen L, Yuan X, Lin D, Liu Q, Zeng X, Ma F. Projecting trends in the disease burden of adult edentulism in China between 2020 and 2030: a systematic study based on the global burden of disease. *Front Pub Health* 2024;12:e1367138.



13. Qin X, He J, He J, Yuan X, Su X, Zeng X. Long-term trends in the burden of edentulism in China over three decades: A Joinpoint regression and age-period-cohort analysis based on the global burden of disease study 2019. *Front Pub Health* 2023;11:e1099194.
14. Nascimento GG, Leite FRM, Conceicao DA, Ferrua CP, Singh A, Demarco FF. Is there a relationship between obesity and tooth loss and edentulism? A systematic review and meta-analysis. *Obes Rev* 2016;17:587-598.
15. Ladha K, Tiwari B. Type 2 Diabetes and Edentulism as Chronic Co-Morbid Factors Affecting Indian Elderly: An Overview. *J Indian Prosthodont Soc* 2013;13:406-412.
16. Sherbaf RA, Kaposvári GM, Nagy K, Álmos PZ, Baráth ZL, Matosovits D. Oral Health Status and Factors Related to Oral Health in Patients with Schizophrenia: A Matched Case-Control Observational Study. *J Clin Med* 2024;13:e1584.
17. Ruospo M, Palmer SC, Craig JC, Gentile G, Johnson DW, Ford PJ, Tonelli M, Petruzzi M, De Benedittis M, Strippoli GFM. Prevalence and severity of oral disease in adults with chronic kidney disease: a systematic review of observational studies. *Neprol Dial Transplant* 2014;29:364-375.
18. Huang Y, Michaud DS, Lu JS, Platz EA. The association of clinically determined periodontal disease and edentulism with total cancer mortality: the National Health and Nutrition Examination Survey III. *Int J Cancer* 2020;147:1587-1596.
19. de Pablo P, Dietrich T, McAlindon TE. Association of periodontal disease and tooth loss with rheumatoid arthritis in the US population. *J Rheumatol* 2008;35:70-76.
20. Dwibendi N, Wiener RC, Findley PA, Shen C, Sambamoorthi U. Asthma, COPD, Tooth Loss, and Edentulism among Adults in the United States: 2016 Behavioral Risk Factor Surveillance Survey. *J Am Dent Assoc* 2020;151:735-744.
21. Kelly N, Winning L, Irwin C, Lundy FT, Linden D, McGarvey L, Linden GJ, El-Karim IA. Periodontal status and chronic obstructive pulmonary disease (COPD) exacerbations: a systematic review. *BMC Oral Health* 2021;21:e425.
22. Tripathi A, Gupta A, Rai P, Sharma P, Tripathi S. Correlation between duration of edentulism and severity of obstructive sleep apnea in elderly edentulous patients. *Sleep Sci* 2022;15:300-305.
23. Bond JC, McDonough R, Alshihayb TS, Kaye EA, Garcia RI, Heaton B. Edentulism is associated with increased risk of all-cause mortality in adult men. *J Am Dent Assoc* 2022;153:625-634.e3.

24. EFP workshop participants and methodological consultants. Prevention and treatment of peri-implant diseases—The EFP S3 level clinical practice guideline. *J Clin Periodontol* 2023;50:4-76.
25. Block MS. Dental Implants: The Last 100 Years. *J Oral Maxillofac Surg* 2018;76:11-26.
26. Wegst UGK, Bai H, Saiz E, Tomsia A, Ritchie RO. Bioinspired structural materials. *Nature Materials* 2015;14:23-36.
27. Oliviera H, Velasco AB, Rios-Santos JV, Lasheras FS, Lemos BF, Gil FJ, Carvalho A, Herrero-Climent. Effect of Different Implant Designs on Strain and Stress Distribution under Non-Axial Loading: A Three-Dimensional Finite Element Analysis. *Int J Environ Res Public Health* 2020;17:e4738.
28. González-Carrasco JL. Metals as bone repair materials. In: Bone repair biomaterial (Chapter: 5). Publisher: Woodhealing Publishing Limited. Editors: Planell J, Best S, Lacroix D, Merolli A, 2009.
29. Cardapoli G, Araújo MG, Lindhe J. Dynamics of bone tissue formation in tooth extraction sites. An experimental study in dogs. *J Clin Periodontol* 2003;30:809-818.
30. Araújo MG, Lindhe J. Dimensional ridge alterations following tooth extraction. An experimental study in the dog. *J Clin Periodontol* 2005;32:212-218.
31. Schropp L, Wenzel A, Kostopoulos L, Karring T. Bone Healing and Soft Tissue Contour Changes Following Single-Tooth Extraction: A Clinical and Radiographic 12-Month Prospective Study. *Int J Periodont Restor Dent* 2003;23:313-323.
32. Van der Weijden F, Dell'Acqua F, Slot DE. Alveolar bone dimensional changes of post-extraction sockets in humans: a systematic review. *J Clin Periodontol* 2009;36:1048–1058.
33. Tan WL, Wong TLT, Wong, MCM, Lang, NP. A systematic review of post-extraction alveolar hard and soft tissue dimensional changes in humans. *Clin Oral Implants Res* 2012;23:1-21.
34. Juodzbaly G, Stumbras A, Goyushov S, Duruel O, Tözüm TF. Morphological Classification of Extraction Sockets and Clinical Decision Tree for Socket Preservation/Augmentation after Tooth Extraction: a Systematic Review. *J Oral Maxillofac Res* 2019;10:e3.
35. Hansson S, Halldin A. Alveolar ridge resorption after tooth extraction: A consequence of a fundamental principle of bone physiology. *J Dent Biomech* 2012;3:e1758736012456543.
36. Bertl K, Kukla EB, Albugami R, Beck F, Gahleitner A, Stavropoulos A. Timeframe of socket cortication after tooth extraction: A retrospective radiographic study. *Clin Oral Implants Res* 2018;29:130-138.

37. Chappuis V, Araújo MG, Buser D. Clinical relevance of dimensional bone and soft tissue alterations post-extraction in esthetic sites. *Periodontology 2000* 2017;73:73-83.
38. Gowd MS, Shankar T, Ranjan R, Singh A. Prosthetic Consideration in Implant-supported Prosthesis: A Review of Literature. *J Int Soc Prev Community Dent* 2017;7:S1-S7.
39. Lekholm U, Zarb GA. Patient selection and preparation. In: Branemark PI, Zarb GA, Albrektsson T, editors. Tissue integrated prostheses: osseointegration in clinical dentistry. Chicago: Quintessence Publishing Company; 1985. p. 199–209.
40. Misch CE. Bone density: A key determinant for clinical success. In: Misch CE., (eds.) Contemporary Implant Dentistry. 2nd edition. St Louis: CV Mosby Company; 1999. p. 109–118.
41. Weiner S, Wagner HD. The material bone: structure mechanical function relations. *Annu Rev Mater Sci* 1998;28:271–298.
42. Tallgren A. The continuing reduction of the residual alveolar ridges in complete denture wearers: A mixed-longitudinal study covering 25 years. *J Prosthetic Dent* 2003;89:427-435.
43. Gabet Y, Kohavi D, Voide R, Mueller TL, Müller R, Bab I. Endosseous implant anchorage is critically dependent on mechanosturctural determinants of peri-implant bone trabeculae. *J Bone Mineral Res* 2010;25:575-583.
44. Oftadeh R, Perez-Viloria M, Villa-Camacho JC, Vaziri A, Nazarian A. Biomechanics and Mechanobiology of Trabecular Bone: A Review. *J Biomech Eng* 2015;137:0108021–01080215.
45. Baggi L, Pastore S, Di Girolamo M, Vairo G. Implant-bone load transfer mechanisms in complete-arch prostheses supported by four implants: a three-dimensional finite element approach. *J Prosthet Dent* 2013;109:9-21.
46. Lang NP, Pun L, Lau KY, Li KY, Wong MCM. A systematic review on survival and success rates of implants placed immediately into fresh extraction sockets after at least 1 year. *Clin Oral Implants Res* 2012;5:39-66.
47. Norton M. Primary stability versus viable constraint--a need to redefine. *Int J Oral Maxillofac Implants* 2013; 28:19-21.
48. Raghavendra S, Wood MC, Taylor TD. Early wound healing around endosseous implants: a review of the literature. *Int J Oral Maxillofac Implants* 2005; 20:425-431.
49. Bumgardner JD, Boring JG, Cooper RC, Gao C, Givaruangsawat S, Gilbert JA, Misch CM, Stefik DE. Preliminary evaluation of a new dental implant design in canine models. *Implant Dent* 2000;9:252-260.

50. Huang YC, Huang YC, Ding SJ. Primary stability of implant placement and loading related to dental implant materials and designs: A literature review. *J Dent Sci* 2023;18:1467-1476.
51. Brunski JB, Puleo DA, Nanci A. Biomaterials and biomechanics of oral and maxillofacial implants: current status and future developments. *Int J Oral Maxillofac Implants* 2000;15:15-52.
52. Trisi P, Perfetti G, Baldoni E, Berardi D, Colagiovanni M, Scogna G. Implant micromotion is related to peak insertion torque and bone density. *Clin Oral Implants Res* 2009;20:467-471.
53. Oh SL, Shiau HJ, Reynolds MA. Survival of dental implants at sites after implant failure: A systematic review. *J Prosthetic Dent* 2020;123:54-60.
54. Tachibana R, Motoyoshi M, Shinohara A, Shigeeda T, Shimizu N. Safe placement techniques for self-drilling orthodontic mini-implants. *Int J Oral Maxillofac Surg* 2012;41:1439–1444
55. Albrektsson T, Branemark PI, Hansson HA, Lindström J. Osseointegrated Titanium Implants: Requirements for Ensuring a Long-Lasting, Direct Bone-to-Implant Anchorage in Man. *Acta Orthop Scand* 2009;52:155–70.
56. Mura P. Immediate loading of tapered implants placed in postextraction sockets: retrospective analysis of the 5-year clinical outcome. *Clin Implant Dent Relat Res* 2012;14:565-574.
57. Caramés JMM, Marques DNS, Caramés GB, Francisco HCO, Vieira FA. Implant Survival in Immediately Loaded Full-Arch Rehabilitations Following an Anatomical Classification System—A Retrospective Study in 1200 Edentulous Jaws. *J Clin Med* 2021;10:e5167.
58. Göcmen G, Bayrakcioglu A, Bayram F. Effect of the level of alveolar atrophy on implant placement accuracy in guided surgery for full-arch restorations supported by four implants: an in vitro study. *Head Face Med* 2023;19:e40.
59. Matsubara VH, Gurbuxani AP, Francis S, Childs RJ. Implant rehabilitation of edentulous maxilla in digital dentistry: A case report utilizing CAD/CAM technologies. *J Dent Res Dent Clin Dent Prospects* 2021;15:115–121.
60. Sakkas A, Wilde F, Heufelder M, Winter K, Schramm A. Autogenous bone grafts in oral implantology—is it still a “gold standard”? A consecutive review of 279 patients with 456 clinical procedures. *Int J Implant Dent* 2017;3:e23.

61. Hof M, Tepper G, Semo B, Arnhart C, Watzek G, Pommer B. Patients' perspectives on dental implant and bone graft surgery: questionnaire-based interview survey. *Clin Oral Implants Res* 2014;25:42-45.
62. Trisi P, Berardini M, Falco A, Vulpiani MP. Effect of Implant Thread Geometry on Secondary Stability, Bone Density, and Bone-to-Implant Contact: A Biomechanical and Histological Analysis. *Implant Dent* 2015;24:384-391.
63. Rosa A, Puija AM, Arcuri C. Complete Full Arch Supported by Short Implant (<8 mm) in Edentulous Jaw: A Systematic Review. *Applied Sci* 2023;13:e7162.
64. Mehta SP, Sutariya PV, Pathan MR, Upadhyay HH, Patel SR, Kantharia NDG. Clinical success between tilted and axial implants in edentulous maxilla: A systematic review and meta-analysis. *J Indian Prosthodont Soc* 2021;21:217-228.
65. Sun X, Cheng K, Liu Y, Ke S, Zhang W, Wang L, Yang F. Biomechanical comparison of all-on-4 and all-on-5 implant-supported prostheses with alteration of anterior-posterior spread: a three-dimensional finite element analysis. *Front Bioeng Biotechnol* 2023;11:e1187504.
66. Barnea E, Tal H, Nissan J, Tarrasch R, Peleg M, Kolerman R. The Use of Tilted Implant for Posterior Atrophic Maxilla. *Clin Implant Dent Relat Res* 2016;18:788-800.
67. King EM, Schofield J. Restoratively driven planning for implants in the posterior maxilla - Part 2: implant planning, biomechanics and prosthodontic planning a proposed prosthodontic complexity index. *British Dental J* 2023;235:695-706.
68. Málo P, Rangert B, Nobre M. "All-on-four" immediate-function concept with Brånemark system® implants for completely edentulous mandibles: A retrospective clinical study. *Clin Implant Dent Relat Res* 2003;5:2-9.
69. Taruna M, Chittaranjan B, Sudheer N, Tella S, Abusaad M. Prosthodontic Perspective to All-On-4® Concept for Dental Implants. *J Clin Diagn Res* 2014;8:ZE16-ZE19.
70. Maló P, Rangert B, Nobre M. All-on-4 immediate-function concept with Brånemark System implants for completely edentulous maxillae: A 1-year retrospective clinical study. *Clin Implant Dent Relat Res* 2005;7:88-94.
71. Soto-Penaloza D, Zaragoza-Alonso R, Penarrocha-Diago M, Penarrocha-Diago M. The all-on-four treatment concept: Systematic review. *J Clin Exp Dent* 2017;9:e474-488.
72. Tironi F, Orlando F, Azzola F, Corbella S, Franceti LA. A Retrospective Analysis on Marginal Bone Loss around Tilted and Axial Implants in Immediate-Loaded All-On-4 with a Long-Term Follow-Up Evaluation. *Prosthesis* 2022;4:15-23.

73. Cattoni F, Chirico L, Merlone A, Manacorda M, Vinci R, Gherlone EF. Digital Smile Designed Computer-Aided Surgery versus Traditional Workflow in “All on Four” Rehabilitations: A Randomized Clinical Trial with 4-Years Follow-Up. *Int J Environ Res Public Health* 2021;18:e3449.
74. Maló P, Nobre MA, Lopes A, Rodrigues R. Double Full-Arch versus Single Full-Arch, Four Implant-Supported Rehabilitations: A Retrospective, 5-Year Cohort Study. *J Prosthodont* 2015;24:263–270.
75. Pera P, Menini M, Pesce P, Bevilacqua M, Pera F, Tealdo T. Immediate Versus Delayed Loading of Dental Implants Supporting Fixed Full-Arch Maxillary Prostheses: A 10-year Follow-up Report. *Int J Prosthodont* 2019;32:27–31.
76. Pera P, Menini M, Bevilacqua M, Pesce P, Signori A, Tealdo T. Factors Affecting the Outcome in the Immediate Loading Rehabilitation of the Maxilla: A 6-year Prospective Study. *Int J Periodont Restor Dent* 2014;34:657–665.
77. Maló P, de Araújo Nobre M, Lopes A, Moss SM, Molina GJ. A longitudinal study of the survival of All-on-4 implants in the mandible with up to 10 Years of follow-up. *J Am Dent Assoc* 2011;142:310–320.
78. Durkan R, Oyar P, Deste G. Maxillary and Mandibular All-on-Four Implant Designs: A Review. *Niger J Clin Pract* 2019;22:1033–1040.
79. Khaohoken A, Sornsuvan T, Chaijareenont, Poovarodom P, Rungsiyakull C, Rungsiyakull P. Biomaterials and Clinical Application of Dental Implants in Relation to Bone Density—A Narrative Review. *J Clin Med* 2023;12:e6924.
80. Steigenga JT, al-Shammari KF, Nociti FH, Misch CE, Wang HL. Dental implant design and its relationship to long-term implant success. *Implant Dent* 2003;12:306-317.
81. Li J, Jansen JA, Walboomers XF, van den Beucken JJJP. Mechanical aspects of dental implants and osseointegration: A narrative review. *J Mech Behav Biomed Mater* 2020;103:e103574.
82. Romanos GE. Bone quality and the immediate loading of implants-critical aspects based on literature, research, and clinical experience. *Implant Dent* 2009;18:203-209.
83. Vogl S, Stopper M, Hof M, Theisen K, Wegscheider WA, Lorenzoni M. Immediate occlusal vs nonocclusal loading of implants: A randomized prospective clinical pilot study and patient centered outcome after 36 months. *Clin Implant Dent Rel Res* 2019;21:766-774.
84. Körtvélyessy G, Szabó ÁL, Pelsöczi-Kovács I, Tarjányi T, Tóth Z, Kárpáti K, Matusovits D, Hangyási DB, Baráth Z. Different Conical Angle Connection of Implant and Abutment

Behavior: A Static and Dynamic Load Test and Finite Element Analysis Study. *Materials* 2023;16:e1988.

85. Torroella-Saura G, Mareque-Bueno J, Cablatosa-Termes J, Hernandez-Alfaro F, Ferrés-Padró E, Calvo-Guirado JL. Effect of implant design in immediate loading. A randomized, controlled, split-mouth, prospective clinical trial. *Clin Oral Implant Res* 2015;26:240-244.

86. Eazhil R, Swaminathan SV, Gunaseelan M, Kannan VG, Alagesan C. Impact of implant diameter and length on stress distribution in osseointegrated implants: A 3D FEA study. *J Int Soc Prev Community Dent* 2016;6:590-596.

87. Javed F, Ahmed HB, Crespi R, Romanos GE. Role of primary stability for successful osseointegration of dental implants: Factors of influence and evaluation. *Interv Med Appl Sci* 2013;5:162-167.

88. Applied Dental Materials, 9th Edition. John F. McCabe (Editor), Angus W. G. Walls (Editor). ISBN: 978-1-405-13961-8, 2008, pp. 320

89. Noyan IC, Cohen JB. Residual Stresses in Materials. *American Sci* 1991;79:142-153.

90. Bandela V, Kanaparthi S. Finite Element Analysis and Its Applications in Dentistry. IntechOpen, 2021. doi: 10.5772/intechopen.94064

91. Niu Y, Du T, Liu Y. Biomechanical Characteristics and Analysis Approaches of Bone and Bone Substitute Materials. *J Funct Biomater* 2023;14:e212.

92. Dieterle MP, Husari A, Steinberg T, Wang X, Ramminger I, Tomakidi P. Role of Mechanotransduction in Periodontal Homeostasis and Disease. *J Dent Res* 2021;100:1210-1219.

93. Atmaram GH, Mohammed H. Stress analysis of single-tooth implants. I. Effect of elastic parameters and geometry of implant. *Implantologist* 1983-84;3:24-9.

94. Nagy ÁL, Tóth Z, Tarjányi T, Práger NT, Baráth ZL. Biomechanical properties of the bone during implant placement. *BMC Oral Health* 2021;21:e86.

95. Geng, J.P.; Tan, K.B.; Liu, G.R. Application of finite element analysis in implant dentistry: A review of the literature. *J. Prosthet. Dent.* 2001, 85, 585–598.

96. Zhang J, Eisentrager J, Duczek S, Song C. Discrete modeling of fiber reinforced composites using the scaled boundary finite element method. *Comp Structures* 2020;235:e111744.

97. Di Fiore A, Montagner M, Sivolella S, Stelini E, Yilmaz B, Brunello G. Peri-Implant Bone Loss and Overload: A Systematic Review Focusing on Occlusal Analysis through Digital and Analogic Methods. *J Clin Med* 2022;11:e4812.

98. Trivedi S. Finite element analysis: A boon to dentistry. *J Oral Biol Craniofacial Res* 2014;4:200–203.
99. Ereiz S, Duvnjak I, Jiménez-Alonso JF. Review of finite element model updating methods for structural applications. *Structures* 2022;41:684-723.
100. Maida CA, Xiong D, Marcus M, Zhou L, Huang Y, Lyu Y, Shen J, Osuna-Garcia A, Liu H. Quantitative data collection approaches in subject-reported oral health research: a scoping review. *BMC Oral Health* 2022;22:e435.
101. Tyndall DA, Price JB, Tetradis S, Ganz SD, Hildebolt C, Scarfe WC, American Academy of Oral and Maxillofacial Radiology. Position statement of the American Academy of Oral and Maxillofacial Radiology on selection criteria for the use of radiology in dental implantology with emphasis on cone beam computed tomography. *Oral Surg Oral Med Oral Pathol Oral Radiol* 2012;113:817-826.
102. Nobel Biocare: How You Can Start with the All-on-4® Treatment Concept. Available online: <https://www.artisbiotech.ro/wp-content/uploads/All-on-4-Manual.pdf> (Accessed on: 2024.05.01.)
103. Javaid MA, Kurshid Z, Zafar MA, Najeeb S. Immediate Implants: Clinical Guidelines for Esthetic Outcomes. *Dent J* 2016;4:e21.
104. Griffin SO, Griffin P, Li CH, Bailey W, Brunson D, Jones J. Changes in Older Adults' Oral Health and Disparities: 1999 to 2004 and 2011 to 2016. *J Am Geriatr Soc* 2019;1:1–6.
105. 3D Slicer Computer Aided Design (CAD) software. Available online: <https://www.slicer.org/> (Accessed on: 2024.05.01.)
106. Fedorov A, Beichel R, Kalpathy-Cramer J, Finet J, Fillion-Robin JC, Pujol S, Bauer C, Jennings D, Fennessy FM, Sonka M et al. 3D Slicer as an Image Computing Platform for the Quantitative Imaging Network. *Magnetic Res Imag* 2012;30:1323–1341.
107. Freedman G, Antal M, Afrashtehfar KI. [An Option for Guided Implantology: The SMART Guide]. *Rev Dent Paciente* 2020;144:10–19.
108. Alpha-Bio Tec Ltd. Product Catalog. Available online: [https://alpha-bio.net/media/10285/product-catalog-2021-r17-english\\_mail.pdf](https://alpha-bio.net/media/10285/product-catalog-2021-r17-english_mail.pdf) (accessed on 2023.01.29.).
109. ANSYS SpaceClaim. Available online: <https://www.ansys.com/products/3d-design/ansys-spaceclaim> (Accessed on: 2024.05.01.)
110. Bathe KJ, Almeida CA. A Simple and Effective Pipe Elbow Element—Linear Analysis. *J Appl Mech* 1980;47:93–100.



111. Hassan AAF, Saleh SA, Jibar ZH. Experimental and Theoretical Study of Hardness and Grain Size Variation in Cold Upset for Pure Copper Cylinder. *Univ J Mech Eng* 2015;3:34–36.
112. Liu T, Mu Z, Wang C, Huang Y. Biomechanical comparison of implant inclinations and load times with the all-on-four treatment concept: A three-dimensional finite element analysis. *Comp Methods Biomech Biomed Eng* 2019;22:585–594.
113. Silva GC, Mendonca JA, Lopes LR, Landre J. Stress patterns on implants in prostheses supported by four or six implants: A three-dimensional finite element analysis. *Int J Oral Maxillofac Implant* 2010;25:239–246.
114. Türker N, Büyükkaplan US, Sadowsky SJ, Özarslan MM. Finite element stress analysis of applied forces to implants and supporting tissues using the „All-on-four” concept with different occlusal scemes. *J Prosthodont* 2019;18:185–194.
115. Huang HL, Fuh LJ, Hsu JT, Tu MG, Shen YW, Wu CL. Effects of implant surface roughness and stiffness of grafted bone on an immediately loaded maxillary implant: A 3D numerical analysis. *J Oral Rehabil* 2008;35:283–290.
116. Shibata Y, Tanimoto Y, Maruyama N, Nagakura M. A review of improved fixation methods for dental implants. Part II: Biomechanical integrity at bone-implant interface. *J Prosthodont Res* 2015;59:84–95.
117. Lakatos É, Magyar L, Bojtár I. Material Properties of the Mandibular Trabecular Bone. *J Med Eng* 2014;2014:e470539.
118. Grimal Q, Laugier P. Quantitative Ultrasound Assessment of Cortical Bone Properties beyond Bone Mineral Density. *IRBM* 2019;40:16–24.
119. Deste G, Durkan R. Effects of All-on-four implant designs in mandible on implants and the surrounding bone: A 3-D finite element analysis. *Nig J Clin Pract* 2020;23:456–463.
120. Uddanwadiker RV, Padole PM, Arya H. Effect of variation of root post in different layers of tooth: Linear vs. nonlinear finite element stress analysis. *J Biosci Bioeng* 2007;104:363–370.
121. dos Santos MBF, de Oliviera Meloto G, Bacchi A, Correr-Sobrinho L. Stress distribution in cylindrical and conical implants under rotational micromovement with different boundary conditions and bone properties: 3-D FEA. *Comp Methods Biomech Biomed Eng* 2017;20:893–900.
122. Ortega-Martínez J, Pérez-Pascual T, Mareque-Bueno S, Hernández-Alfaro F, Ferrés-Padró E. Immediate implants following tooth extraction. A systematic review. *Med Oral Patol Oral Cir Bucal* 2012;17:e251–e261.

123. Becker K, Mihatovic I, Golubovic V, Schwarz F. Impact of abutment material and dis-/re-connection on soft and hard tissue changes at implants with platform-switching. *J Clin Periodontol* 2012;39:774–780.
124. Santos JS, Santos TS, Filho PRSM, von Krockow N, Weigl P, Pablo H. One Abutment at One Time Concept for Platform-Switched Morse Implants: Systematic Review and Meta-Analysis. *Braz Dent J* 2018;29:7–13.
125. Do TA, Le HS, Shen YW, Huang HL, Fuh LJ. Risk Factors related to Late Failure of Dental Implant—A Systematic Review of Recent Studies. *Int J Environ Res Public Health* 2020;17:e3931.
126. Romanidi M, Cordaro M, Donno S, Cordaro L. Discrepancy Between Patient Satisfaction and Biologic Complication Rate in Patients Rehabilitated with Overdentures and Not Participating in a Structured Maintenance Program After 7 to 12 Years of Loading. *Int J Oral Maxillofac Implant* 2019;4:1143–1151.
127. Schwarz MS. Mechanical complications of dental implants. *Clin Oral Implants Res* 2000;11:156–158.
128. Patzelt SBM, Bahat O, Reynolds MA, Strub JR. The All-on-Four Treatment Concept: A Systematic Review. *Clin Implant Dent Relat Res* 2014;16:836–855.
129. Nishigawa G, Matsunaga T, Maruo Y, Okamoto M, Natusaki N, Minagi S. Finite element analysis of the effect of the bucco-lingual position of artificial posterior teeth under occlusal force on the denture supporting bone of the edentulous patient. *J Oral Rehabil* 2003;30:646–652.
130. Hürzeler M, Fickl S, Zuhr O, Wachtel H. Peri-implant bone level around implants with platform-switched abutments: Preliminary data from a prospective study. *J Oral Maxillofac Surg* 2007;65:33–39.
131. Widmark G, Andersson B, Carlsson GE, Lindval AM, Ivanoff CJ. Rehabilitation of patients with severely resorbed maxillae by means of implants with or without bone grafts: A 3- to 5-year follow-up clinical report. *Int J Oral Maxillofac Implant* 2001;16:73–79.
132. Makary C, Menhall A, Zammarie C, Lombardi T, Lee SY, Stacchi C, Park KB. Primary Stability Optimization by Using Fixtures with Different Thread Depth According To Bone Density: A Clinical Prospective Study on Early Loaded Implants. *Materials* 2019;12:e2398.
133. Barone A, Ricci M, Romanos GE, Tonelli P, Alfonsi F, Covani U. Buccal bone deficiency in fresh extraction sockets: A prospective single cohort study. *Clin Oral Implants Res.* 2015;26:823–830.

134. Roe P, Kan JY, Rungcharassaeng K, Caruso JM, Zimmerman G, Mesquida J. Horizontal and vertical dimensional changes of peri-implant facial bone following immediate placement and provisionalization of maxillary anterior single implants: A 1-year cone beam computed tomography study. *Int J Oral Maxillofac Implant* 2012;27:393–400.
135. Maló P, de Araújo Nobel M, Lopes A, Ferro A, Gravito I. All-on-4® Treatment Concept for the Rehabilitation of the Completely Edentulous Mandible: A 7-Year Clinical and 5-Year Radiographic Retrospective Case Series with Risk Assessment for Implant Failure and Marginal Bone Level. *Clin Implant Dent Relat Res* 2015;17:e531–e541.
136. Bevilacqua M, Tealdo T, Pera F, Menini M, Mossolov A, Drago C, Pera P. Three-dimensional finite element analysis of load transmission using different implant inclinations and cantilever lengths. *Int J Prosthodont* 2008;21:539–542.
137. Moneiro DR, Silva EVF, Pellizzer EP, Filho OM, Goiato MC. Posterior partially edentulous jaws, planning a rehabilitation with dental implants. *World J Clin Cases* 2015;3:65–76.
138. Rubo JH, Souza EAC. Finite element analysis of stress in bone adjacent to dental implants. *J Oral Implantol* 2008;34:248–255.
139. Fernandes, GVO, Costa BMGN, Trindade HF, Castilho RM, Fernandes JCH. Comparative analysis between extra-short implants ( $\leq 6$  mm) and 6 mm-longer implants: A meta-analysis of randomized controlled trial. *Aust Dent J* 2022;67:194-211.
140. Katada H, Arakawa T, Ichimura K, Sueishi K, Sameshima GT. Stress distribution in mandible and temporomandibular joint by mandibular distraction: A 3-dimensional finite-element analysis. *Bull Tokyo Dent Coll* 2009;50:161–168.
141. Hart NH, Nimphius S, Rantalainen T, Ireland A, Siafarikas A, Newton RU. Mechanical basis of bone strength: Influence of bone material, bone structure and muscle action. *J Muscoskelet Neuronal Interact* 2017;17:114–139.
142. Bonnet AS, Postaire M, Lipinski, P. Biomechanical study of mandible bone supporting a four-implant retained bridge. Finite element analysis of the influence of bone anisotropy and foodstuff position. *Med Eng Phys* 2009;31:806–815.
143. Darwich A, Alammar A, Heshmeh O, Szabolcs S, Nazha H. Fatigue Loading Effect in Custom-Made All-on-4 Implants System: A 3D Finite Elements Analysis. *IRBM* 2022;43:372–379.
144. Ayali A, Altagar M, Ozan O, Kurtulmus-Yilmaz S. Biomechanical comparison of the All-on-4, M-4, and V-4 techniques in an atrophic maxilla: A 3D finite element analysis. *Comp Biol Med* 2020;123:e103880.

145. Chowdhary R, Kumararama, S.S. “Simpli5y” a novel concept for fixed rehabilitation of completely edentulous maxillary and mandibular edentulous arches: A 3-year randomized clinical trial, supported by a numerical analysis. *Clin. Implant Dent. Relat. Res.* 2018, 20, 749–755.
146. Liu C, Xing Y, Li Y, Lin Y, Xu J, Wu D. Bone quality effect on short implants in the edentulous mandible: A finite element study. *BMC Oral Health* 2022;22:e139.
147. Omi M, Mishina Y. Roles of osteoclasts in alveolar bone remodeling. *Genesis* 2022;60:e23490.
148. Malo P, de Araujo Nobre M, Lopes A, Ferro A. The All-on-4 treatment concept for the rehabilitation of the completely edentulous mandible: A longitudinal study with 10 to 18 years of follow-up. *Clin Implant Dent Relat Res* 2019;21:565–577.
149. Misch CE, Qu Z, Bidez MW. Mechanical properties of trabecular bone in the human mandible: Implications for dental implant treatment planning and surgical placement. *J Oral Maxillofac Surg* 1999;57:700–706.
150. Fernández-Ruiz JA, Sánchez-Siles M, Guerrero-Sánchez Y, Pato-Mourelo J, Camacho-Alonso F. Evaluation of Quality of Life and Satisfaction in Patients with Fixed Protheses on Zygomatic Implants Compared with the All-on-Four Concept: A Prospective Randomized Clinical Study. *Int J Environ Res Public Health* 2021;18:e3426.
151. Zincir ÖÖ, Parlar A. Comparison of stresses in monoblock tilted implants and conventional angled multiunit abutment-implant connection systems in the all-on-four procedure. *BMC Oral Health* 2021;21:e646.
152. Tu MG, Hsu JT, Fuh LJ, Lin DJ, Huang HL. Effects of cortical bone thickness and implant length on bone strain and interfacial micromotion in an immediately loaded implant. *Int J Oral Maxillofac Implant* 2010;25:706–714.
153. Beviacqua M, Tealdo T, Menini M, Mossolov A, Drago C, Pera P. The influence of cantilever length and implant inclination on stress distribution in maxillary implant-supported fixed dentures. *J Prosthet Dent* 2011;105:5–13
154. Malhotra AO, Padmananbhan TV, Mohamed K, Natarajan S, Elavia U. Load transfer in tilted implants with various cantilever lengths in an all-on-four situation. *Australian Dent J* 2012;57:440–445.
155. van Zyl PP, Grundling NL, Jooste CH, Terblanche E. Three-dimensional finite element model of a human mandible incorporating six osseointegrated implants for stress analysis of mandibular cantilever protheses. *Int J Oral Maxillofac Implant* 1995;10:51–57.

156. Hajizadeh F, Kermani ME, Sadafszaz M, Motlagh AM. Evaluation of stress and strain magnitude in tapered and cylindrical implant surrounding bone, used for restoration of mandibular teeth: Finite element analysis in All-on-Four concept. *J Long-Term Eff Med Implant* 2021;31:51–58.
157. Orsini E, Giavaresi G, Triré A, Ottani V, Salgarello, S. Dental implant thread pitch and its influence on the osseointegration process: An in vivo comparison study. *Int J Oral Maxillofac Implant* 2012;27:383–392.
158. Wu AYJ, Hsu JT, Fuh LJ, Huang HL. Biomechanical effect of implant design on four implants supporting mandibular full-arch fixed dentures: In vitro test and finite element analysis. *J Formosan Med Assoc* 2020;119:1514–1523.
159. Horita S, Sugiura T, Yamamoto K, Murakami K, Imai Y, Kirita T. Biomechanical analysis of immediately loaded implants according to the “All-on-Four” concept. *J Prosthodont Res* 2017;61:123–132.
160. Almeida EO, Rocha EP, Freitas AMJ, Anchieta RB, Poveda R, Gupta N, Coelho PG. Tilted and short implants supporting fixed prosthesis in an atrophic maxilla: A 3D-FEA biomechanical evaluation. *Clin Implant Dent Relat Res* 2015;17:e332–e342.
161. Bhering CLB, Mesquita MF, Kemmoku DT, Noritomi PY, Consani RLX, Barao VAR. Comparison between all-on-four and all-on-six treatment concepts and framework material on stress distribution in atrophic maxilla: A prototyping guided 3D-FEA study. *Mat Sci Eng C* 2016;69:715–725.
162. Sigiura T, Yamamoto K, Horita S, Murakami K, Kirita T. Micromotion analysis of different implant configuration, bone density, and crestal bone thickness in immediately loaded mandibular full-arch implant restorations: A nonlinear finite element study. *Clin Implant Dent Relat Res* 2018;20:43–49.
163. Daas M, Dubois G, Bonnet AS, Lipinski P, Rignon-Bret C. A complete finite element model of a mandibular implant-retained overdenture with two implants: Comparison between rigid and resilient attachment configurations. *Med Eng Phys* 2008;30:218–225.
164. Dastgerdi AK, Rouhi G, Dehghan MM, Farzad-Mohajeri S, Barikani HR. Linear Momenta Transferred to the Dental Implant-Bone and Natural Tooth—PDL-Bone Constructs Under Impact Loading: A Comparative in-vitro and in-silico Study. *Front Bioeng Biotechnol* 2020;8:e544.

## XII. ACKNOWLEDGEMENTS

I would like to offer my gratitude to my thesis supervisor **Prof. Dr. Zoltán Baráth**, for the opportunity to work on this topic. Furthermore, I wish to thank my supervisor for the valuable comments, advice and scientific inspiration. The supportive environment created by **Prof. Dr. Zoltán Baráth** considerably contributed to the success of this research. After graduating from university, Professor Baráth helped me as a mentor in my professional development and in the development of my practice.

I am grateful for **Dr. Éva Ilona Lakatos** and **Haydar Slyteen** for their support during the 3D finite element analysis studies.

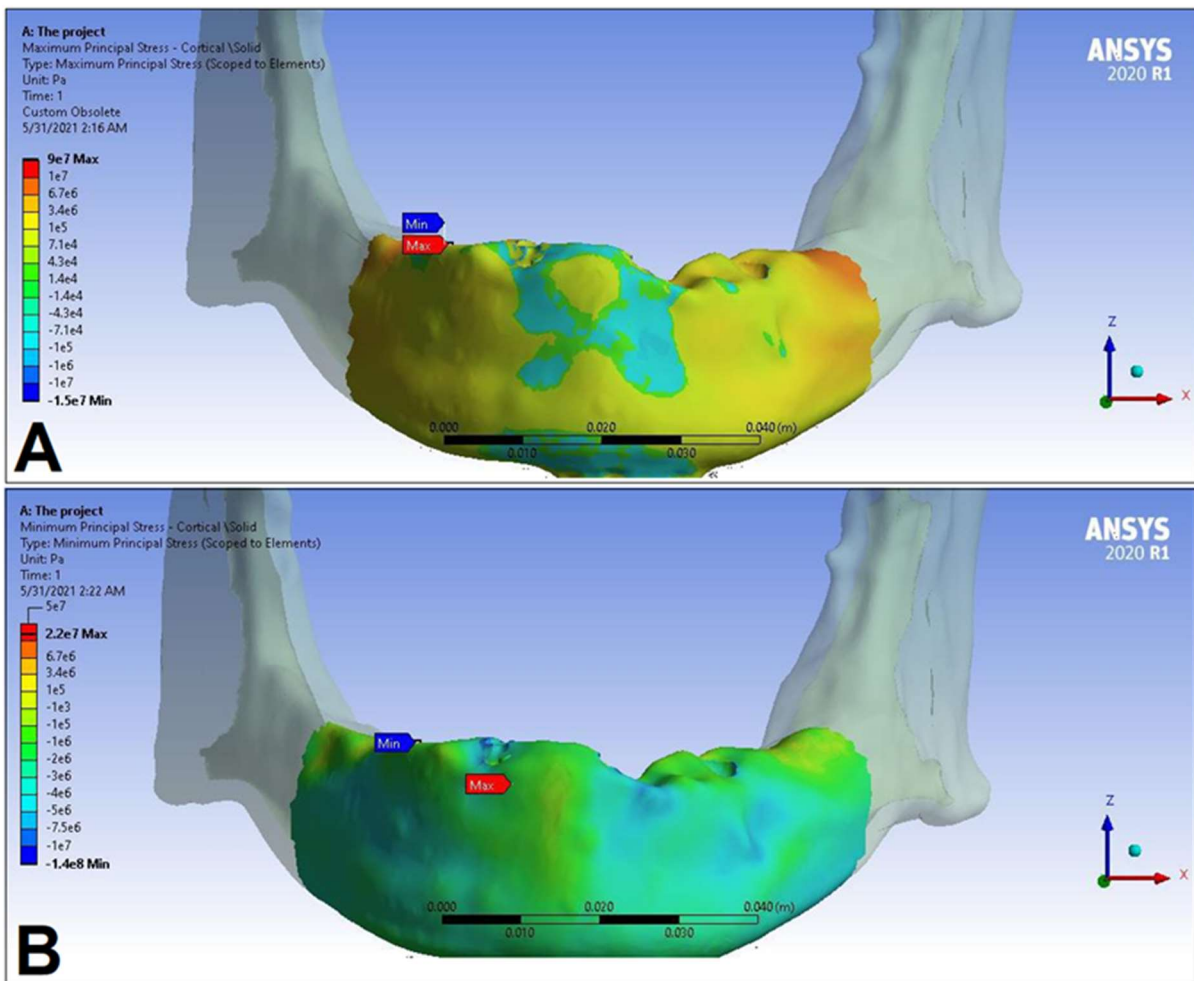
I wish to thank **Dr. Ádám László Nagy**, **Dr. Péter Bencsik** and **Dr. Csaba Lászlófy** for their professional collaboration in the retrospective clinical study.

I would like to acknowledge the support of **Dr. Márió Gajdács** and the Study Group for Dental Research Methodology and Health Sciences, University of Szeged.

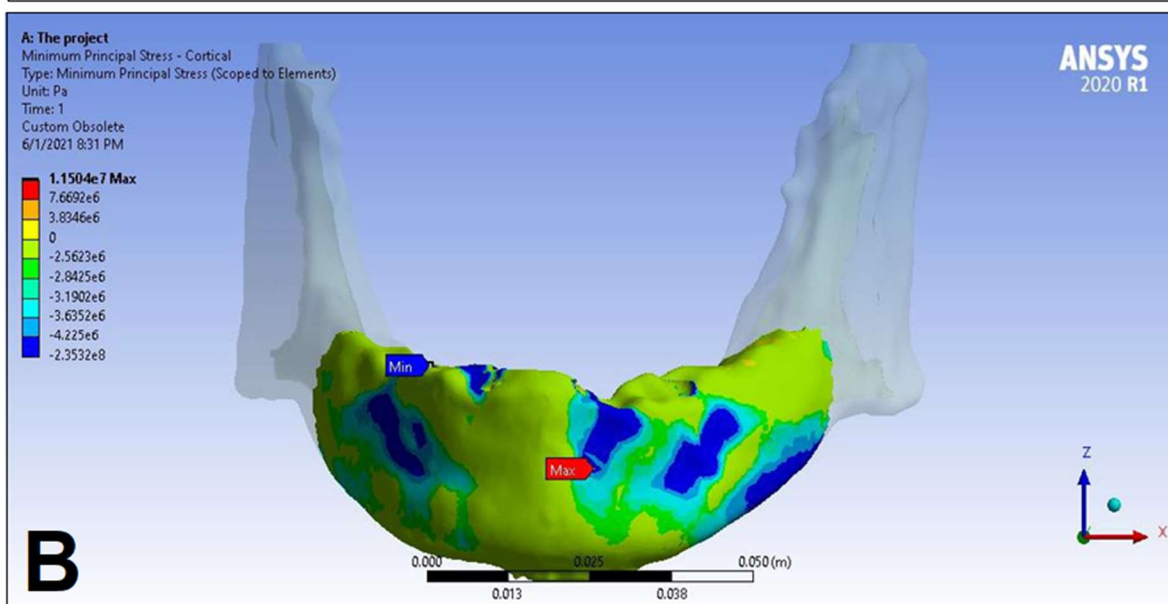
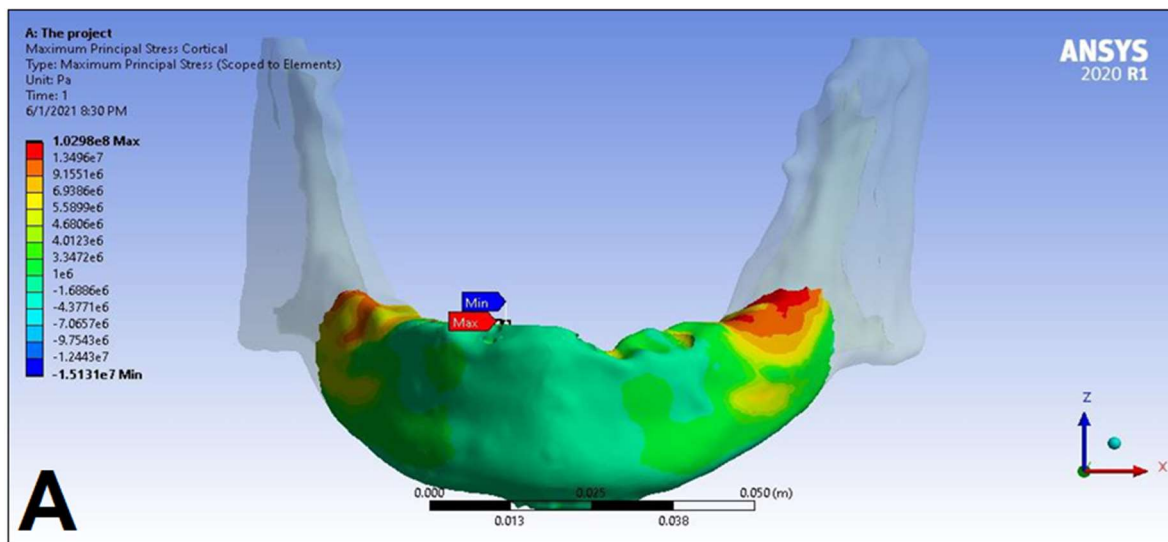
I would also like to extend my thanks to the **Oral Centrum** Dentistry and Oral Surgery for the opportunity to perform the implant surgery and analyze the X-ray / CBCT images.

Finally, I am grateful to my **family** and my **fiancée** for their persistent patience and support, which also contributed to the creation of this study.

### XIII. APPENDIX

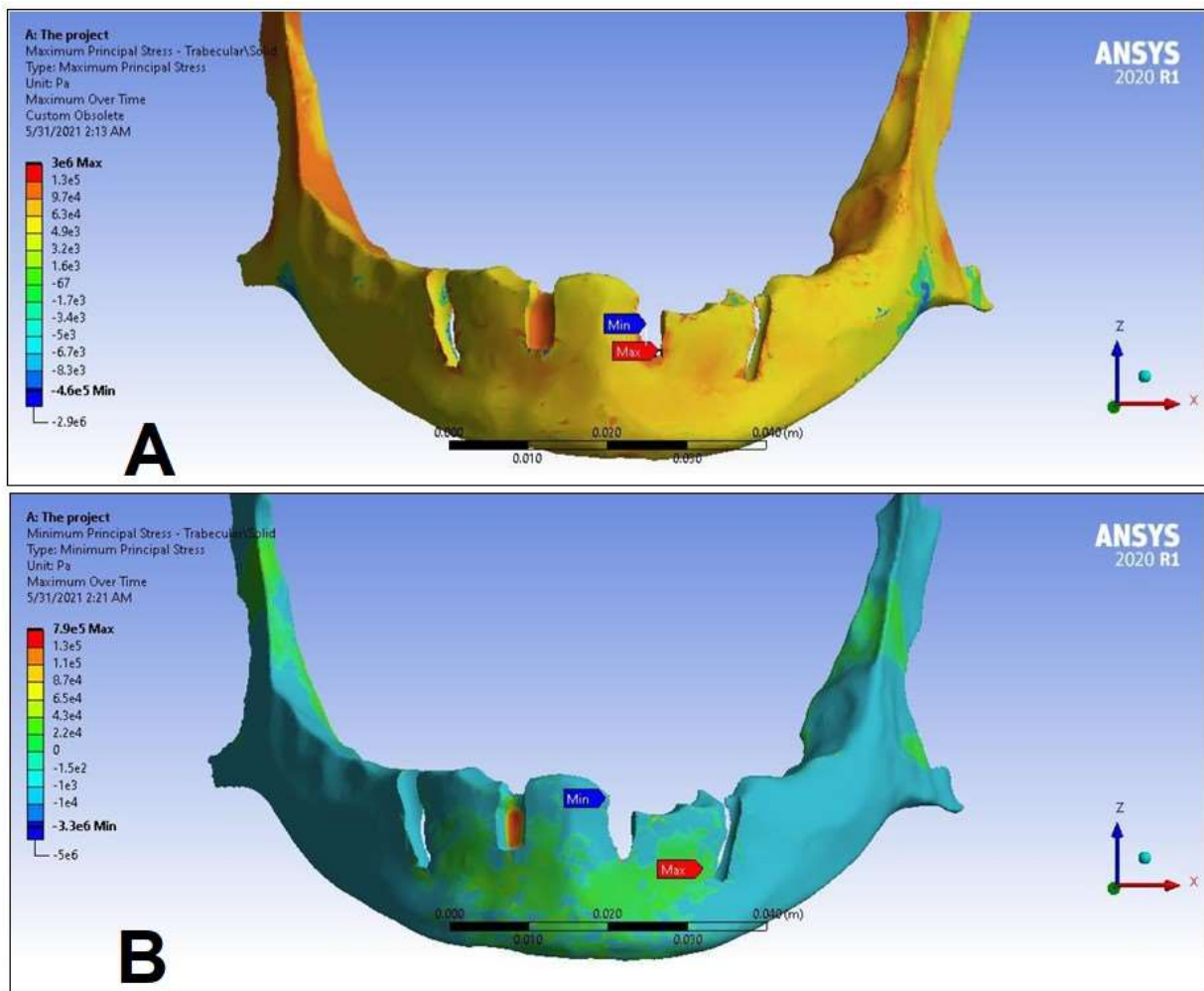


**Appendix 1.** Maximum ( $P_{\max}$ , **A**) and minimum ( $P_{\min}$ , **B**) principal stress distributions in the *cortical* bone segment of the mandible for the S1 LC2 simulation case. The heatmap shows the distribution of stresses according to the color scale, while the maximum and minimum values for stresses are also denoted (e.g., 8E3 corresponds to  $8 \times 10^3$ ).

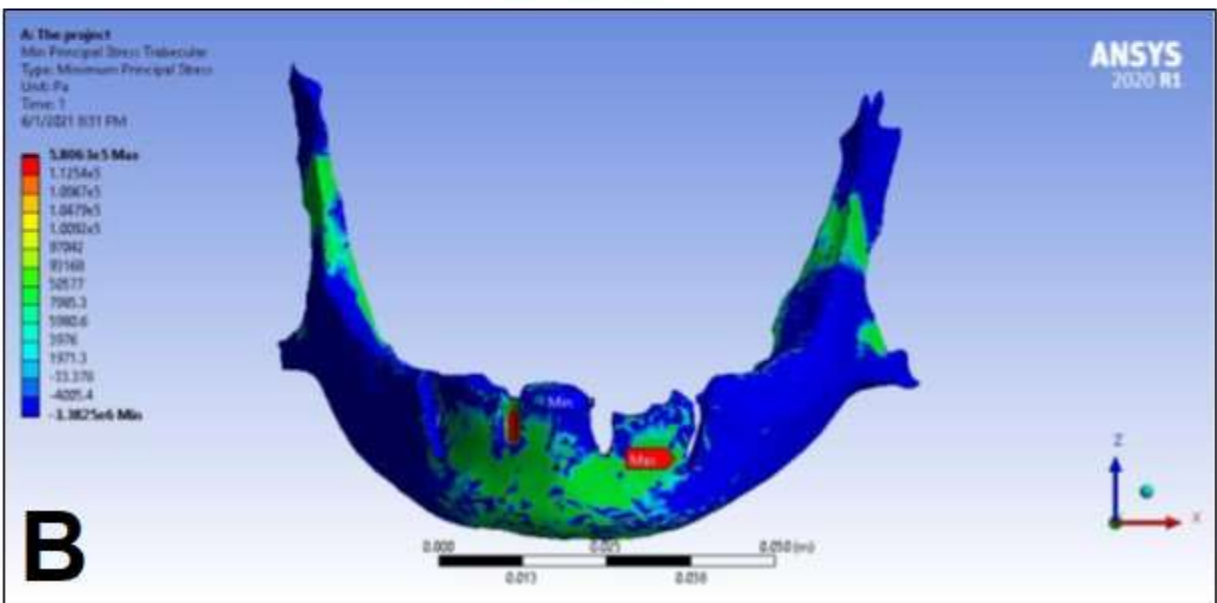
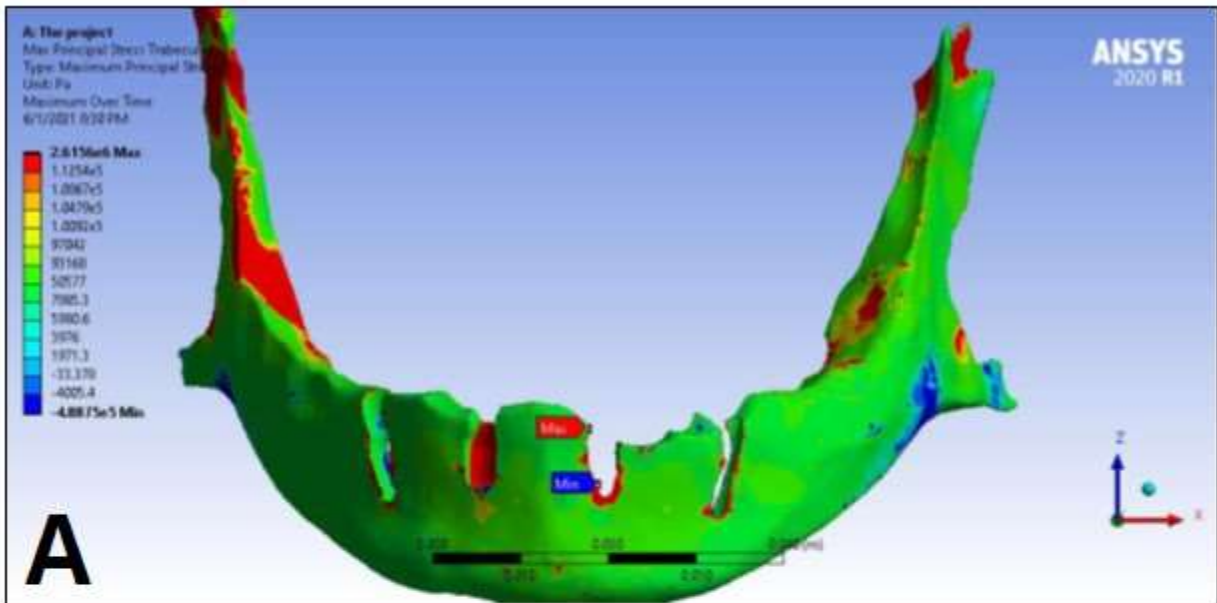


**Appendix 2.** Maximum ( $P_{\max}$ , **A**) and minimum ( $P_{\min}$ , **B**) principal stress distributions in the *cortical* bone segment of the mandible for the S2 LC2 simulation case. The heatmap shows the distribution of stresses according to the color scale, while the maximum and minimum values for stresses are also denoted (e.g., 8E3 corresponds to  $8 \times 10^3$ ).

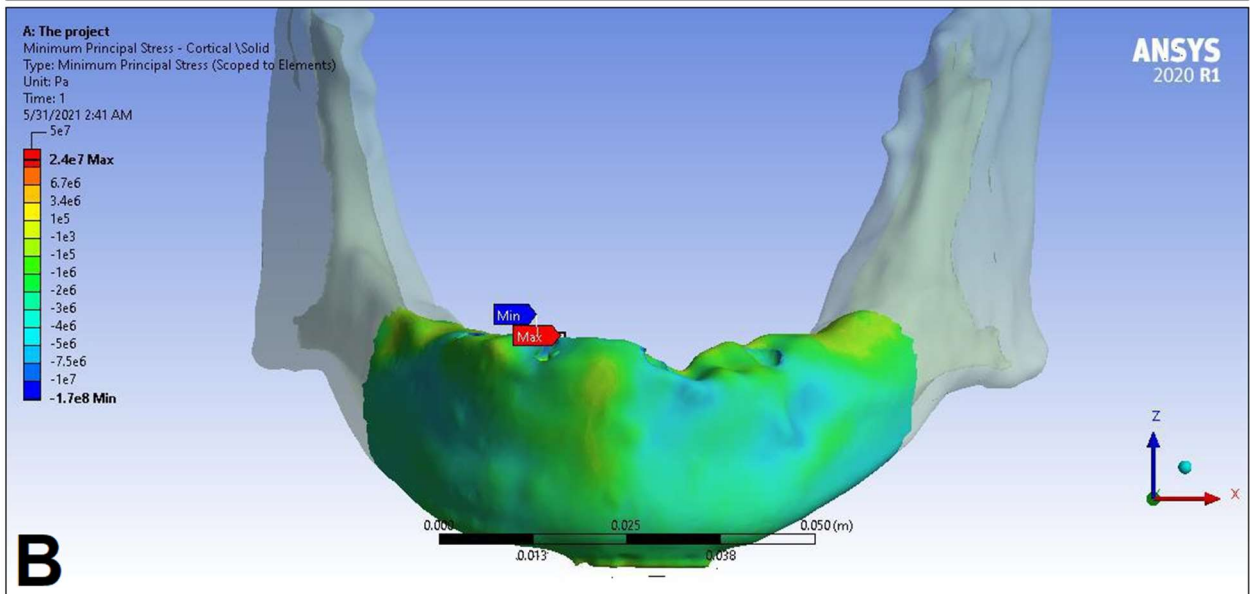
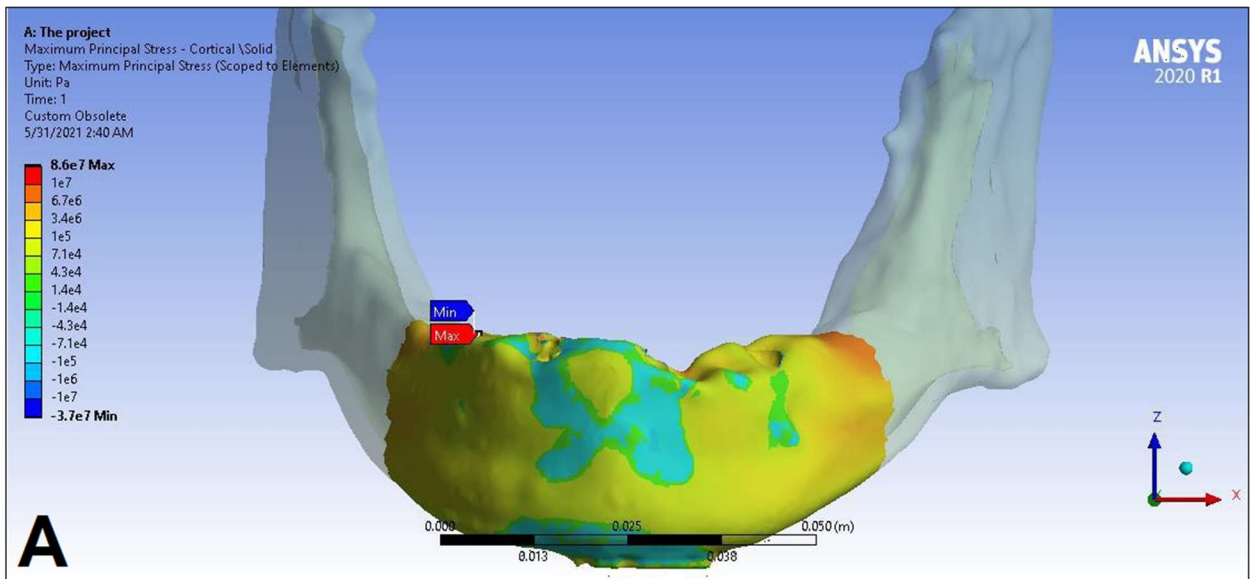




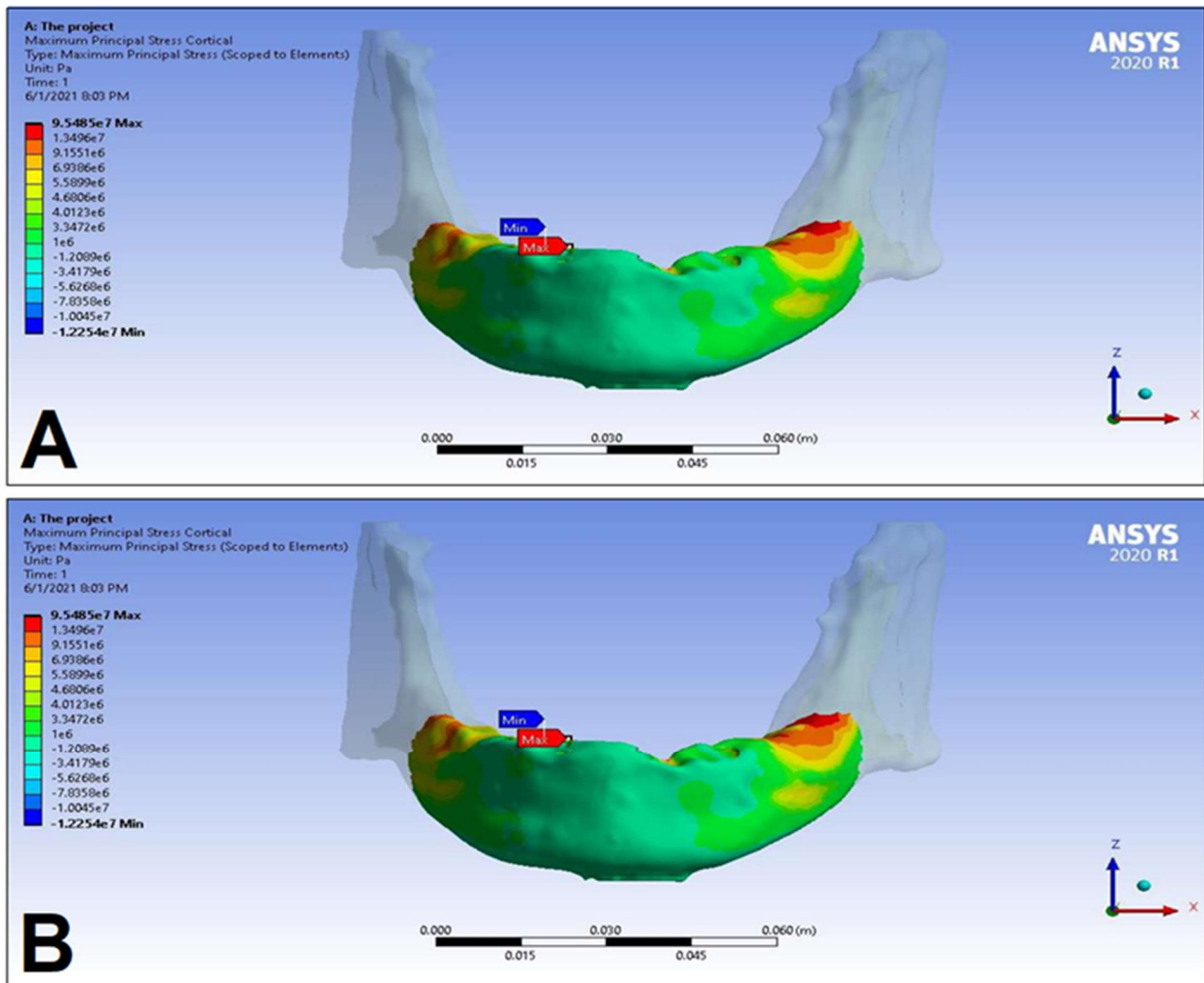
**Appendix 3.** Maximum ( $P_{\max}$ , **A**) and minimum ( $P_{\min}$ , **B**) principal stress distributions in the *trabecular* bone segment of the mandible for the S1 LC2 simulation case. The heatmap shows the distribution of stresses according to the color scale, while the maximum and minimum values for stresses are also denoted (e.g., 8E3 corresponds to  $8 \times 10^3$ ).



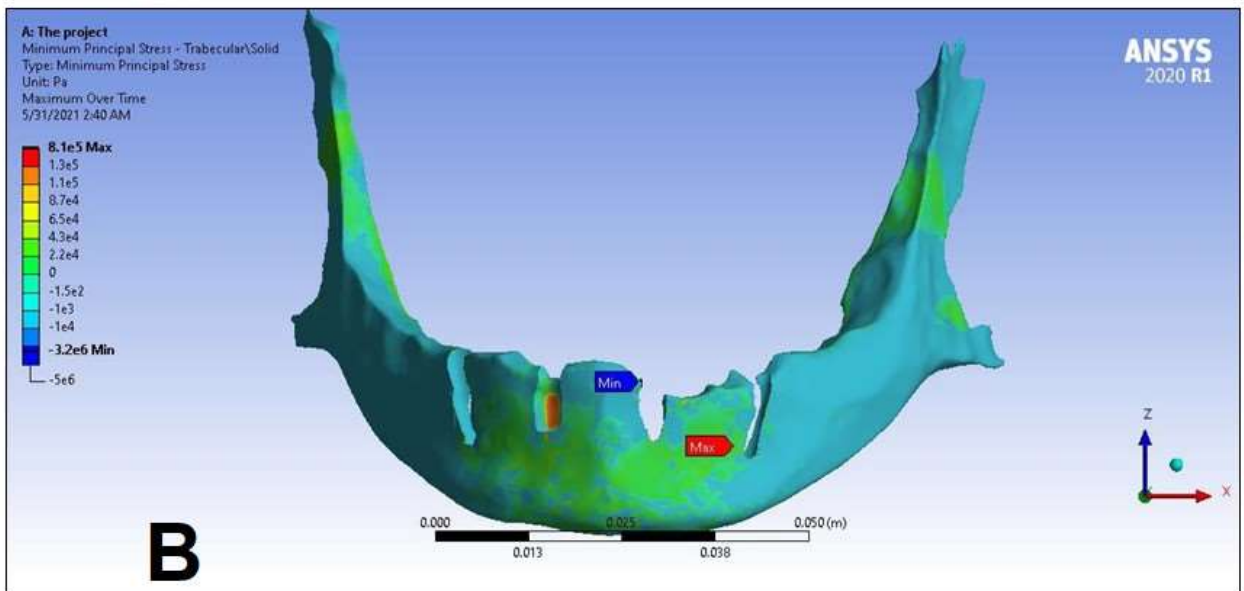
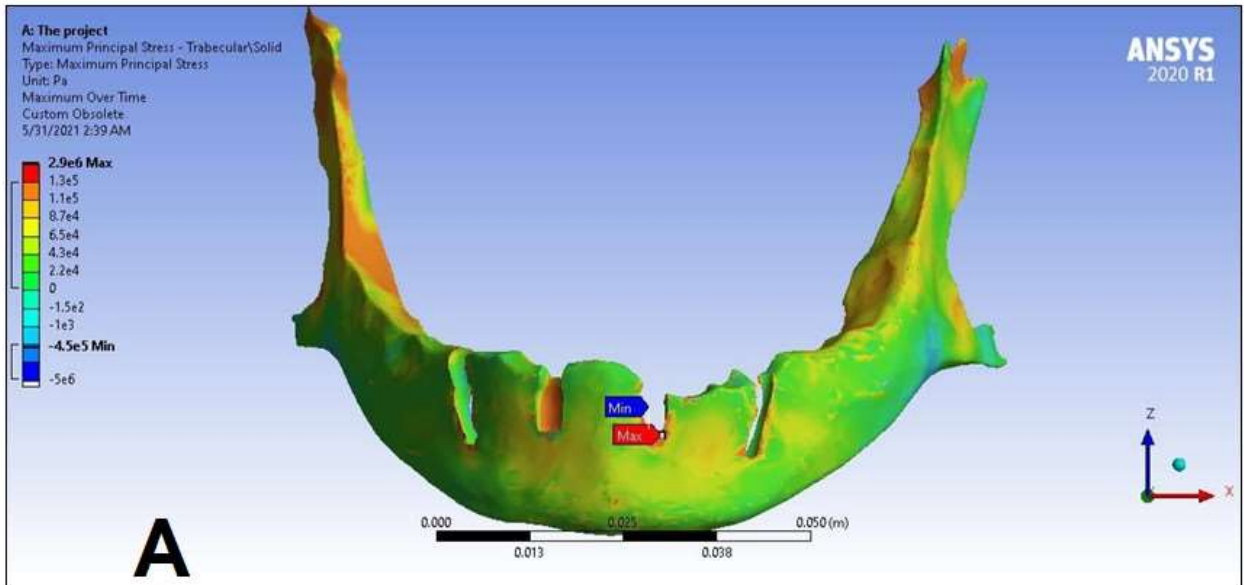
**Appendix 4.** Maximum ( $P_{\max}$ , **A**) and minimum ( $P_{\min}$ , **B**) principal stress distributions in the *trabecular* bone segment of the mandible for the S2 LC2 simulation case. The heatmap shows the distribution of stresses according to the color scale, while the maximum and minimum values for stresses are also denoted (e.g., 8E3 corresponds to  $8 \times 10^3$ ).



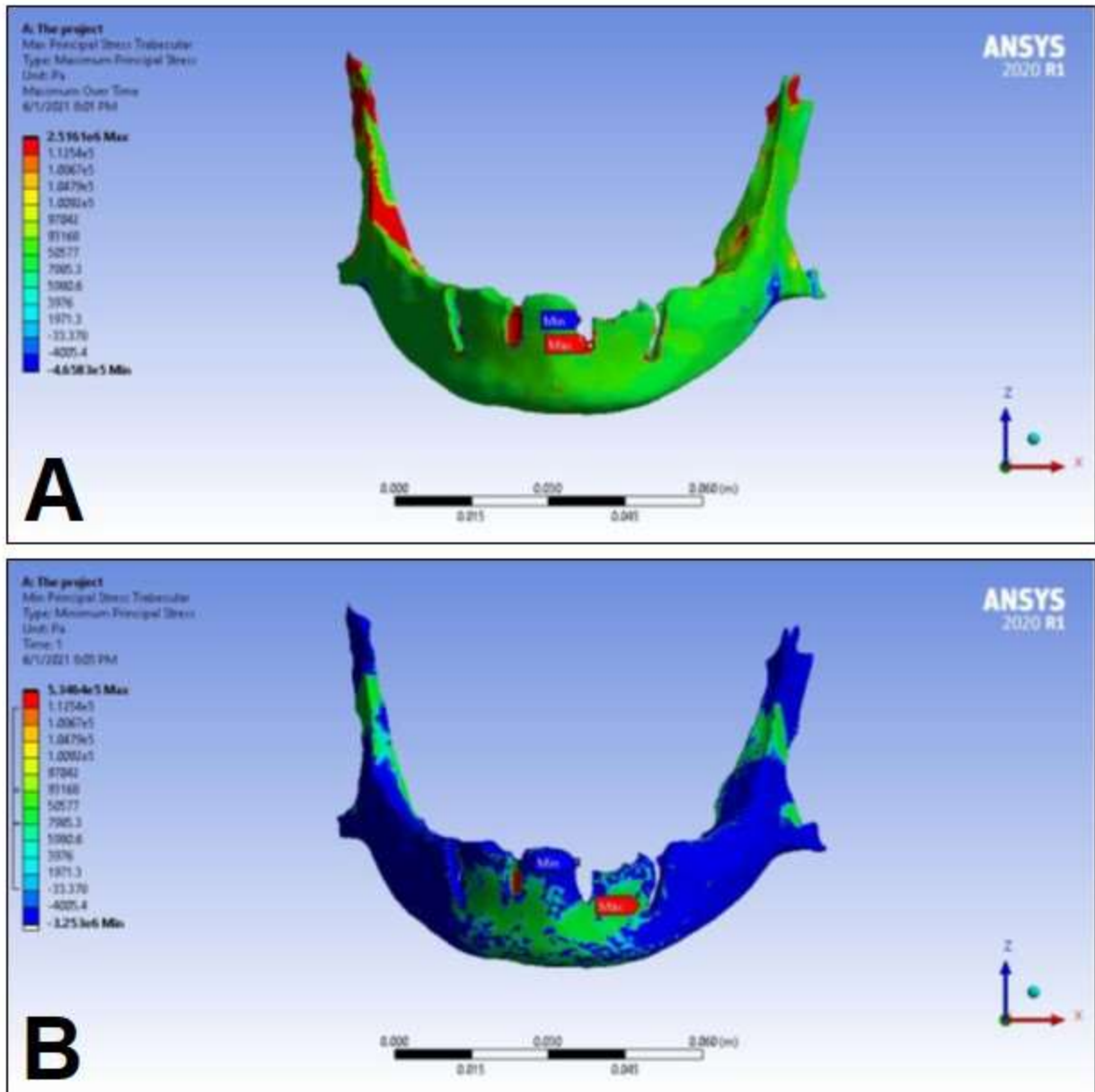
**Appendix 5.** Maximum ( $P_{\max}$ , **A**) and minimum ( $P_{\min}$ , **B**) principal stress distributions in the *cortical* bone segment of the mandible for the S1 LC3 simulation case. The heatmap shows the distribution of stresses according to the color scale, while the maximum and minimum values for stresses are also denoted (e.g., 8E3 corresponds to  $8 \times 10^3$ ).



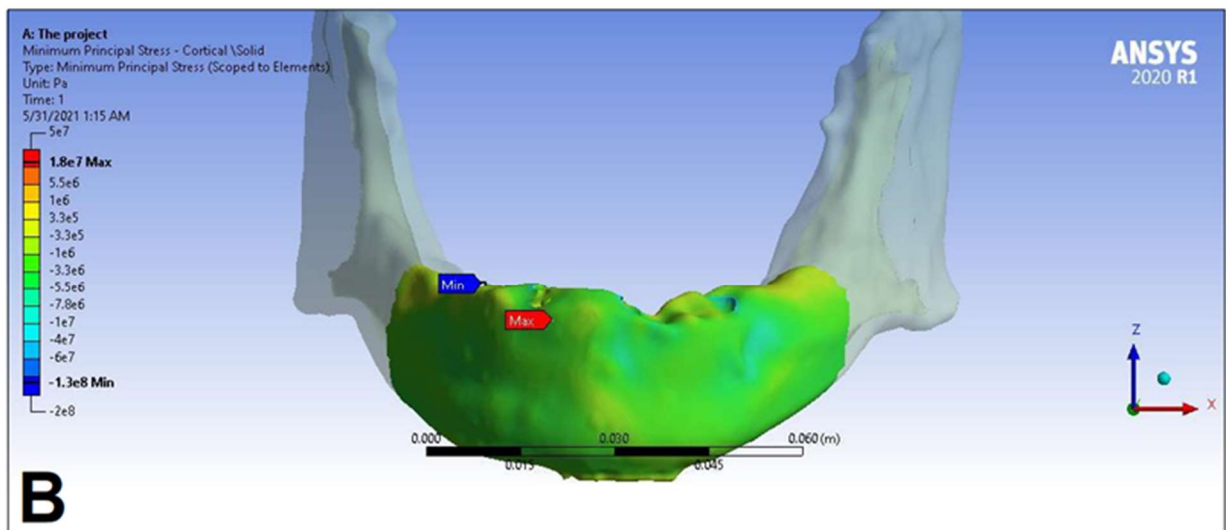
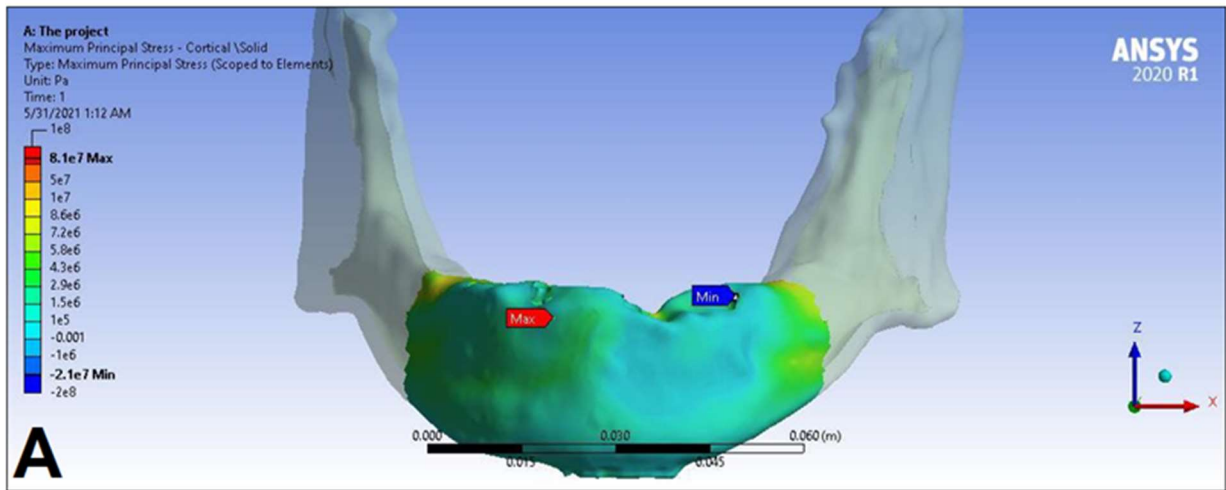
**Appendix 6.** Maximum ( $P_{\max}$ , **A**) and minimum ( $P_{\min}$ , **B**) principal stress distributions in the *cortical* bone segment of the mandible for the S2 LC3 simulation case. The heatmap shows the distribution of stresses according to the color scale, while the maximum and minimum values for stresses are also denoted (e.g., 8E3 corresponds to  $8 \times 10^3$ ).



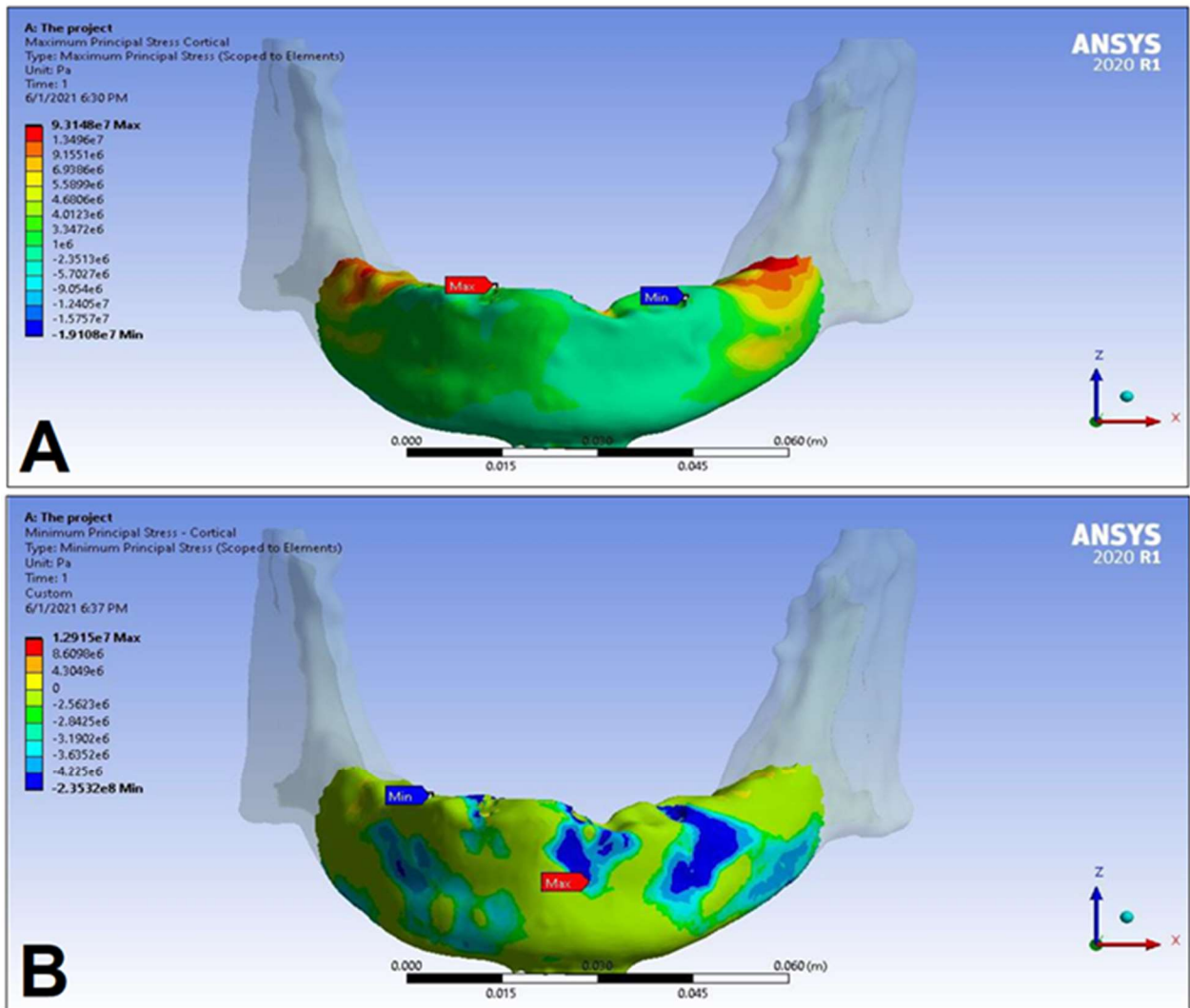
**Appendix 7.** Maximum ( $P_{\max}$ , **A**) and minimum ( $P_{\min}$ , **B**) principal stress distributions in the *trabecular* bone segment of the mandible for the S1 LC3 simulation case. The heatmap shows the distribution of stresses according to the color scale, while the maximum and minimum values for stresses are also denoted (e.g., 8E3 corresponds to  $8 \times 10^3$ ).



**Appendix 8.** Maximum ( $P_{\max}$ , **A**) and minimum ( $P_{\min}$ , **B**) principal stress distributions in the *trabecular* bone segment of the mandible for the S2 LC3 simulation case. The heatmap shows the distribution of stresses according to the color scale, while the maximum and minimum values for stresses are also denoted (e.g., 8E3 corresponds to  $8 \times 10^3$ ).

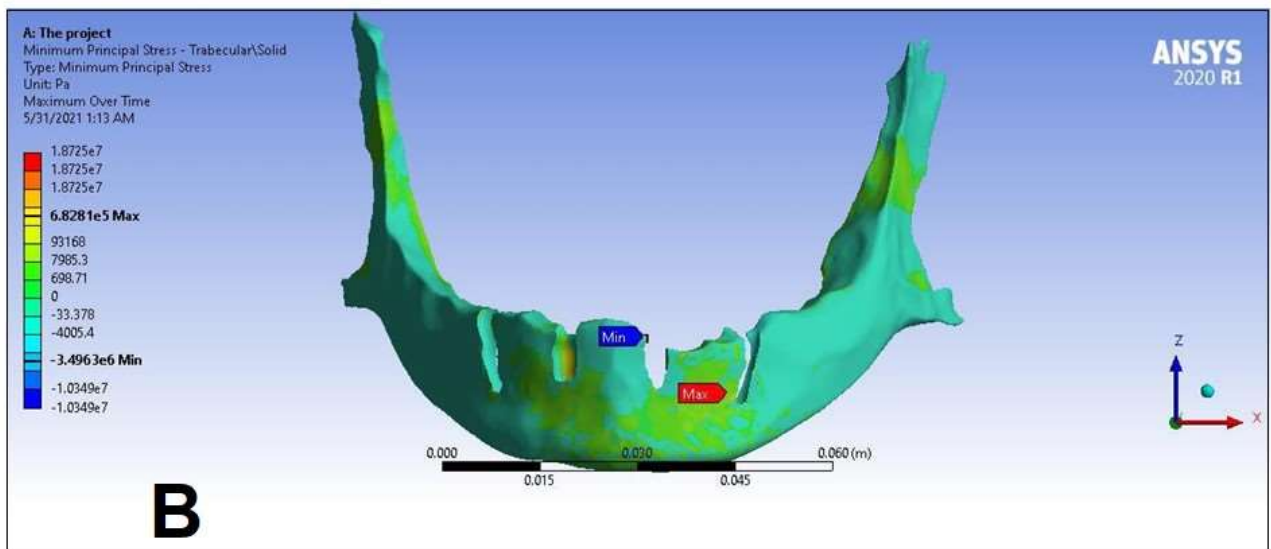
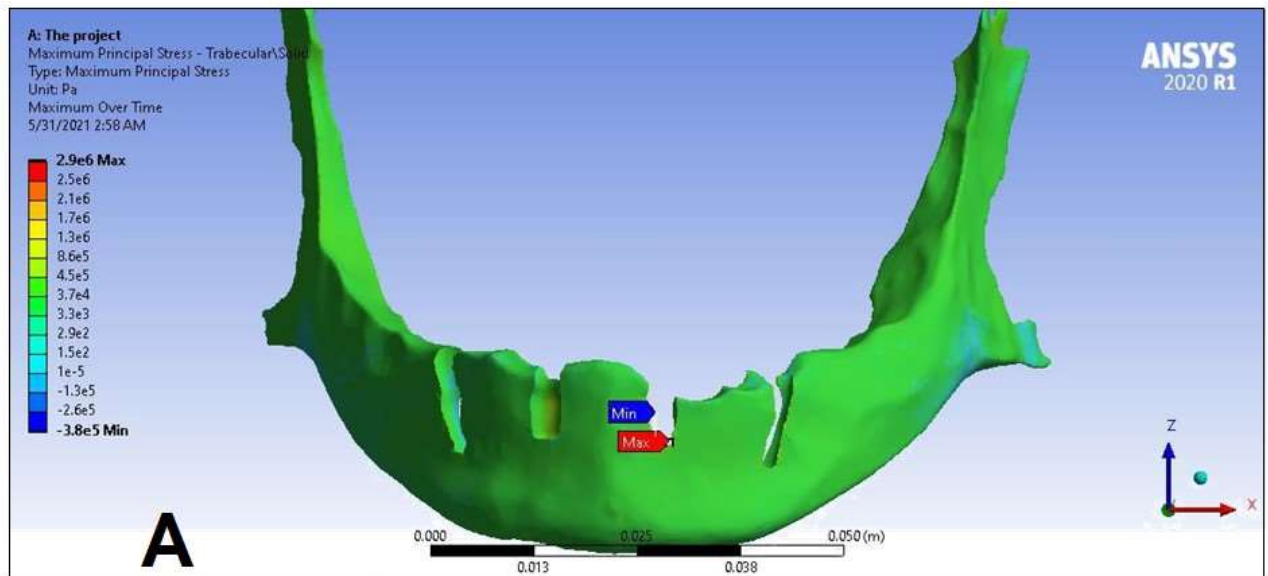


**Appendix 9.** Maximum ( $P_{\max}$ , **A**) and minimum ( $P_{\min}$ , **B**) principal stress distributions in the *cortical* bone segment of the mandible for the S1 LC4 case. The heatmap shows the distribution of stresses according to the color scale, while the maximum and minimum values for stresses are also denoted (e.g., 8E3 corresponds to  $8 \times 10^3$ ).

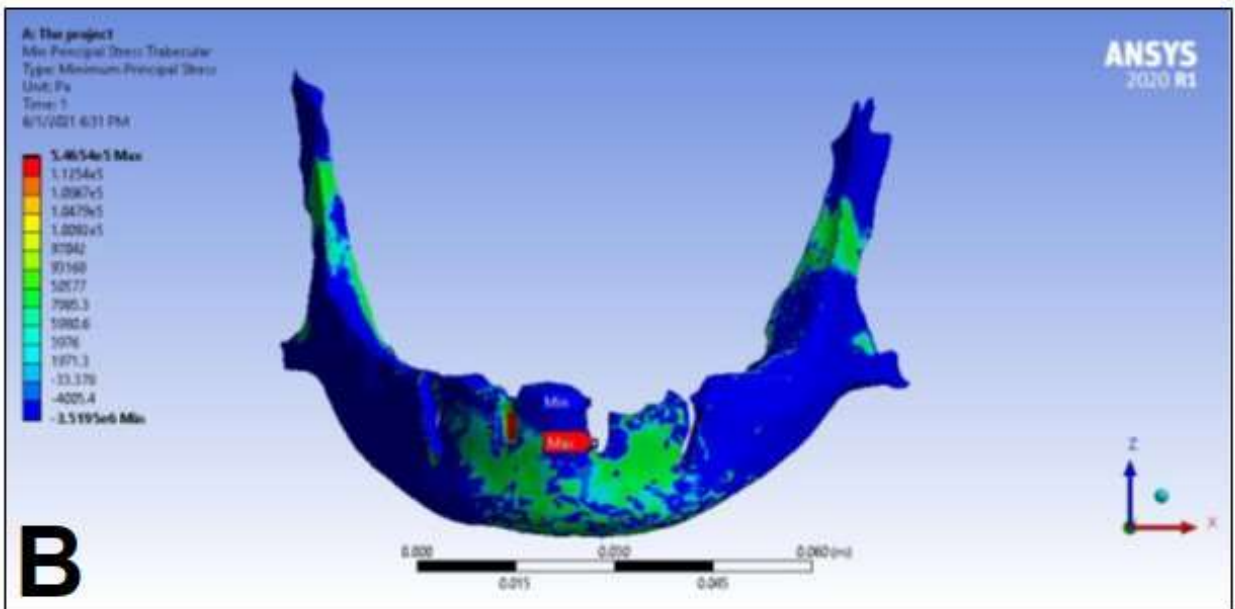
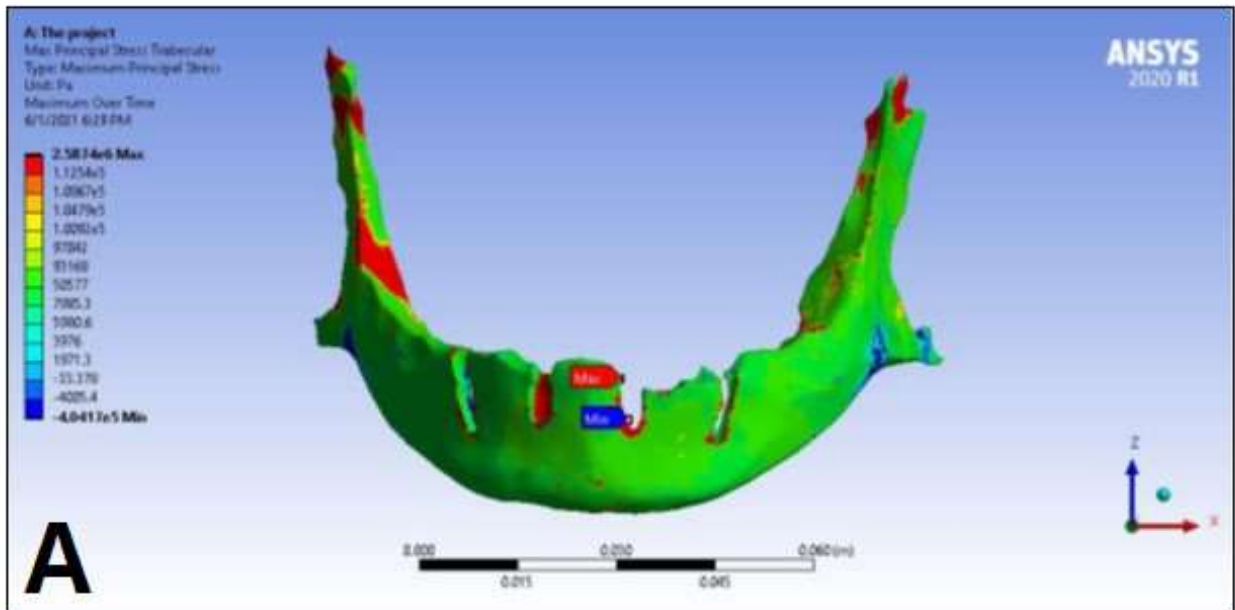


**Appendix 10.** Maximum ( $P_{\max}$ , **A**) and minimum ( $P_{\min}$ , **B**) principal stress distributions in the *cortical* bone segment of the mandible for the S2 LC4 simulation case. The heatmap shows the distribution of stresses according to the color scale, while the maximum and minimum values for stresses are also denoted (e.g., 8E3 corresponds to  $8 \times 10^3$ ).





**Appendix 11.** Maximum ( $P_{\max}$ , **A**) and minimum ( $P_{\min}$ , **B**) principal stress distributions in the *trabecular* bone segment of the mandible for the S1 LC4 simulation case. The heatmap shows the distribution of stresses according to the color scale, while the maximum and minimum values for stresses are also denoted (e.g., 8E3 corresponds to  $8 \times 10^3$ ).



**Appendix 12.** Maximum ( $P_{\max}$ , A) and minimum ( $P_{\min}$ , B) principal stress distributions in the *trabecular* bone segment of the mandible for the S2 LC4 simulation case. The heatmap shows the distribution of stresses according to the color scale, while the maximum and minimum values for stresses are also denoted (e.g., 8E3 corresponds to  $8 \times 10^3$ ).

## Co-author certification

I, **Éva Ilona Lakatos, Ph.D. MSc.** as a corresponding author of the following publications declare that the authors have no conflict of interest, and **Árpád László Szabó, D.M.D., Ph.D.** candidate had significant contribution to the jointly published researches. The results discussed in his thesis were not used and not intended to be used in any other qualification process for obtaining a Ph.D. degree.

Szeged, 2024. 05. 05.

.....  
Éva Ilona Lakatos, Ph.D. MSc.

The publication(s) relevant to the applicant's thesis:

**II. Szabó ÁL,** Matusovits D, Sylteen H, Lakatos ÉI, Baráth ZL: Biomechanical Effects of Different Load Cases with an Implant-Supported Full Bridge on Four Implants in an Edentulous Mandible: A Three-Dimensional Finite Element Analysis (3D-FEA). *Dent J* 2023; 11(11): e261.

## Co-author certification

I, **Zoltán Lajos Baráth, Ph.D. Habil. Prof.** as a corresponding author of the following publications declare that the authors have no conflict of interest, and **Árpád László Szabó, D.M.D.**, Ph.D. candidate had significant contribution to the jointly published researches. The results discussed in his thesis were not used and not intended to be used in any other qualification process for obtaining a Ph.D. degree.

Szeged, 2024. 05. 05.

.....  
Zoltán Lajos Baráth, Ph.D. Habil. Prof.

The publication(s) relevant to the applicant's thesis:

**I. Szabó ÁL**, Nagy ÁL, Lászlófy C, Gajdács M, Bencsik P, Kárpáti K, Baráth ZL: Distally Tilted Implants According to the All-on-Four<sup>®</sup> Treatment Concept for the Rehabilitation of Complete Edentulism: A 3.5-Year Retrospective Radiographic Study of Clinical Outcomes and Marginal Bone Level Changes. *Dent J* 2022; 10(5): e82.

**II. Szabó ÁL**, Matusovits D, Sylteen H, Lakatos ÉI, Baráth ZL: Biomechanical Effects of Different Load Cases with an Implant-Supported Full Bridge on Four Implants in an Edentulous Mandible: A Three-Dimensional Finite Element Analysis (3D-FEA). *Dent J* 2023; 11(11): e261.